

AN ANALYSIS OF THE ORTHOGONAL METAL CUTTING PROCESS

A THESIS

Presented to

The Faculty of the Graduate Division

by

Cecil Reid Attaway

In Partial Fulfillment

of the Requirements for the Degree

Doctor of Philosophy in the School of Mechanical Engineering

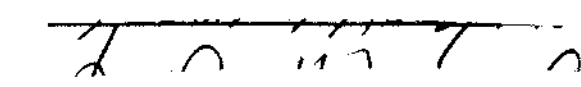
Georgia Institute of Technology

December, 1968

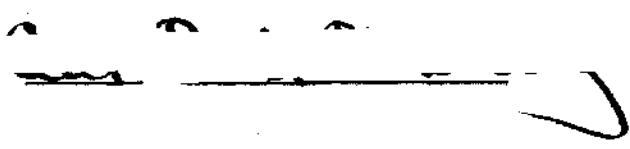
AN ANALYSIS OF THE ORTHOGONAL METAL CUTTING PROCESS

Approved:

  
Chairman

  
Date approved by Chairman: February 13 1969

In presenting the dissertation as a partial fulfillment of the requirements for an advanced degree from the Georgia Institute of Technology, I agree that the Library of the Institute shall make it available for inspection and circulation in accordance with its regulations governing materials of this type. I agree that permission to copy from, or to publish from, this dissertation may be granted by the professor under whose direction it was written, or, in his absence, by the Dean of the Graduate Division when such copying or publication is solely for scholarly purposes and does not involve potential financial gain. It is understood that any copying from, or publication of, this dissertation which involves potential financial gain will not be allowed without written permission.



7/25/68

## ACKNOWLEDGMENTS

A great deal of thanks is given to Dr. John A. Bailey, without whose suggestions, aid, and timely and constructive criticism this investigation would not have been successful. Appreciation is also extended to Dr. G. Boothroyd who introduced the author to the subject of machining and provided the basic foundation for this analysis, and to Dr. Robert F. Hochman, Dr. John H. Murphy, Dr. Wilham R. Clough, and Dr. James M. Bradford who served on the examining and reading committee. Thanks are also due to Mr. David Keibel and Mr. Robert Collins whose aid in the machine shop was invaluable.

Sincere appreciation is extended to the American Society of Tool and Manufacturing Engineers, the National Science Foundation, and the United States Army Research Office - Durham, for support of portions of this research, and to Mrs. Cecil L. Reid, for her steadfast encouragement during the extended period of this research.

Special permission was received from the Graduate Division of the Georgia Institute of Technology to deviate from the standard procedure for figure titles in order to maintain a more uniform appearance.



## TABLE OF CONTENTS

	Page
ACKNOWLEDGMENTS . . . . .	ii
LIST OF TABLES . . . . .	v
LIST OF ILLUSTRATIONS . . . . .	vi
SUMMARY . . . . .	ix
Chapter	
I. PROBLEM DEFINITION . . . . .	1
II. REVIEW OF LITERATURE . . . . .	2
Problem History	
Chip Formation	
Tool Forces and Their Measurement	
Specific Cutting Pressure	
Mean Shear Strength of the Work Material	
Chip Thickness	
Regions of Interest	
Review of Cutting Theories	
Critique of Existing Work	
III. EXPERIMENTAL PROCEDURE . . . . .	34
Introduction	
Equipment	
Procedure	
IV. MODEL DESCRIPTION . . . . .	46
Introduction	
Proposed Model	
Model Analysis	
V. MODEL APPLICATION . . . . .	66
VI. MODEL UTILIZATION . . . . .	72
Introduction	
Utilization	

## TABLE OF CONTENTS (Continued)

Chapter	Page
VII. DISCUSSION . . . . .	77
Basic Assumptions	
Model Geometry Assumptions	
Independent Correlation	
VIII. CONCLUSIONS . . . . .	85
IX. RECOMMENDATIONS . . . . .	86
APPENDICES	
I. EXPERIMENTAL RESULTS . . . . .	87
II. RATE OF WORK IN PRIMARY DEFORMATION ZONE . . . . .	107
III. LIST OF SYMBOLS USED . . . . .	115
IV. COMPUTER PROGRAMS . . . . .	121
BIBLIOGRAPHY . . . . .	177
VITA . . . . .	181

## LIST OF TABLES

Table		Page
1.	Nominal and Actual Cutting Speeds and Rake Angles . . . .	88
2.	Experimental Cutting Test Results . . . . .	89
3.	Stress $S_s \times 10^{-3}$ in psi . . . . .	90
4.	Stress Ratio $\frac{S_s}{S_o}$ . . . . .	91
5.	Stress $S_o \times 10^{-3}$ in psi . . . . .	92
6.	Stress $S_f \times 10^{-3}$ in psi . . . . .	93
7.	Percent Error in Predicting $S_f$ . . . . .	94
8.	Percent Error in Predicting $\frac{S_s}{S_o}$ . . . . .	95

## LIST OF ILLUSTRATIONS

Figure	Page
1. Oblique Cutting . . . . .	3
2. Orthogonal Cutting . . . . .	4
3. Metal Cutting Deformation Zones . . . . .	6
4. Characteristic Forces of Metal Cutting . . . . .	9
5. Idealized Orthogonal Cutting Model . . . . .	11
6. Idealized Orthogonal Cutting Forces . . . . .	12
7. Ernst and Merchant Orthogonal Cutting Model . . . . .	16
8. Shear Stress vs. Normal Stress on Shear Plane . . . . .	19
9. Ideal Plastic Stress-Strain Curve . . . . .	21
10. Lee and Shaffer Slip Line Field Solution . . . . .	22
11. Palmer and Oxley Orthogonal Cutting Model . . . . .	25
12. Stress Strain-rate Temperature Relationship for Aluminum . . . . .	27
13. Theoretical Model Used by Boothroyd to Predict Brass Cutting Results . . . . .	29
14. Some Theoretical and Experimental Shear Angle Relationships . . . . .	30
15. Dynamometer Configuration . . . . .	36
16. Strain Gage Layout and Schematic for Vertical Force Component of Dynamometer . . . . .	37
17. Workpiece with Dynamometer . . . . .	38
18. Cutting Force vs. Undeformed Chip Thickness . . . . .	41
19. Thrust Force vs. Undeformed Chip Thickness . . . . .	42

## LIST OF ILLUSTRATIONS (Continued)

Figure	Page
20. Microhardness Distribution of a Suddenly Stopped Chip Sample . . . . .	43
21. Typical Flow Lines Observed in a Suddenly Stopped Chip . . . . .	45
22. Developed Model of Orthogonal Metal Cutting . . . . .	48
23. Model with Stresses Shown on Applicable Planes . . . . .	50
24. Individual Zones of Proposed Model . . . . .	51
25. Force Polygon Across Surface EBF of Model . . . . .	56
26. Force Polygons of Triangles BDF and ABE of Model . . . . .	57
27. Primary Deformation Zone of Model . . . . .	60
28. Block Diagram of Iterative Process . . . . .	74
29. Shear Angle vs. Difference Between Friction Angle and Rake Angle . . . . .	96
30. Friction Angle vs. Rake Angle for Various Cutting Speeds . . . . .	97
31. Friction Angle vs. Cutting Speed for Various Rake Angles . . . . .	98
32. Shear Angle vs. Rake Angle for Various Cutting Speeds . . . . .	99
33. Shear Angle vs. Cutting Speed for Various Rake Angles . . . . .	100
34. Chip Thickness vs. Rake Angle . . . . .	101
35. Chip Thickness vs. Cutting Speed . . . . .	102
36a. Cutting & Thrust Forces vs. Rake Angle for Various Cutting Speeds . . . . .	103
36b. Cutting & Thrust Forces vs. Rake Angle for Various Cutting Speeds . . . . .	104

## LIST OF ILLUSTRATIONS (Continued)

Figure	Page
37a. Cutting & Thrust Forces vs. Cutting Speeds for Various rake Angles . . . . .	105
37b. Cutting & Thrust Forces vs. Cutting Speeds for Various rake Angles . . . . .	106
38. Shear Plane Model Used to Determine Deformation as a Function of Shear and Compression . . . . .	109

## SUMMARY

Previous analyses concerning the mechanics of the orthogonal metal cutting process have produced relationships between the various angle parameters. These relationships cannot be used to predict the geometry of cutting or tool forces, and hence are limited in applicability and usefulness.

The purpose of the investigation is two-fold; first to determine experimentally the effect of changes in the rake angle and cutting speed on the type of chip produced during orthogonal machining of aluminum and then to develop a generalized model of the orthogonal metal cutting process which will predict the chip geometry and the effects of changes in rake angle and cutting speed on tool forces from a knowledge of the effects of strain, strain rate, and temperature on the mechanical properties of the work material.

It is believed that the present work represents considerable progress in the understanding of the mechanics of the machining process. The analysis shows excellent qualitative agreement between the predicted and experimentally measured cutting forces, friction angle, and chip thickness.

## CHAPTER I

### PROBLEM DEFINITION

Because of the complex nature of the metal cutting process no comprehensive theory has been proposed which will accurately describe the process without use of artificial parameters such as the shear angle, the friction angle, or a machinability constant. The problem is compounded by the fact that changes in cutting speed as well as changes in rake angle alter the chip geometry and tool forces during cutting.

The purpose of this research is to develop a comprehensive model of the metal cutting process which will qualitatively predict the effects of changes in rake angle and cutting speed on the tool forces and geometry of the cutting process.



## CHAPTER II

### REVIEW OF LITERATURE

#### Problem History

The metal cutting process is one of the oldest methods of reducing a metal workpiece to a given shape and is directly or indirectly involved in the manufacture of most of the items used today. Much work of an empirical nature has been carried out in the past concerning the development of new cutting techniques and methods to obtain reductions in machining costs and improvements in dimensional control. A much smaller amount of work has been carried out concerning attempts to understand the fundamental principals of the machining process. In recent years the amount of basic research has increased since it has been recognized that fundamental knowledge of the machining process can help in the solution of many practical production problems.

The machining process involves the systematic removal of layers of metal in the form of chips from a workpiece by the action of a wedge shaped cutting tool. Figure 1 illustrates the general case of cutting known as oblique cutting in which the cutting edge of the tool is straight and parallel with the original plane surface of the workpiece. The special case where the cutting edge of the tool is perpendicular to the direction of relative work tool motion is known as orthogonal cutting and is illustrated in Figure 2.

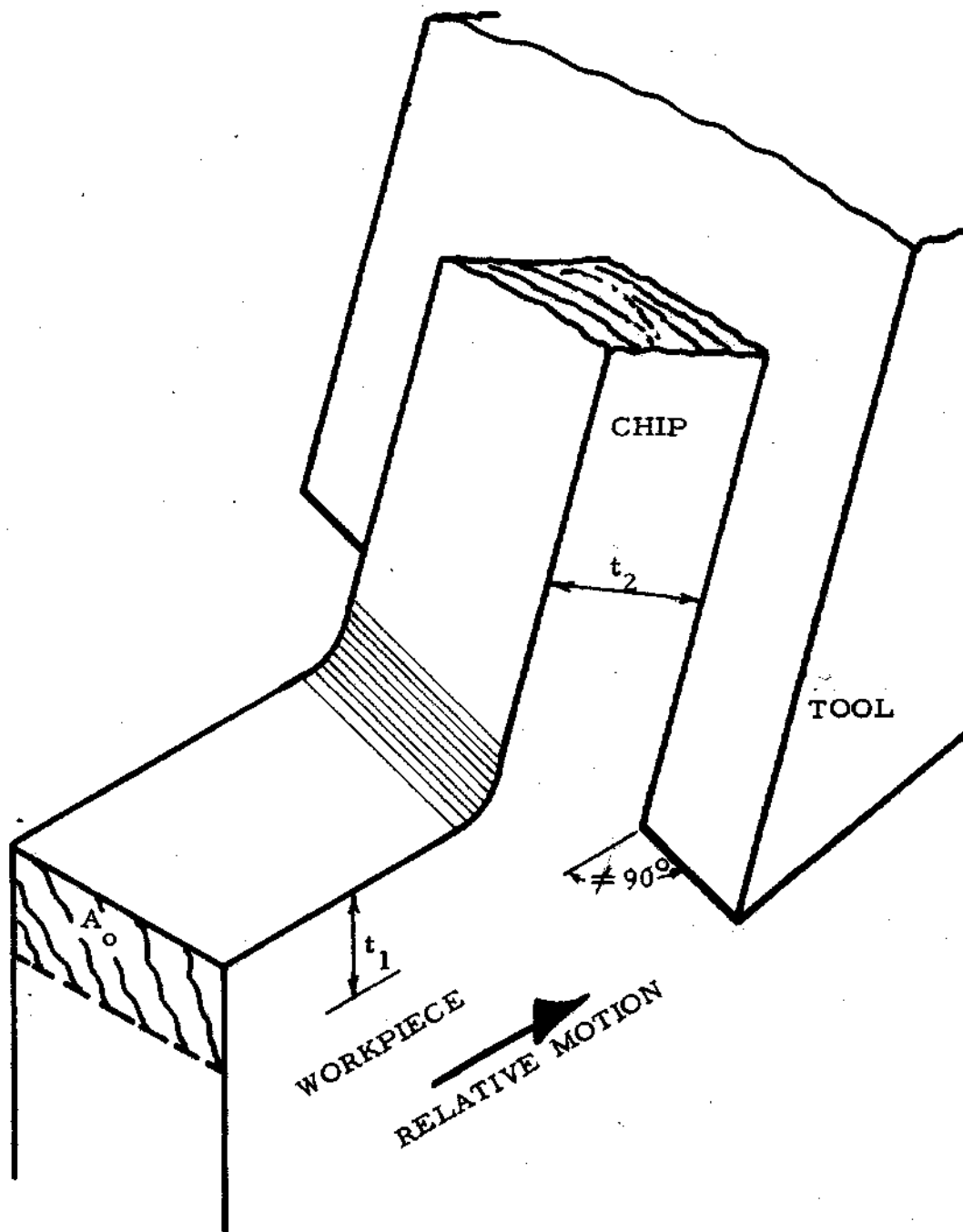


Figure 1: Oblique Cutting

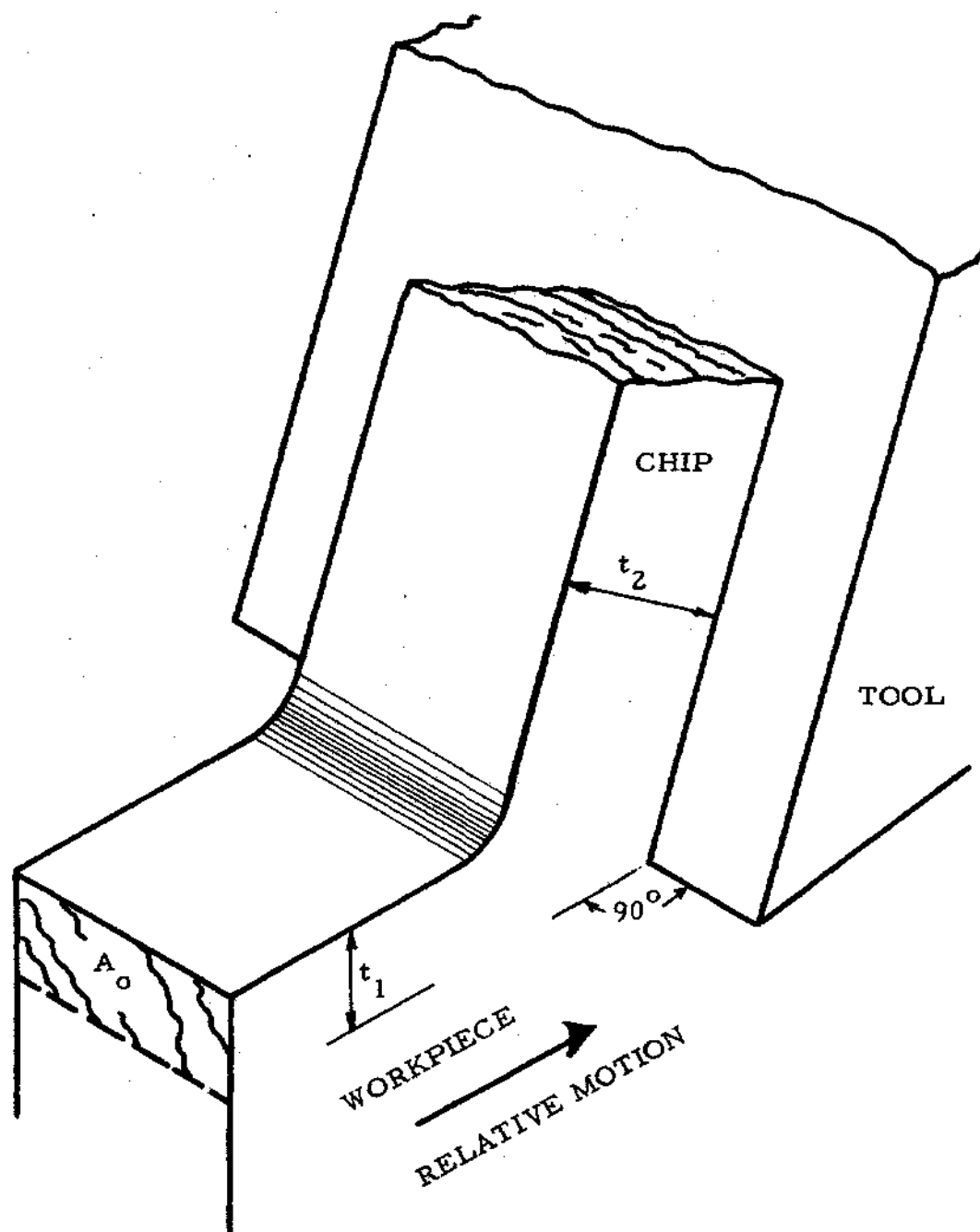


Figure 2: Orthogonal Cutting

### Chip Formation

Since orthogonal cutting represents a two-dimensional or plane strain process rather than a three-dimensional process it lends itself well to analytical investigations where it is desirable to eliminate as many of the independent variables as possible.

In practical machining it is possible to produce three types of chip, namely:

- (1) a continuous chip
- (2) a continuous chip with a built-up edge on the  
tool face
- (3) a discontinuous chip.

The type of chip produced in a particular machining operation is a function of the work and tool materials, the geometry and speed of the cutting process, and whether or not a lubricant is present.

When machining ductile materials such as mild steel, brass, or copper, continuous chips with the absence of a built-up edge on the tool face can be produced under certain conditions. Cutting under these conditions is a steady state process, and for this reason most of the work conducted in metal cutting research has dealt with continuous chip formation.

The formation of the chip takes place by shear in a zone extending from the tool cutting edge to the junction between the surfaces of the chip and the workpiece. This is known as the primary deformation zone, and is shown in Figure 3. The chip, which is substantially workhardened flows up the tool rake face under the action of large normal and frictional stresses. In unlubricated cutting the normal stress is such that

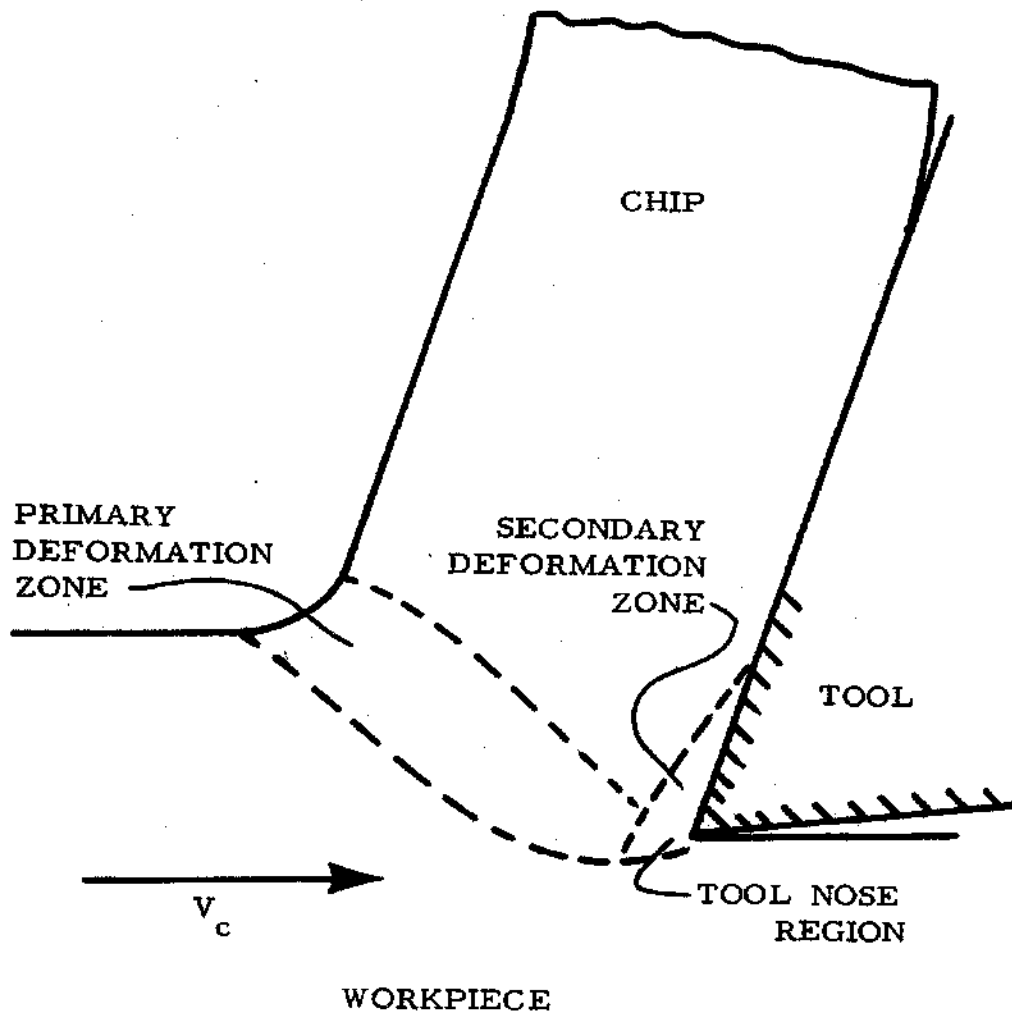


Figure 3: Metal Cutting Deformation Zones

the real and apparent areas of contact are equal over a portion of the chip-tool contact length. In this portion there is no relative motion at the chip-tool interface and deformation takes place in the lower layers of the chip (Secondary Deformation). This is also shown in Figure 3. Over the remaining portion of the chip-tool contact length the real area of contact is less than the apparent and relative motion at the interface can take place.

In the slow speed machining of certain ductile materials, it has been observed that a built-up edge forms on the tool rake face. Under these conditions a portion of the chip material becomes anchored to the tool face and shearing takes place in a zone within the chip itself. During machining this built-up edge often grows until it becomes unstable and breaks away from the tool face. As the built-up edge disintegrates some fragments are carried past the tool by the new workpiece surface and some past the rake face by the underside of the chip causing damage in these regions.

Built-up edge formation in machining is usually an undesirable characteristic. It is one of the principal factors affecting surface finish and has a considerable influence on power consumption. The built-up edge is on occasion beneficial in that it reduces cutting tool wear when machining very abrasive materials by protection of the tool rake face. The built-up edge can be eliminated in a number of ways. It has generally been accepted that an increase in the workhardened state of the work material, the application of a lubricant, and an increase in rake angle all lead to a decrease in the speed below which a built-up edge will appear.

In machining brittle materials or ductile materials at very low speeds and high rates of feed, discontinuous chips are produced. In this case fracture occurs in the primary deformation zone and the chip becomes segmented.

### Tool Forces and Their Measurement

In orthogonal cutting, the resultant force (R) applied to the chip by the tool lies in a plane normal to the cutting edge (Figure 4). This force is usually determined from the measurement of two orthogonal components; one in the direction of cutting (known as the cutting force,  $F_c$ ); the other normal to the direction of cutting (known as the thrust force,  $F_t$ ). The two components,  $F_c$  and  $F_t$ , are measured with a dynamometer.

### Specific Cutting Pressure

The work done during cutting ( $W_{tl}$ ) is the product of the cutting speed ( $V_c$ ) and the cutting force ( $F_c$ ), and is given by the expression:

$$W_{tl} = F_c V_c \quad (1)$$

A parameter which should give an indication of the efficiency of the metal cutting process, independent of cutting speed, is the work done per unit volume of metal removed (commonly known as the specific cutting pressure). This is given by the expression:

$$P_s = \frac{W_{tl}}{A_o V_c} \quad (2)$$

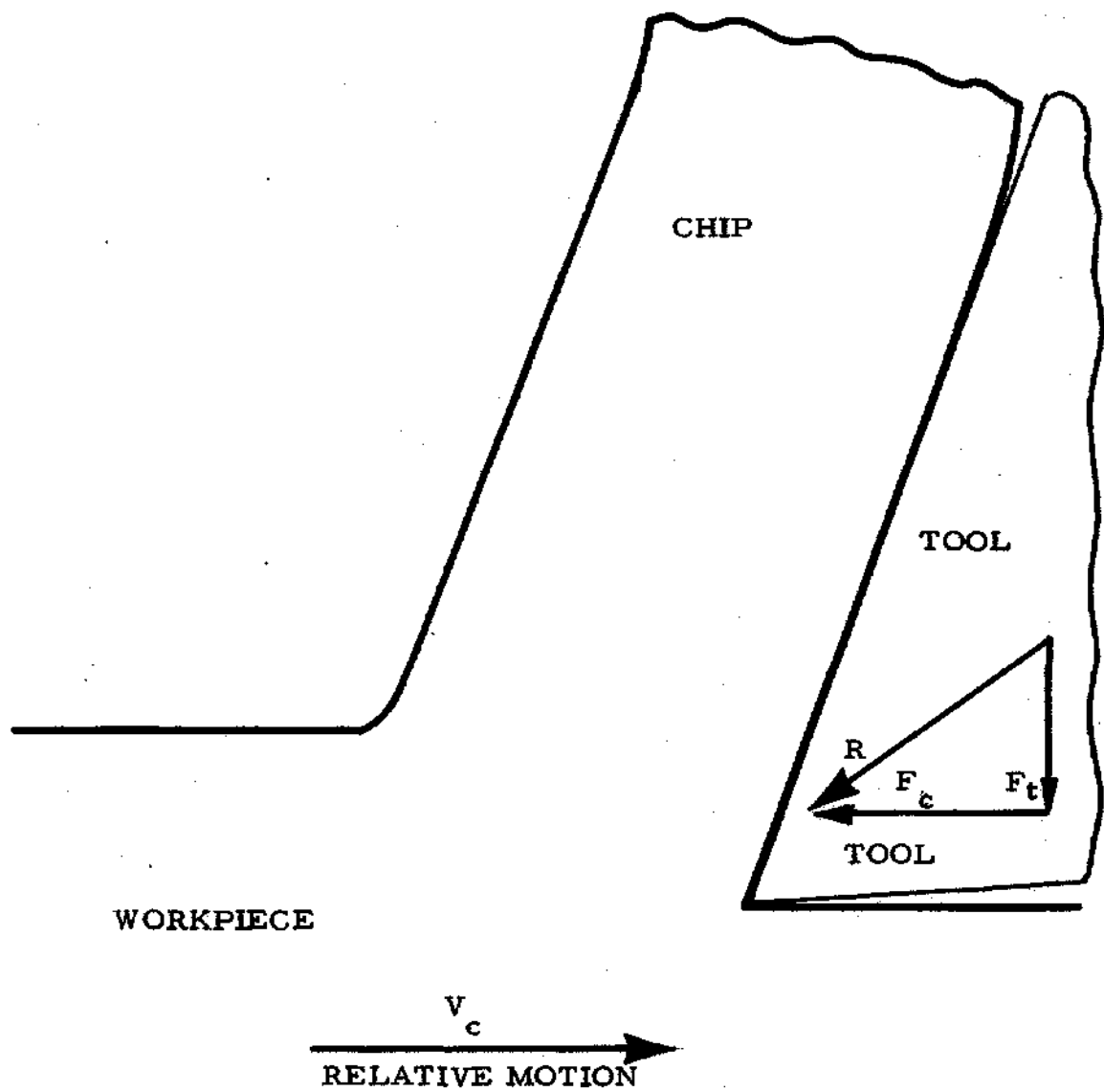


Figure 4. Characteristic Forces of Metal Cutting



Combining Equations (1) and (2) gives:

$$P_s = \frac{F_c}{w t_1} \text{ psi} \quad (3)$$

The specific cutting pressure can vary considerably for a given material and is affected by changes in cutting speed, tool rake angle, and undeformed chip thickness, at small values of  $t_1$ .

#### Mean Shear Strength of the Work Material

Figures 5 and 6 show the idealized model of the orthogonal metal cutting process where a continuous chip is produced with the absence of a built-up edge on the tool face. In this model the shear zone or primary deformation zone is represented by a plane, known as the shear plane. The angle of inclination of the shear plane, ( $\phi$ ), may be obtained from the expression:

$$\tan \phi = \frac{r_c \sin \alpha}{1 - r_c \cos \alpha} \quad (4)$$

where  $r_c$  is the cutting ratio and is given by:

$$r_c = \frac{t_1}{t_2} \quad (5)$$

In the experimental work, the tool rake angle ( $\alpha$ ) and the undeformed chip thickness ( $t_1$ ) are known. The chip thickness ( $t_2$ ) can be obtained by measurement with a ball ended micrometer or from the weight of a known length of chip.

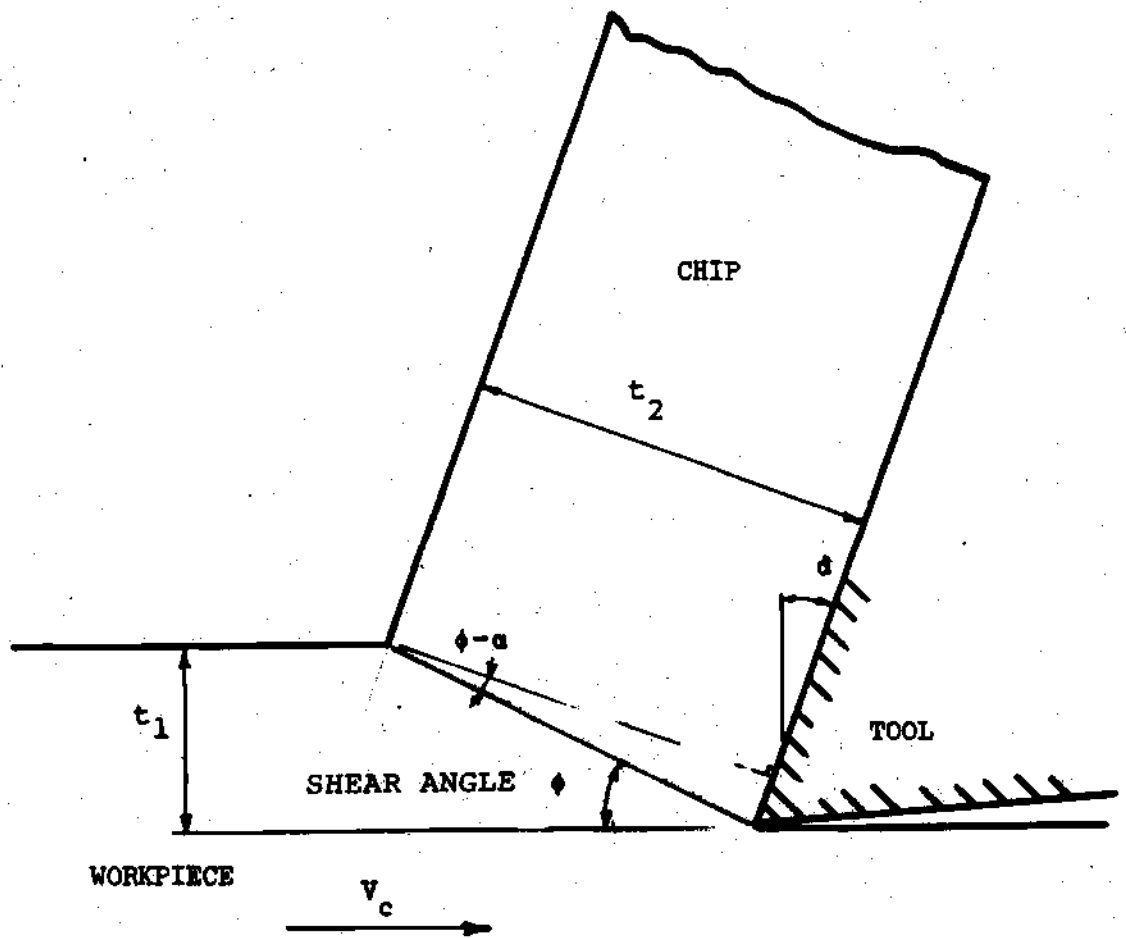


Figure 5: Model of Orthogonal Metal Cutting Process

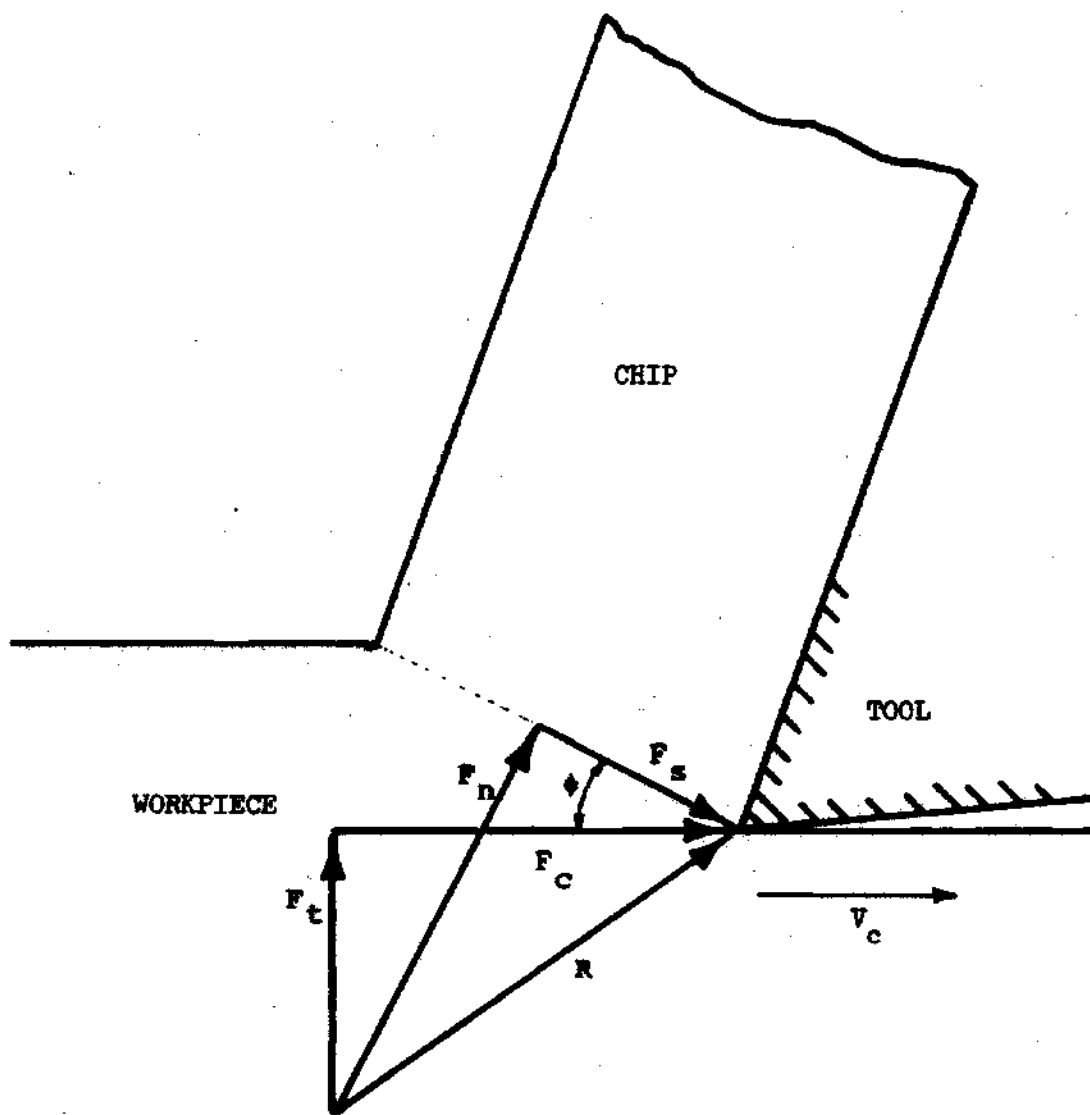


Figure 6: Cutting Forces in Orthogonal Cutting

If the resultant tool force is resolved in a direction parallel to the shear plane, the force  $F_s$  required to shear the work material to form the chip is obtained. This force may be expressed in terms of the cutting ( $F_c$ ) and thrust ( $F_t$ ) forces, the components of the resultant tool force resolved parallel to, and perpendicular to the direction of relative work-tool motion, respectively. From Figure 5 it can be seen that

$$F_s = F_c \sin \phi - F_t \cos \phi \quad . \quad (6)$$

The shear stress along the shear plane is given by the expression:

$$S = \frac{F_s}{w l_s} \text{ psi} \quad , \quad (7)$$

where  $l_s$  is the length of the shear plane.

From Equation (5) and Equation (6)

$$S = \frac{(F_c \sin \phi - F_t \cos \phi) \sin \phi}{w t_1} \text{ psi} \quad . \quad (8)$$

Much previous work has shown that  $S$ , calculated from Equation (8), remains constant for a given work material over a wide range of cutting conditions. However, it has been observed that  $S$  increases with a decrease in feed, ( $t_1$ ). This can be explained by the existence of a tool nose force,  $P$ . If  $P$  is subtracted from the resultant cutting force  $R$ , then the apparent shear strength of the work material remains constant with respect to changes in undeformed chip thickness. Thus, the apparent shear strength of the work material may be said to be constant and a property of the work material, and independent of cutting conditions.

### Chip Thickness

The chip thickness,  $(t_2)$ , is not defined by the geometry of the cutting tool and the undeformed chip thickness,  $(t_1)$ . It is in this respect that the cutting process differs fundamentally from other metal forming processes where the final shape of the deformed material is determined by the shape of the tool. It is this lack of control of chip thickness which has made analysis of the cutting process extremely difficult, since before any prediction of cutting forces can be made the chip thickness  $(t_2)$  must be known.

It can be seen from Equation (4) that a knowledge of chip thickness  $(t_2)$  will allow the shear angle  $(\phi)$  to be determined for a given set of cutting conditions. Experimentally, it has been found that the cutting ratio  $(r_c)$ , and hence the shear angle  $(\phi)$ , depend on the work and tool materials and the cutting conditions. A number of attempts have been made in the past to establish a relationship which can be used to predict the shear angle from a knowledge of  $t_1$  and  $t_2$ .

### Regions of Interest

The principal regions of interest in the orthogonal metal cutting process are illustrated in Figure 3. These are:

1. The primary deformation zone where the work material is continuously sheared to form the chip.
2. The tool nose region where the effect of friction between the tool flank and the newly generated workpiece surface and the ploughing effect of the tool edge are thought to combine to produce a force acting on the tool which does not contribute directly to chip production. (Tool

nose force.)

3. The secondary deformation zone where large chip-tool frictional forces can cause further deformation of the chip material.

Much of the published work on the mechanics of the metal cutting process has been concerned with deformation in the primary deformation zone. A number of analyses have appeared based on a "shear plane" model of the cutting process. The most important of these will now be considered.

### Review of Cutting Theories

#### Theory of Ernst and Merchant

The first complete analysis resulting in a so-called "shear angle solution" was presented by Ernst and Merchant<sup>1</sup>. The model of the cutting process used by these authors is shown in Figure 7. For convenience, the resultant tool force ( $R$ ) is shown acting at the tool cutting edge and is resolved into components  $\bar{N}$  and  $F$  in directions normal to and along the tool rake face, respectively, and into components  $F_n$  and  $F_s$ , normal to and along the shear plane, respectively. The cutting ( $F_c$ ) and thrust ( $F_t$ ) components of the resultant tool force are also shown. It is assumed that the entire resultant cutting force is transmitted across the chip-tool interface and that no force acts on the tool edge or flank (i.e., the tool nose force  $P$  is zero and the tool is perfectly sharp).

The basis of Ernst and Merchant's theory was the suggestion that the shear angle,  $\phi$ , would assume such a value as to make the work done per unit time in cutting a minimum. Since the work done in cutting is proportional to  $F_c$  it was necessary to develop an expression for  $F_c$  in

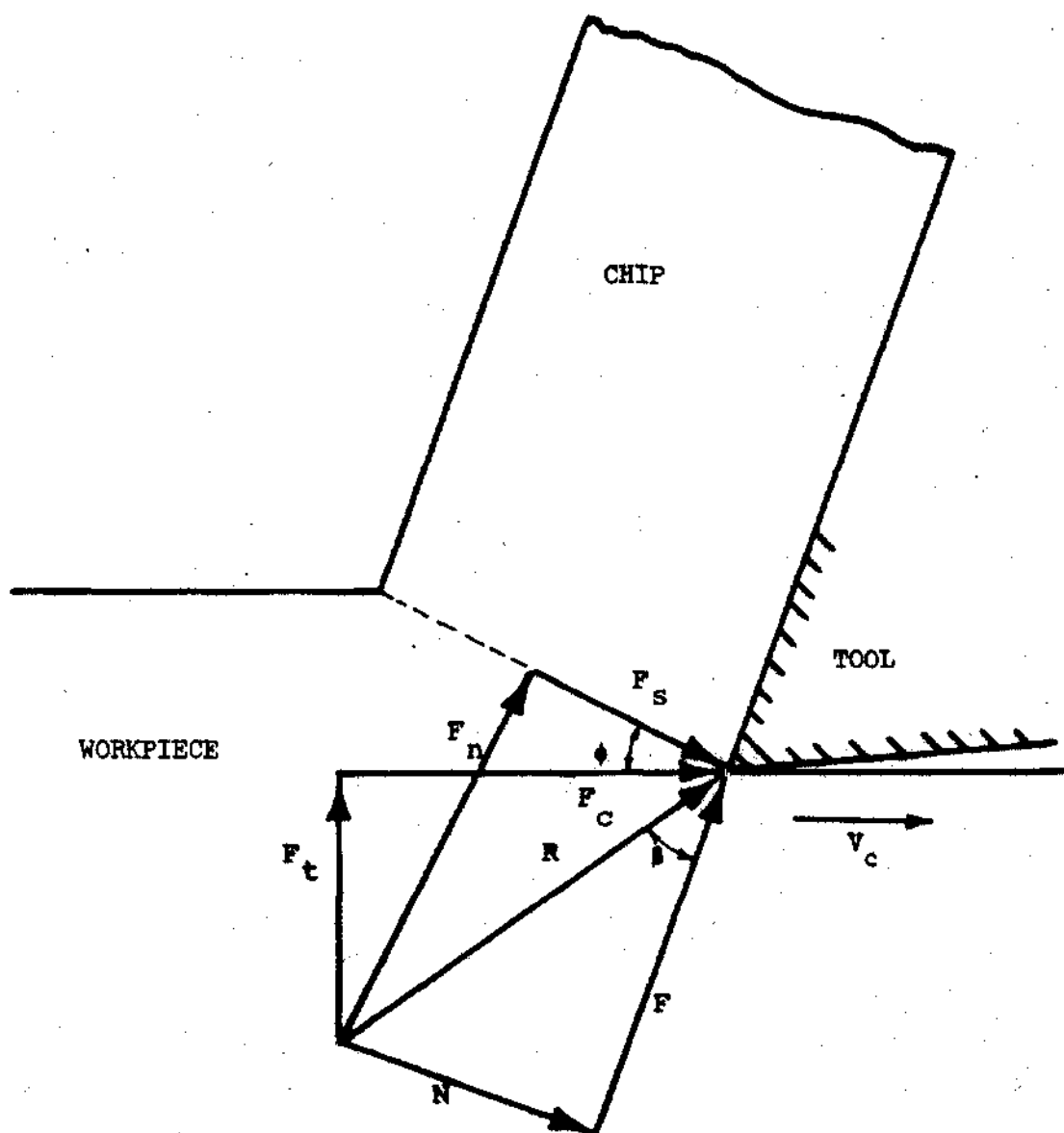


Figure 7: Ernst and Merchant Orthogonal Cutting Model<sup>1,2</sup>

terms of  $\phi$  and then to obtain the values of  $\phi$  for which  $F_c$  was a minimum.

It can be shown from Figure 5 that

$$F_c = \frac{S A_o \cos(\beta - \alpha)}{\sin \phi \cos(\phi + \beta - \alpha)} \quad (9)$$

where  $S$  is the shear stress on the shear plane,  $A_o$  is the cross sectional area removed during cutting,  $\beta$  is the friction angle,  $\alpha$  is the rake angle, and  $\phi$  is the shear angle. Equation (9) may now be differentiated with respect to  $\phi$  and equated to zero to find the value of  $\phi$  for which  $F_c$  is a minimum. The required value is given by:

$$2\phi + \beta - \alpha = 90^\circ \quad (10)$$

Merchant<sup>2</sup> found that this theory gave good agreement with experimental results obtained when cutting synthetic plastics but gave poor agreement for steel machined with a sintered carbide tool. In differentiating Equation (9) with respect to  $\phi$ , it was assumed that  $A_o$  and  $S$  would be independent of  $\phi$ . Merchant attributed the poor agreement between theory and experiment in the machining of steel to the fact that large normal stresses are transmitted across the shear plane and that these could affect the shear stress on the shear plane. Accordingly, Merchant included in a new analysis the relationship:

$$S = S_o + K S_n \quad (11)$$

where  $S_n$  is the normal stress on shear plane,  $K$  is a constant for the material, and  $S_o$  is the value of  $S$  when  $S_n$  is zero.



This indicates that the shear strength of the material increases linearly with increases in normal stress across the shear plane (Figure 8). The value of  $S$  is affected by changes in  $S_n$  and may be inserted in Equation (9) to give a new equation for  $F_c$  in terms of  $\phi$ , namely:

$$F_c = \frac{S_o A_o \cos(\beta - \alpha)}{\sin \phi \cos(\phi + \beta - \alpha) [(1-K) \tan(\phi + \beta - \alpha)]} \quad (12)$$

If it is now assumed that  $K$  and  $S_o$  are constants for the particular work material, and that  $A_o$  and  $\alpha$  are constants for the cutting operation, Equation (12) may be differentiated and equated to zero to give the new value of  $\phi$ . The resulting relationship is

$$2\phi + \beta - \alpha = C \quad , \quad (13)$$

where the machining constant ( $C$ ) is  $\cot^{-1}K$ , where  $K$  is the slope of Shear Stress versus Normal Stress curve, as shown in Figure 8.

#### Theory of Lee and Shaffer

The theory of Lee and Shaffer<sup>5</sup> was the result of an attempt to apply plasticity theory to the problem of orthogonal metal cutting. In dealing with problems in plasticity theory it is necessary to make certain assumptions regarding the behavior of the work material when deformed.

Some of these assumptions are:

1. The workpiece behaves as perfectly plastic material, i.e., it does not workharden and any elastic deformation can be neglected.
2. The material is rigid up to its yield point and the effects of variations in strain rate and temperature can be neglected.

These assumptions imply a stress-strain curve for the work material of

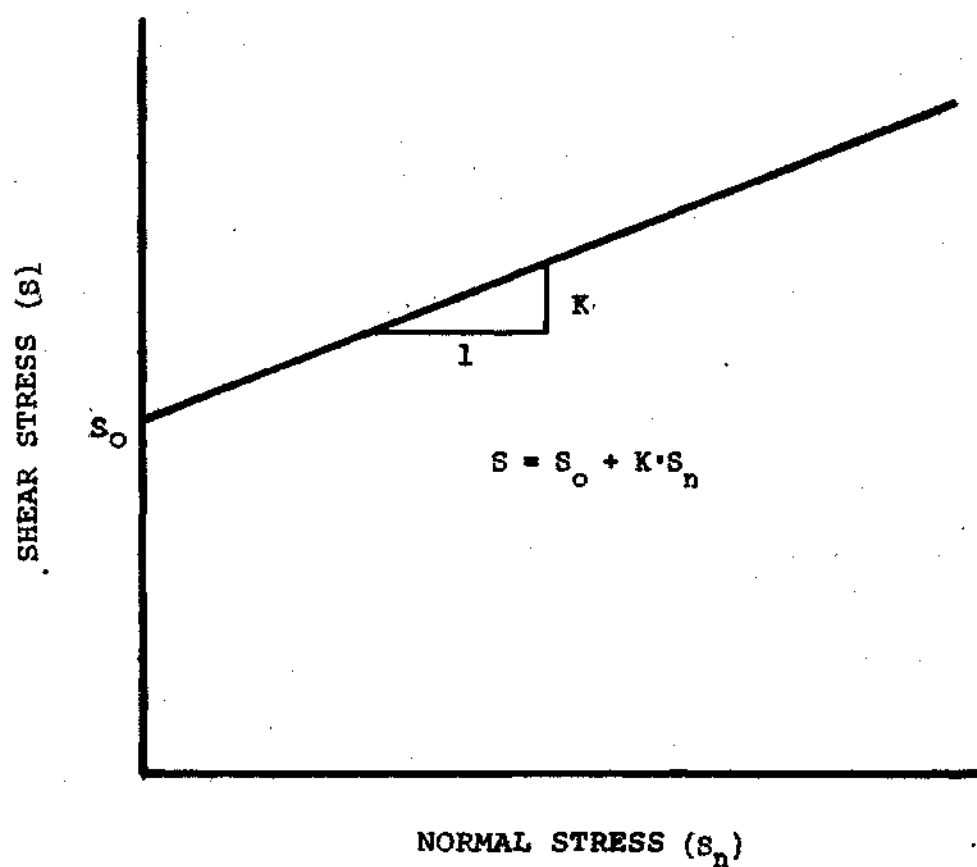


Figure 8: Shear Stress vs. Normal Stress on Shear Plane

the form shown in Figure 9, where the material undergoes no strain until the yield point is reached, when it yields at constant stress throughout the entire deformation process. Such assumptions have led to useful solutions of many problems in metal working.

It is known that the rate of workhardening of many metals decreases rapidly with increasing strain and that the effect of a high strain rate is to raise the yield stress of the metal with respect to its ultimate strength. Thus, with the high strains and strain rates known to exist in metal cutting, the material may approach the ideal plastic condition. Further, with the high plastic strains, the elastic strain would form a negligible proportion of the total strain. Thus, the stress-strain curve for the work material could approximate the ideal case shown in Figure 9.

In the solution of problems in plasticity, the construction of a slip line field is necessary; this consists of two orthogonal sets of lines (called slip lines) indicating, at each point in the plastic zone, the two orthogonal directions of maximum shear stress.

The slip line field proposed by Lee and Shaffer<sup>5</sup> for orthogonal cutting with the production of a continuous chip with the absence of a built-up edge on the tool face is shown in Figure 10. It can be seen that Lee and Shaffer have employed the idealized shear plane model of the cutting process where all the deformation takes place in a plane extending from the tool cutting edge to the point of intersection of the free surfaces of the workpiece and chip. From Figure 10 it can be shown that:

$$\phi + 45^\circ + \beta - \alpha = 90^\circ \quad , \quad (14)$$

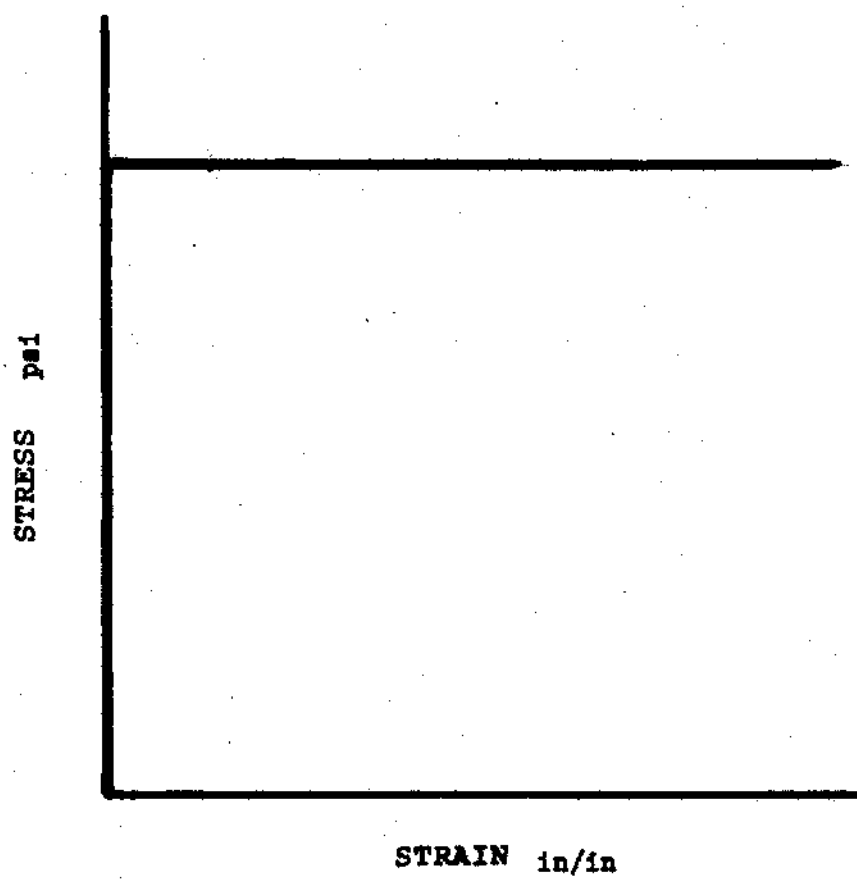


Figure 9: Ideal Plastic Stress-Strain Curve

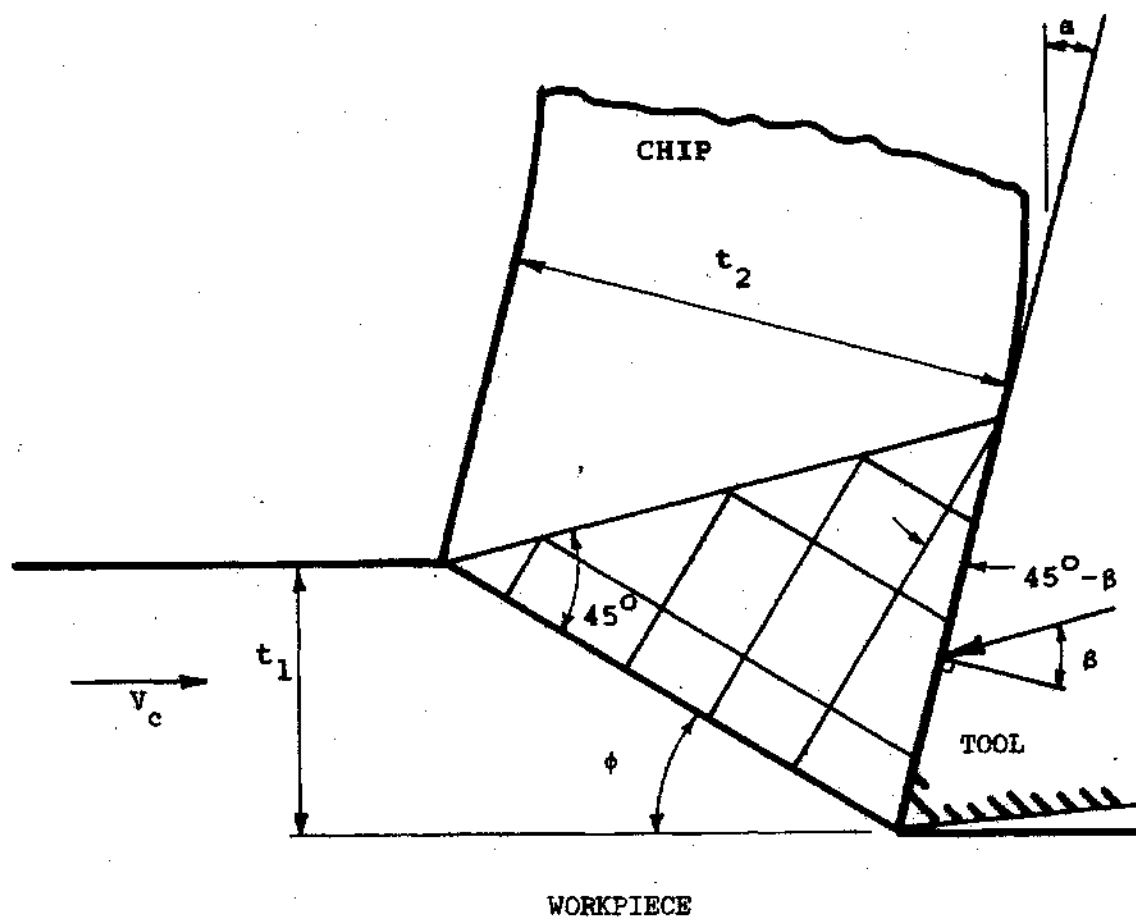


Figure 10: Lee and Shaffer Slip Line Field Solution

or

$$\phi + \beta - \alpha = 45^{\circ} \quad , \quad (15)$$

which is the required shear angle solution.

Lee and Shaffer<sup>5</sup> realized that Equation (15) could not apply where  $\beta$  is  $45^{\circ}$  and  $\alpha$  is  $0^{\circ}$  since with these values  $\phi$  would be equal to zero. The authors considered that conditions of high friction and low tool rake angles were those which could lead to the formation of a built-up edge. In order to account for this, a second solution<sup>5</sup> was presented with a new geometry in which a built-up edge was present on the tool rake face.

#### Other Shear Angle Theories

In addition to the theories of Ernst and Merchant<sup>1,2</sup> and Lee and Shaffer<sup>5</sup>, several other shear angle relationships have been developed. Huck<sup>6,8</sup> proposed the relationships:

$$\phi = 45^{\circ} - \omega + \alpha \quad (16)$$

and

$$\phi = \frac{1}{2} \cot^{-1} C - \beta + \alpha \quad , \quad (17)$$

where  $\omega$  is given by the expression

$$\omega = \frac{1}{2} \tan^{-1}(2\mu) \quad , \quad (18)$$

where  $\mu$  is the coefficient of friction and  $C$  is the machining constant.

Stabler<sup>7</sup> has proposed the relationship:

$$\phi = 45^\circ - \beta + \frac{1}{2} \alpha \quad . \quad (19)$$

Shaw, et al.<sup>9</sup> proposed that the shear plane was not the plane of maximum shear stress and suggested the relationship:

$$\phi = 45^\circ + \eta - \beta + \alpha \quad , \quad (20)$$

where  $\eta$  is the angle between the shear plane and the direction of maximum shear stress.

Oxley<sup>13</sup> developed a strain hardening model of chip formation (see also Figure 11 after Palmer and Oxley<sup>18</sup>) in which the shear angle is given by the equation:

$$\phi = \beta - \alpha - \theta \quad , \quad (21)$$

where

$$\theta = \tan^{-1} \frac{P_A + P_B}{2k} \quad , \quad (22)$$

and where  $P_A$  and  $P_B$  are the hydrostatic stresses at A and B and  $k$  is the shear stress along AB (Figure 11).

An important implication of the analysis of Oxley<sup>13</sup> and Palmer and Oxley<sup>18</sup> is the existence of a tensile stress at the nose of the tool and the extension of the plastic zone below the nose of the tool. Variable flow stress properties of the workpiece material were considered by Oxley<sup>33-37</sup> in an extensive analysis of a shear zone which was wide in proportion to its length. In these analyses estimates of the forces involved during cutting were made for various cutting speeds.

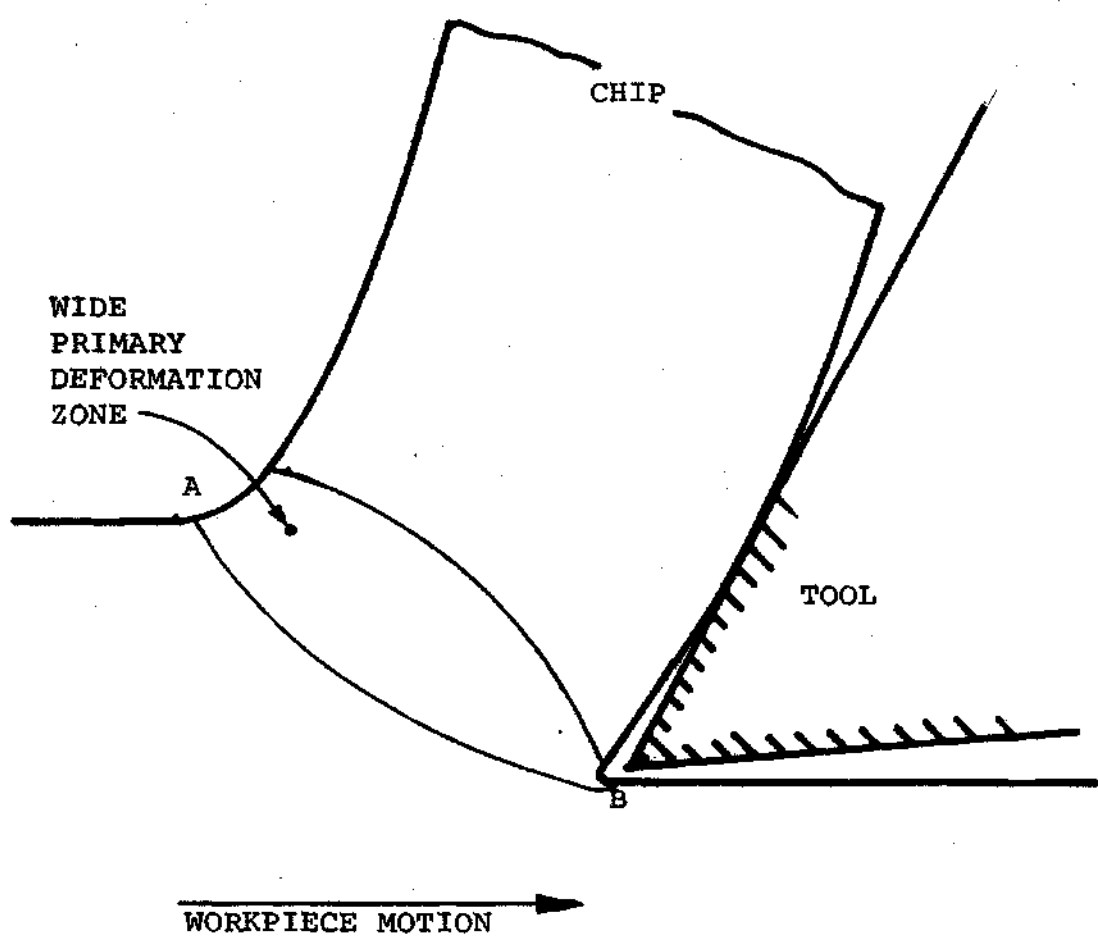


Figure 11: Palmer and Oxley Model



A minimum energy solution for the shear plane angle was developed by Rowe and Spick<sup>38</sup>; however, the simplifying assumptions involved provide little further advancement and the minimum energy criterion as applied to the metal cutting process is also open to question.

Several other shear angle relationships have been developed including those by Weisz<sup>6,10</sup>, Colding<sup>6,11</sup>, Sata and Mizuno<sup>6,12</sup>, Kullberg<sup>30</sup>, and Zorev<sup>14</sup>. A comparison of some of these has been made by Sata<sup>6</sup>.

#### Theory of Boothroyd

A new approach to the analysis of the mechanics of the orthogonal cutting process under unlubricated cutting conditions has been presented by Boothroyd<sup>24</sup> and Boothroyd and Bailey<sup>15</sup>. The assumptions made in this analysis were:

1. The apparent shear strength of the metal in the primary deformation zone is a constant for the material and is independent of the undeformed chip thickness, tool rake angle, cutting speed, and the work-hardened state of work material.
2. The deformation process is one of plane strain where the effect of side spread of the chip during its formation is neglected.
3. A continuous chip is produced with an absence of a built-up edge on the tool face.
4. The work material is a single phase metal whose behavior at high strains and at different strain rates and temperatures may be represented qualitatively by the curve shown for aluminum in Figure 12 (after Bailey)<sup>16</sup>.
5. The cutting process is not lubricated either by the application of a fluid or through the presence of inclusions of a lubricating nature

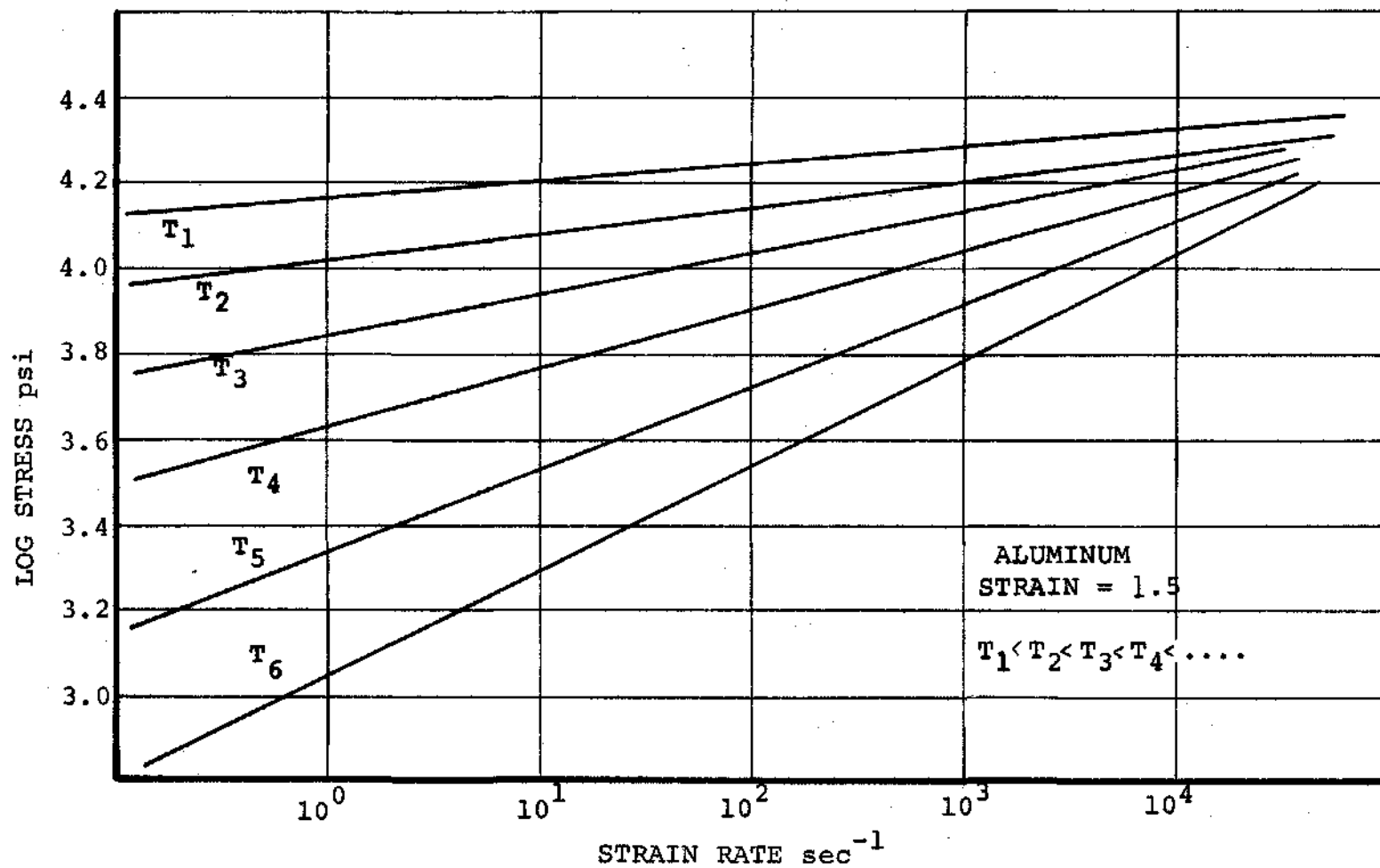


Figure 12: Stress, Strain Rate, Temperature Relationship For Aluminum<sup>16</sup>

in the workpiece.

From a force analysis of the model<sup>15</sup> it was shown that the dimensionless stress ratio,  $\frac{S_s}{S_o}$ , was given by the expression:

$$\frac{S_s}{S_o} = \frac{(1 + \tan \psi) \tan(\gamma - \alpha) - (1 - \tan \psi)}{1 + \tan^2(\gamma - \alpha)}, \quad (23)$$

and the ratio  $\frac{S_f}{S_o}$  by:

$$\frac{S_f}{S_o} = \frac{(1 + 2 \tan \psi) \tan \beta}{1 + 2 \tan \beta - \tan \alpha}, \quad (24)$$

where  $\beta$  is the mean angle of friction and the remaining angles are defined in Figure 13; the stress  $S_s$  is the shear stress along the line AB in Figure 13 and is that stress obtained at a high strain rate for a highly strained material; the stress  $S_o$  is the shear stress along line BE obtained at much lower strain rate; the stress  $S_f$  is the shear stress along the tool rake face and may be higher, lower, or equal to the shear stress ( $S_o$ ) on line BD.

From cutting test data on 85-15 Brass,  $\frac{S_s}{S_o}$  was found to be a constant for the work material and independent of changes in rake angle or cutting speed. The ratio  $\frac{S_f}{S_o}$  was found to vary with rake angle and cutting speed and was controlled by the conditions of strain rate and temperature at the tool rake face.

#### Critique of Existing Work

Two of the shear angle solutions outlined above have been compared with the results of independently conducted experiments<sup>17</sup>. Figure 14



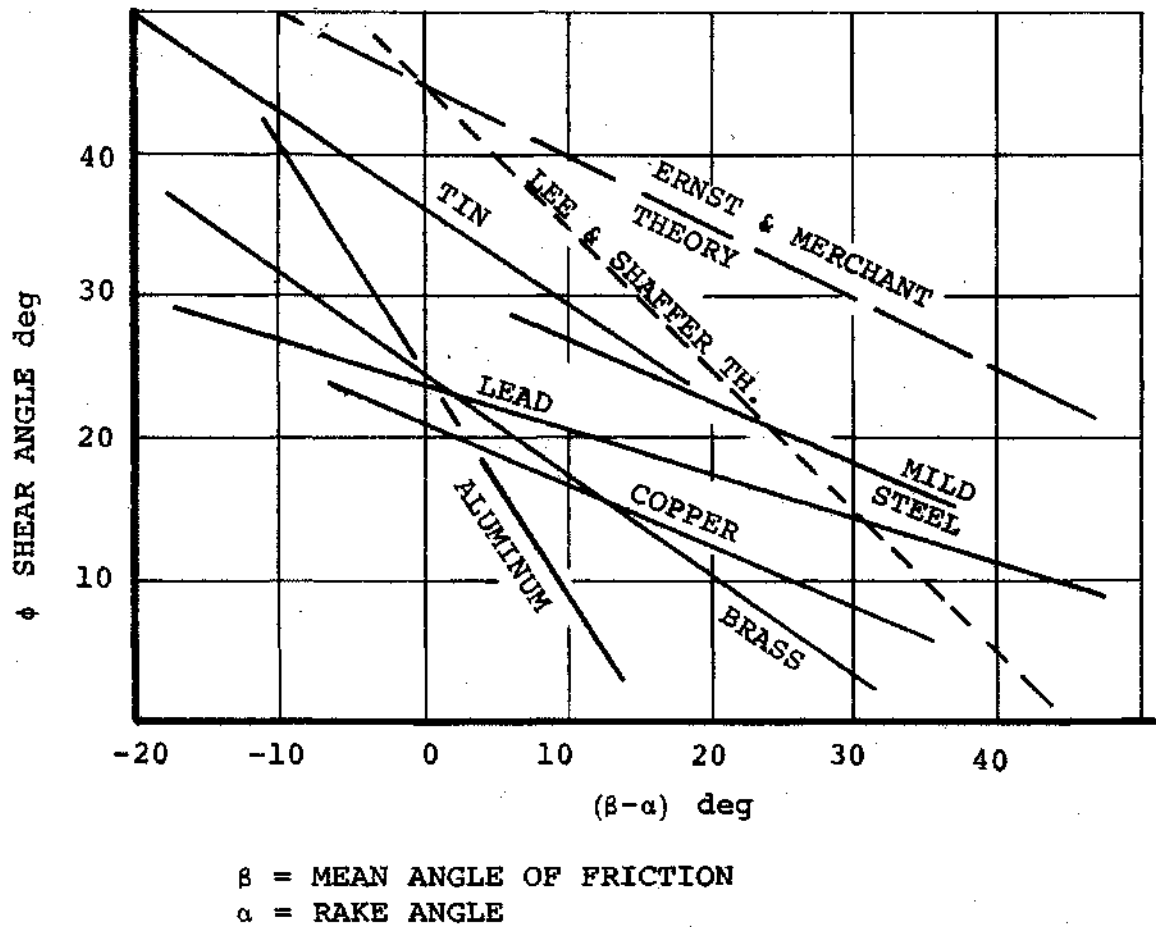


Figure 14: Some Theoretical and Experimental Shear Angle Relationships

shows the most convenient way of making such comparisons; the shear angle  $\phi$  is plotted against the difference between the friction angle and the rake angle; i.e.,  $(\beta - \alpha)$ . On such a graph, the relationships obtained by the Ernst and Merchant and by the Lee and Shaffer theories form straight lines. It can be seen that neither of these theories approach quantitative agreement with any of the experimental relationships for the various materials tested. However, comparing them in a qualitative sense, both the theories and the experimental results show that a linear relationship exists between  $\phi$  and  $(\beta - \alpha)$  and that a decrease in  $(\beta - \alpha)$  always results in an increase in  $\phi$ . For a given rake angle a decrease in the mean friction angle on the tool rake face results in an increase in the shear angle. Since the mean shear strength of the work material along the shear plane is approximately constant, the force required to form the chip will be reduced and a corresponding reduction in shear plane length will occur.

The results plotted in Figure 14 shows that no unique relationship of the kind predicted by the Ernst and Merchant<sup>1</sup> and by the Lee and Shaffer<sup>5</sup> theories could possibly agree with all the experimental results. Even the modified Merchant theory<sup>2</sup> in which the shear stress on the shear plane is assumed to be linearly dependent on the normal stress could not agree with all the results. Substituting various values for the machining constant in Equation (13) could only give a series of parallel lines on the graph in Figure 14. Clearly, the experimental lines are not parallel and could not all be represented by Equation (13). It is for this reason that other attempts have been made to develop machining constants for individual materials; usually they have met with little success.

Recent work<sup>18,19</sup> has also shown that the range over which the

primary deformation zone can be regarded as a shear plane is not as large as it had been thought previously. For example, Palmer and Oxley<sup>18</sup> used motion pictures to observe the flow of grains in a steel workpiece during slow speed cutting. Their investigation showed that the primary deformation zone had the form shown in Figure 11. Work by Nakayama<sup>19</sup> has also shown the primary deformation zone to be wide and to have constant proportions for cutting speeds of up to 500 feet per minute. In these experiments the side of the workpiece was coated with lamp black and a series of lines were scribed on the prepared surface parallel to the cutting direction. During cutting, these lines formed stationary material flow lines and could be photographed. From the resulting photographic records it was possible to plot the boundaries of the primary deformation zone.

The above shear angle theories and the experimental results indicate that the friction on the tool rake face is a most important parameter in metal cutting, and in virtually all the theories produced to date the simplifying assumption has been made that frictional condition on the tool face can be represented by a single parameter, the mean angle of friction  $\beta$ .

The theory proposed by Boothroyd and Bailey<sup>15</sup> does have direct application to the machining of 85-15 Brass and to a certain degree predicts the geometry and forces of cutting for that one material. However, when application to the machining of aluminum was attempted by this author, unsatisfactory results were obtained. Certain other limitations in previous analyses have been observed, namely:

1. Most authors completely neglect secondary deformation.

2. Under certain cutting conditions the secondary deformation zone extends below the tool nose into the workpiece<sup>18</sup>.

3. A velocity flow diagram of most of the previously defined models is inconsistent. It is not reasonable to expect material to change its direction of motion instantaneously as it passes the shear plane. In this respect the analyses by Boothroyd and Bailey<sup>15,24</sup> and Oxley<sup>34-37</sup> are definite advancements over the shear plane type analyses.

4. The normal stress on plane BE of the Boothroyd model is not necessarily small and for materials which exhibit large secondary deformation zones may be large.

5. A velocity flow diagram of the Boothroyd model in the secondary deformation zone is inconsistent.

Thus, it is evident that an improved model of the orthogonal metal cutting process is needed.



## CHAPTER III

### EXPERIMENTAL PROCEDURE

#### Introduction

An aluminum (1100 - 0) tube was orthogonally end-machined on a lathe using a two component, strain gage, cutting force dynamometer. The dynamometer output was amplified and recorded on a two-channel pen recorder. The undeformed chip thickness was measured with a ball-end micrometer and verification made by weighing a known length of chip and neglecting the small amount of side spread of the chip. The tool rake angle was varied through use of replaceable HSS tool inserts rigidly mounted in the dynamometer. The rake angle was measured with a tool maker's microscope. Tools were ground with a small tool and cutter grinder.

#### Equipment

The design of the metal cutting dynamometer used in these experiments is based on one described by Boothroyd<sup>47</sup>. Improvements were made in the method of supporting the tool and in the strain gage Wheatstone Bridge arrangement. The dynamometer tool holder was so designed that it supported a 3/8-inch square HSS tool at a 45 degree angle from the vertical. The tool was held rigidly against the dynamometer by two set screws which were recessed into the toolholder. Tools of various rake angles were produced by grinding the tool surface inclined from the horizontal at the appropriate rake angle. An appropriate flank relief angle of five degrees was ground on each tool. The tool and the functional por-

tions of the dynamometer are shown in Figure 15.

Strain gages were mounted on the horizontal and vertical struts of the dynamometer in such a manner as to negate the effects of bending of the strut and give a change of resistance proportional to compressive stress within the strut. Temperature compensation was accomplished by mounting strain gages on the reverse side of each strut perpendicular to the direction of loading. These compensating gages also increased the sensitivity of the dynamometer by adding the effect of the strain due to Poisson's ratio to the net effective difference in resistance across the measuring terminals of the Wheatstone bridge. The position of the strain gages on the struts and in the Wheatstone bridge was such that a variation in the position of the tool and consequent change of moment resisted by the dynamometer did not affect the bridge output. A layout of gage positions and a schematic diagram of gage placement in a Wheatstone bridge for one component of the forces of cutting is shown in Figure 16.

A sketch of the set-up used on the 15" x 60", 5 horsepower, variable speed Cincinnati lathe is shown in Figure 17. The output of the dynamometer was amplified by a Sanborn Model 366-1100-B carrier preamplifier and recorded on a Sanborn Model 296 dual-channel recorder. The gain of the preamplifier was adjusted so that a 1 volt change across each bridge resulted in a 30 mm. deflection of the associated recorder pen.

Calibration of the dynamometer was accomplished by a dead weight loading technique and showed excellent linearity and very little inter-channel interaction for the dynamometer-recorder system. This procedure has been described in the literature<sup>47</sup>.

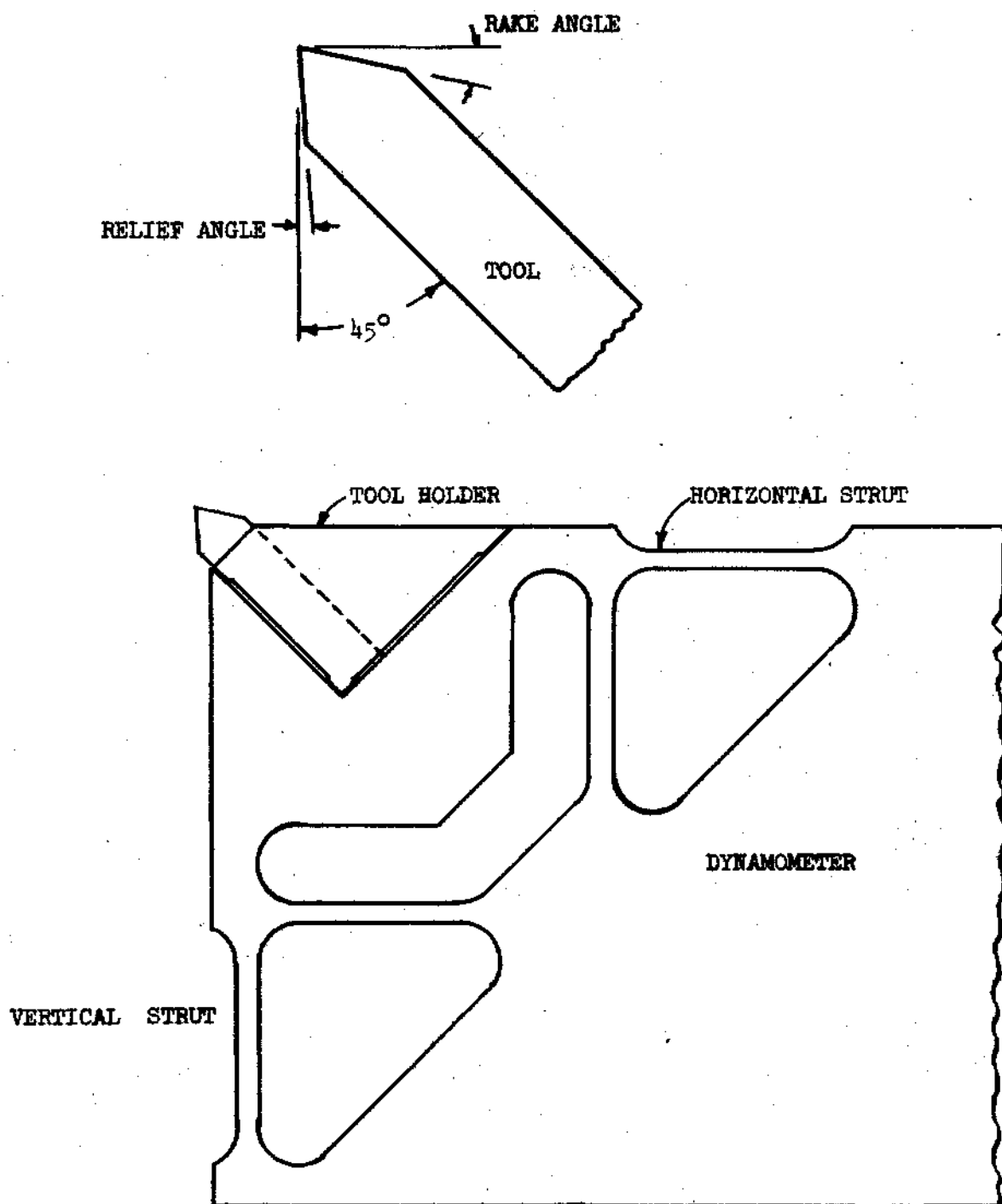
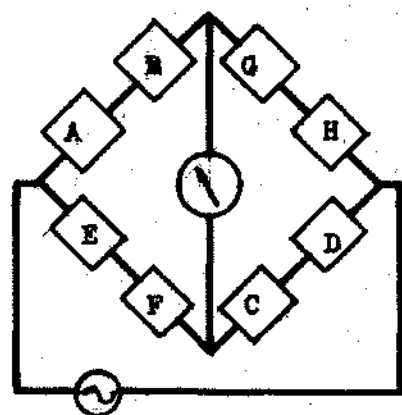
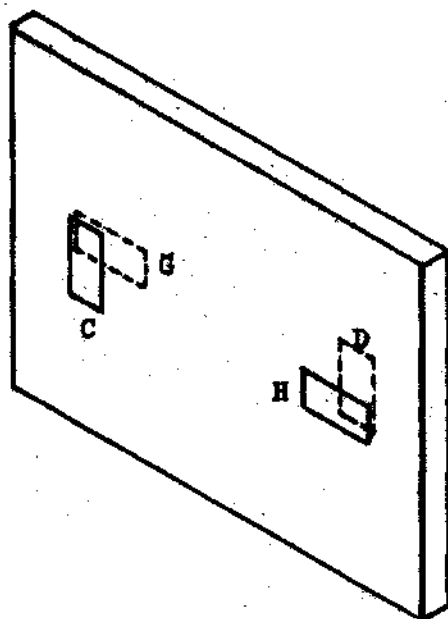
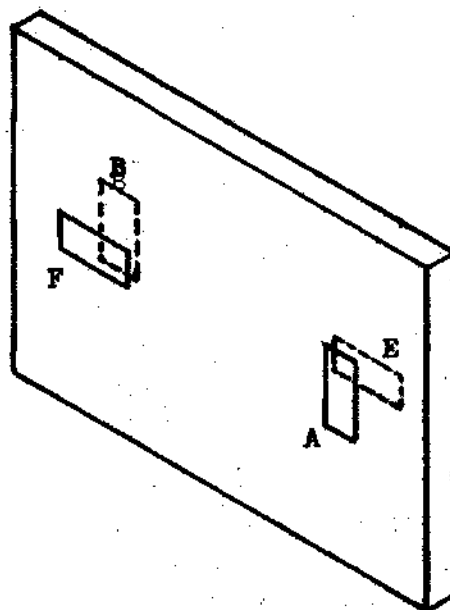


Figure 15: Dynamometer Configuration.



SCHEMATIC



ACTIVE  
STRAIN  
GAGES

A  
B  
C  
D

COMPENSATING  
STRAIN  
GAGES

E  
F  
G  
H

Figure 16: Strain Gage Layout and Schematic for  
Vertical Force Component of Dynamometer

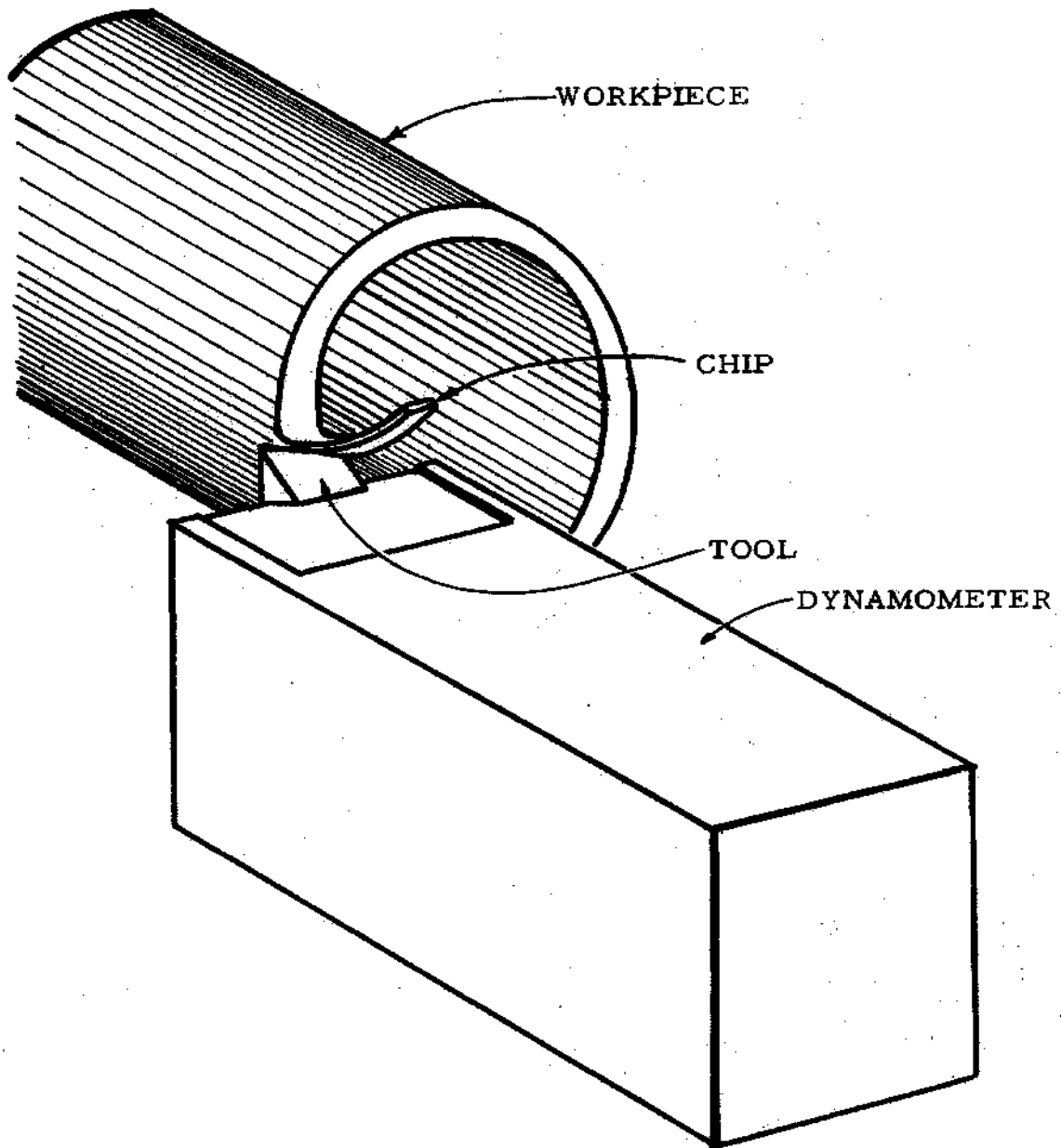


Figure 17: Workpiece With Dynamometer

### Procedure

Orthogonal machining was realized by end machining a 3 inch outside diameter tube with a 0.28 inch wall thickness. The tube was produced by machining a solid aluminum billet to the required dimensions in the Cincinnati lathe. The cutting tests performed were chosen to cover the entire range of cutting conditions possible within the material and equipment limitations. An undeformed chip thickness of 0.0202 inches was chosen because this was the minimum value which would give good delineation between the cutting and thrust force for a variety of cutting speeds.

The maximum cutting speed was 480 SFPM because higher speeds required more power than the lathe motor could provide. The minimum cutting speed was 80 SFPM because the chip produced at lower speeds tended to be discontinuous or irregular with a built-up edge.

The maximum rake angle was 45 degrees. To exceed this would seriously weaken the tool and result in direct rubbing contact between the chip and the toolholder leading to extraneous dynamometer output and negation of the experimental results. The minimum rake angle used was approximately 20 degrees. Results of the tests with this rake angle are questionable because of irregularities in chip thickness and the presence of an unstable built-up edge on the rake face. The results of these tests will be included in the analysis, however, in spite of the questionable continuity of cutting conditions. Therefore, variations of results of this rake angle with predictions of the model may be expected. Nominal rake angles of 20, 25, 30, 35, 40, and 45 degrees and velocities of 80, 120, 160, 240, 320, and 480 SFPM were used in the work. Cutting

speeds in SFPM were determined from the product of the average circumference of the tubular workpiece and the angular velocity of the lathe as measured by the lathe tachometer. The recorded experimental data of this series of orthogonal metal cutting tests were the cutting and thrust forces and the chip thickness. Smoothed values of these results are tabulated in Table 2 (shown in Appendix I) where an averaging of several test points was made in order to prevent excessive experimental error.

A series of controlled contact length experiments was also performed in order to ascertain the magnitude of the tool nose forces. The tool nose forces result from the ploughing effect of the tool and friction between the tool flank and freshly machined workpiece surface. The controlled contact length resulted in a similar geometry of cutting for a variety of undeformed chip thicknesses when the ratio of contact length to undeformed chip thickness was maintained constant. Tool nose forces were calculated by extrapolating the total cutting tool forces to zero undeformed chip thickness.

Typical results of this investigation for a single set of cutting conditions are shown in Figures 18 and 19. These figures indicate that the tool nose force (as determined by the zero undeformed chip thickness) is of sufficiently small magnitude to neglect its effects when performing cutting tests with a  $t_1$  value greater than 0.020 inches. (Sufficiently small magnitude being less than the resolution of the pen recorder for the thrust force, i.e., 1/2 mm or 10 pounds thrust force, or 10 percent of the cutting force).

A determination of the microhardness distribution of a suddenly stopped chip specimen was also made and is shown in Figure 20. The iso-

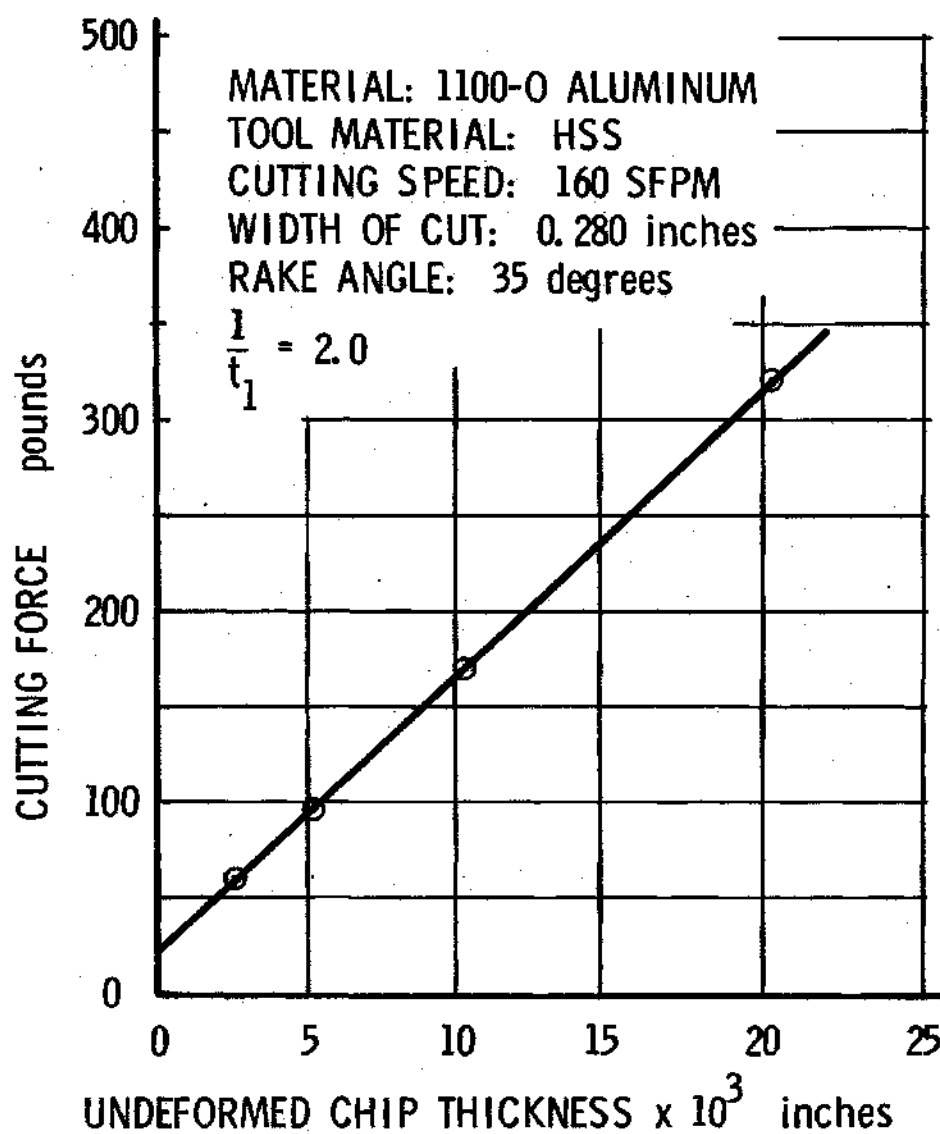


FIGURE 18: CUTTING FORCE vs. UNDEFORMED CHIP THICKNESS



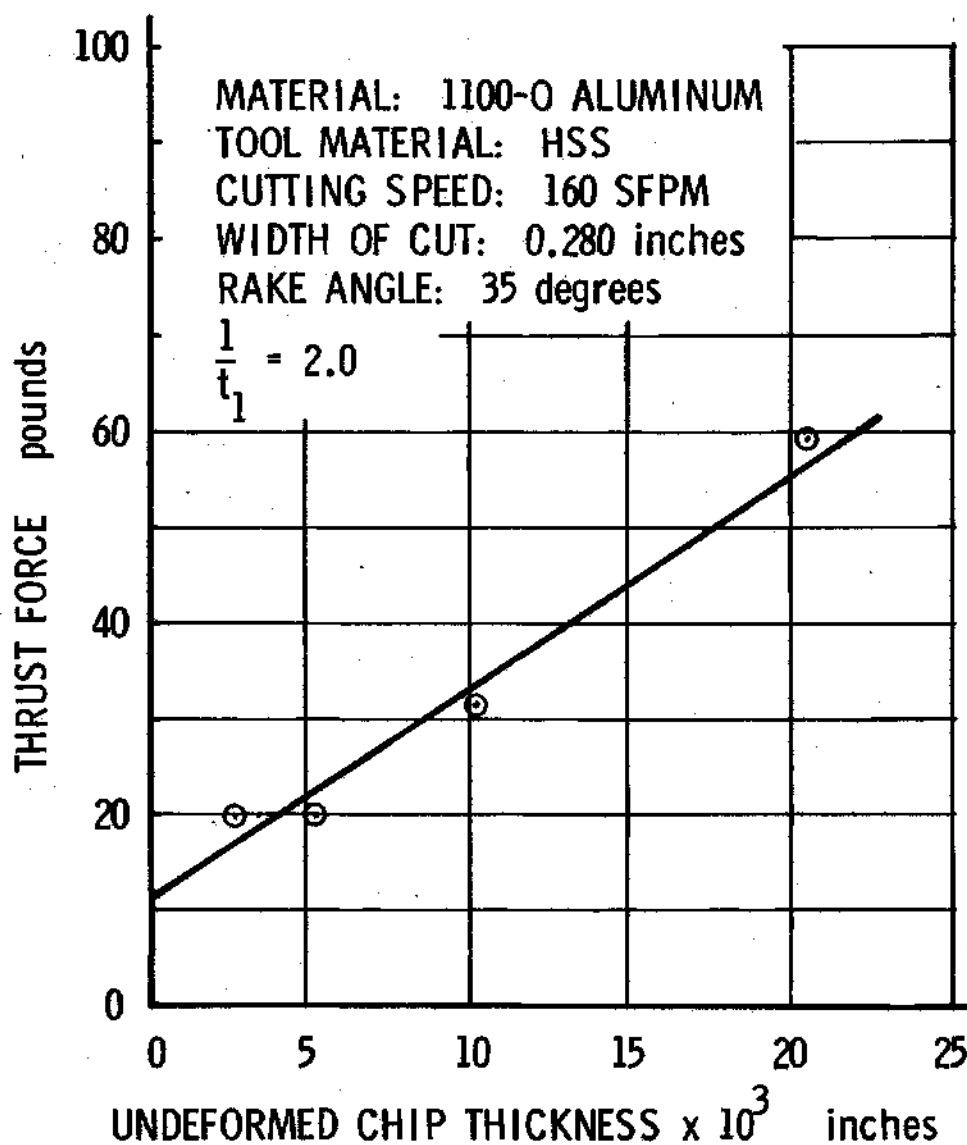


FIGURE 19: THRUST FORCE vs. UNDEFORMED CHIP THICKNESS

MATERIAL: 1100-O ALUMINUM  
TOOL MATERIAL: HSS  
CUTTING SPEED: 40 SFPM  
RAKE ANGLE: 30 DEGREES  
UNDEFORMED CHIP THICKNESS: 0.0202 INCHES

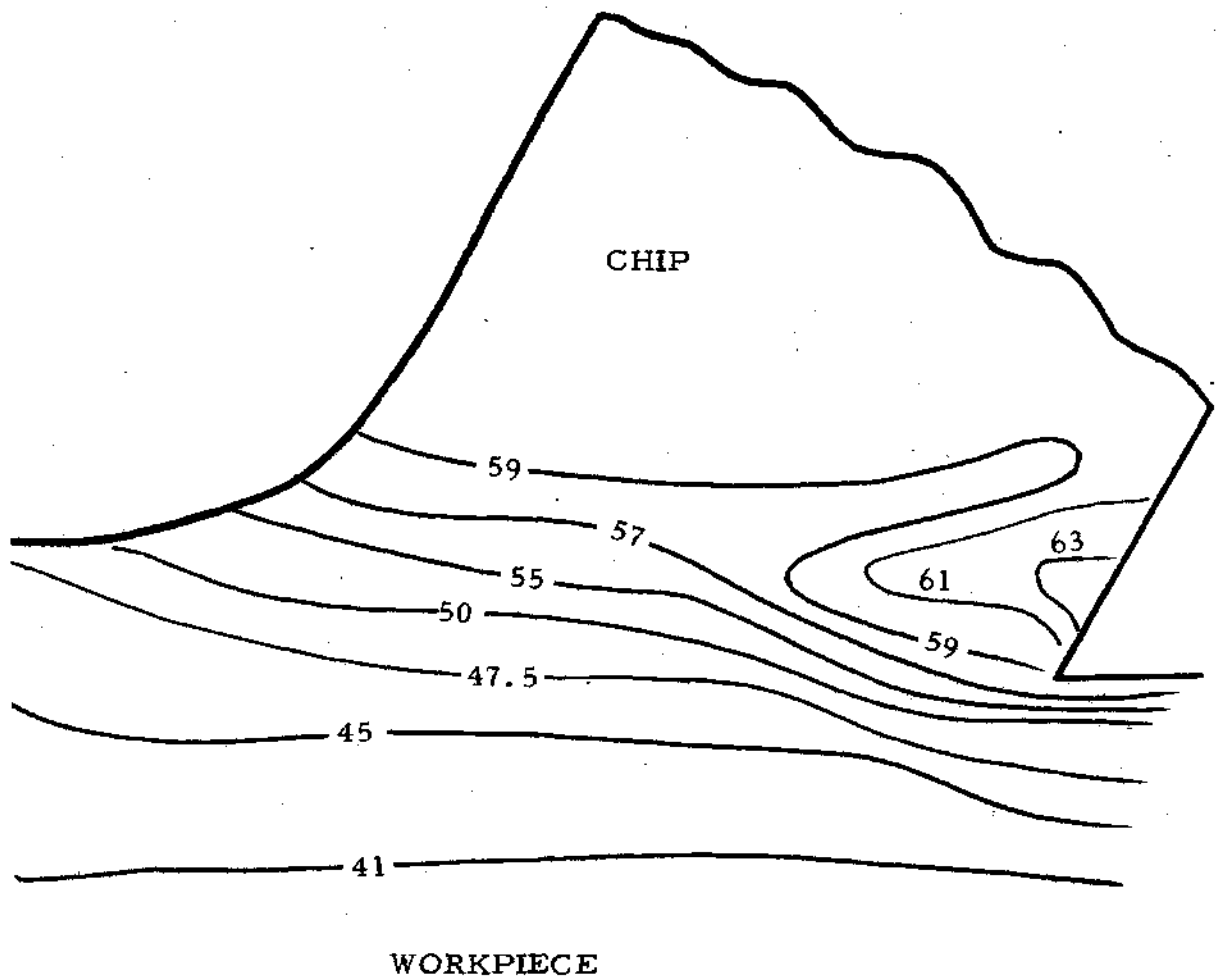


Figure 20: Microhardness Distribution of Suddenly Stopped Chip Sample

grams of equal microhardness give an indication of the amount of workhardening which has occurred at any specific point. The key quantitative results of the investigation are that the material has been workhardened (therefore deformed) below the freshly machined workpiece surface well ahead of the nose of the tool and that workhardening due to secondary deformation has occurred along the chip-tool interface.

A representation of typical flow lines discernable in a suddenly stopped chip sample which has been polished and etched is given in Figure 21. A photomicrograph of this deformation did not give a sufficiently distinct image to be of value.

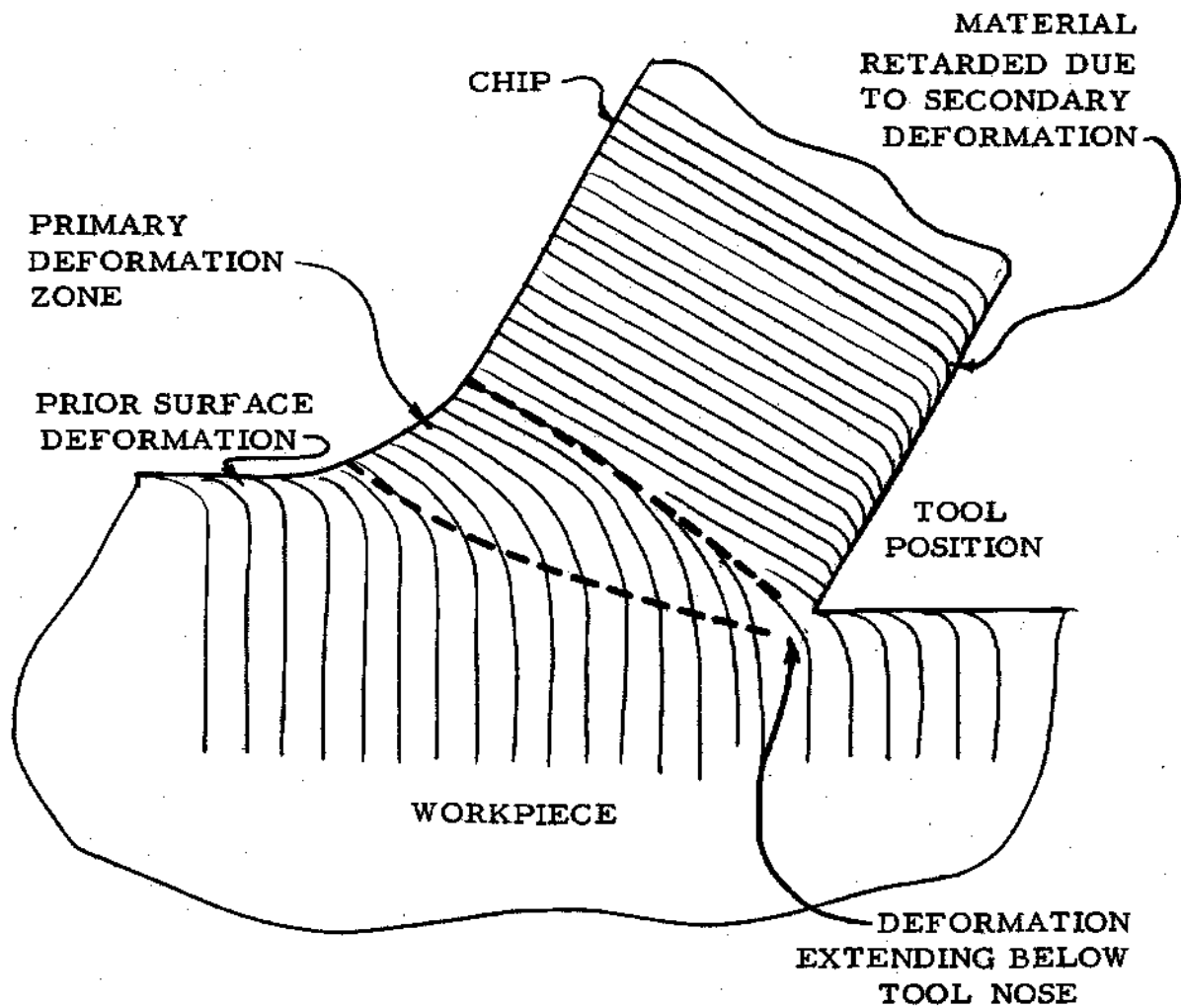


Figure 21: Typical Flow Lines Observed in a Suddenly Stopped Chip Sample

## CHAPTER IV

### MODEL DESCRIPTION

#### Introduction

The physical phenomena which occur during the orthogonal metal cutting process are extremely complex. An exact mathematical analysis would require a large number of variables and generally would not be feasible from an engineering viewpoint. Furthermore, the validity of such an analysis would be questionable because the primary criteria available to verify the sum total of all assumptions would be the applicability and accuracy of the model in predicting such parameters as tool forces and cutting geometry for a wide range of cutting conditions. Albrecht<sup>22</sup> stated this principle in the form that the predictability of a model of the metal cutting process increases as the simplicity of the model decreases (the predictability approaching 100 percent as the number of factors considered becomes very large).

The following analysis is a compromise between simplicity and the need for an accurate model as measured by its applicability and the requirement that material deformation occur in a reasonable and logical manner. The deciding criteria for any assumption therefore is that it be reasonable in light of known characteristics of the material and the flow of metal during the orthogonal metal cutting process. The proposed analysis will include most of the important characteristics enunciated by Shaw<sup>23</sup> with the exception of the condition where the built-up edge

occurs, which is usually present only at low cutting speeds and rake angles.

### Proposed Model

The proposed model of the orthogonal metal cutting process is shown in Figure 22. The following initial assumptions are made:

1. The deformation process is one of plane-strain, where the effects of side spread of the chip material during deformation are negligible.

2. A continuous chip is formed and no built-up edge exists on the tool rake face.

3. The work material is a single phase metal whose behavior at different strains, strain rates, and temperatures may be represented by an equation of the form

$$\sigma = \sigma_0 G^T e^{(A+BT)} e^{(C+DT+F[\ln s]T)} \quad (24)$$

which is similar to that proposed by Lubahn<sup>21</sup>.

4. The cutting process is unlubricated, either by the application of a fluid or through the presence of inclusions in the workpiece of a lubricating nature.

In order to perform the analysis, the region in which the chip is formed was divided into several zones for convenience. These zones are as follows (see Figure 22):

1. The zone CGBEA, which is an approximation to the primary deformation zone as it actually occurs in the machining process, zone CGBEA, is divided into two portions by line AB.

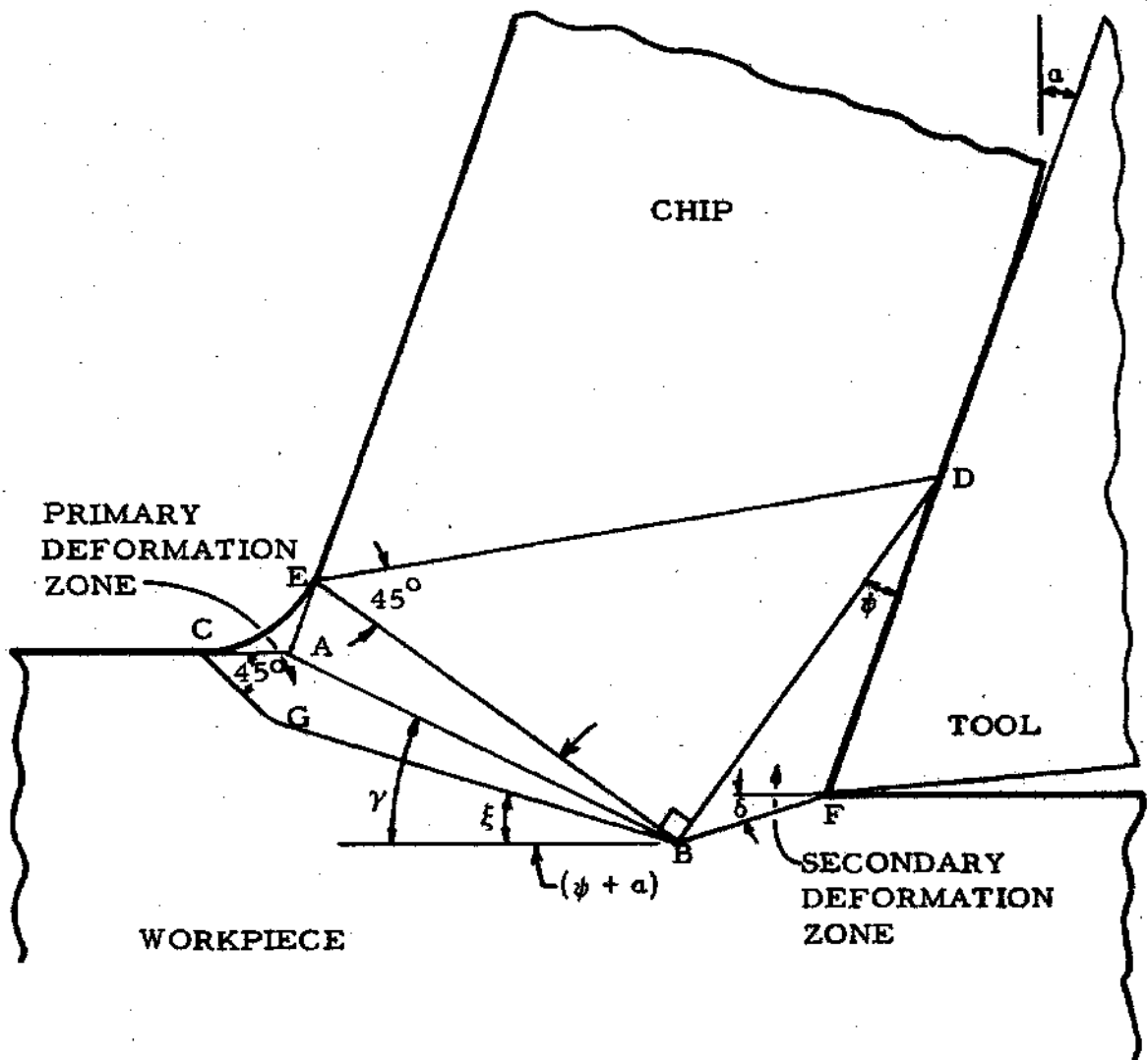


Figure 22. Developed Model of Orthogonal Metal Cutting Process

2. The zone EDB through which stresses are transmitted to the primary deformation zone, but where no deformation occurs.

3. The zone BDF which is an approximation to the secondary deformation zone as it actually occurs and where the chip material is subjected to further deformation due to the high normal and shear stresses at the chip tool interface.

The stresses acting on these individual zones are shown in Figures 23 and 24.

The behavior of the work material as it passes through the various zones is assumed to be as follows.

#### 1. Primary Deformation Zone - CGBEA

Plastic deformation begins at the boundary CGB as the material approaches the cutting tool. The shear stress along CGB is a constant for the workpiece material and is denoted by  $S_i$ , the initial shear strength of the work material. Plane CG intersects the free surface of the undeformed workpiece at  $45^\circ$ , at point C. The shear and normal stresses on plane CG are assumed to be of equal magnitude and plane BG is assumed to be of a length equal to that of plane AB. (This may be in slight error but a 10 percent change in the length of plane BG was found to have a negligible effect on the resulting model geometry.)

After crossing surface CGB the material is deformed by a process of shear at a rapidly increasing rate until it reaches the plane AB, which is assumed to be the plane of maximum shear stress and shear strain rate. The stress along plane AB will be dependent upon the strain, strain rate, and temperature in the primary deformation zone



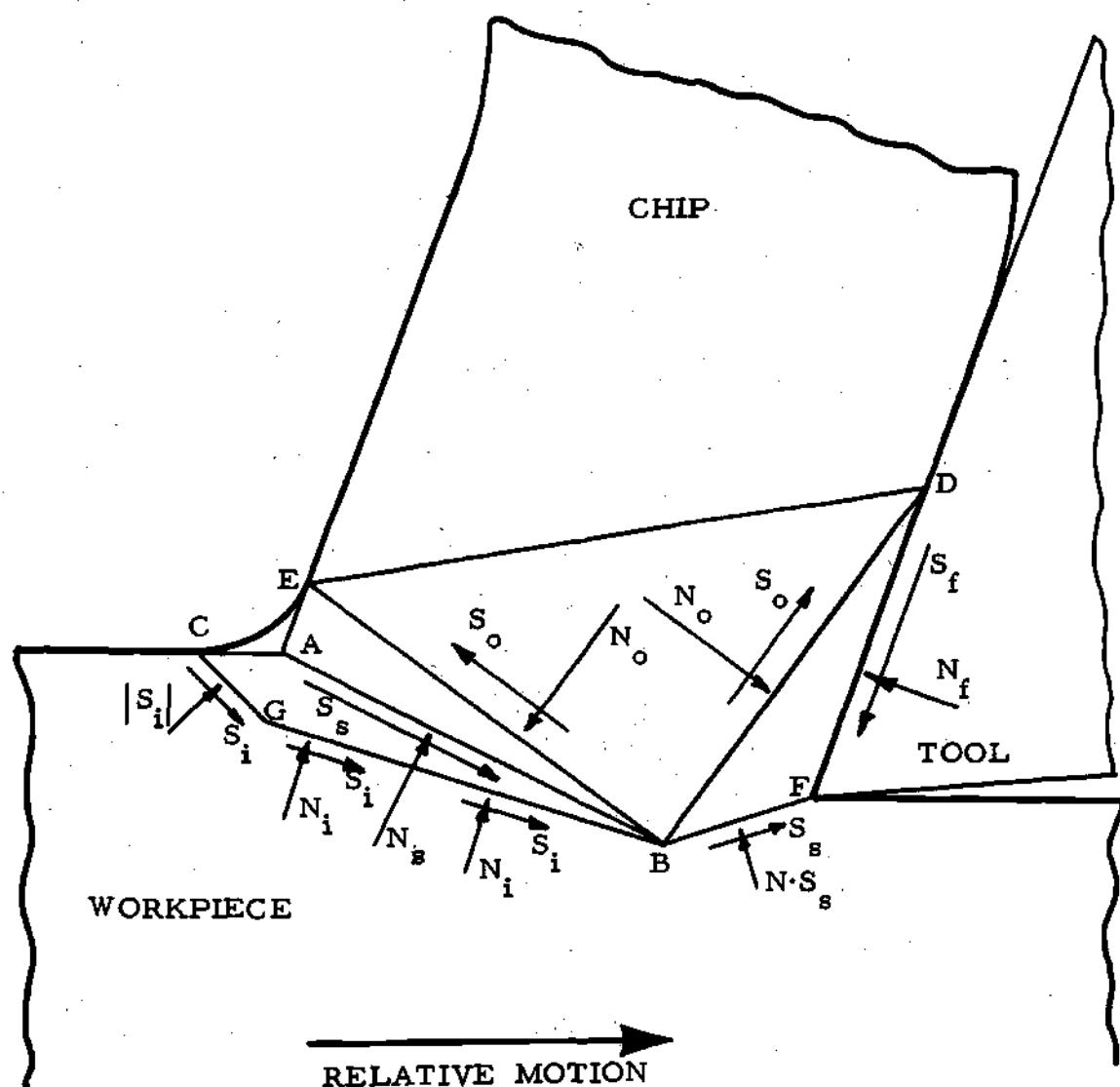


Figure 23: Model with Stresses Shown on Applicable Planes

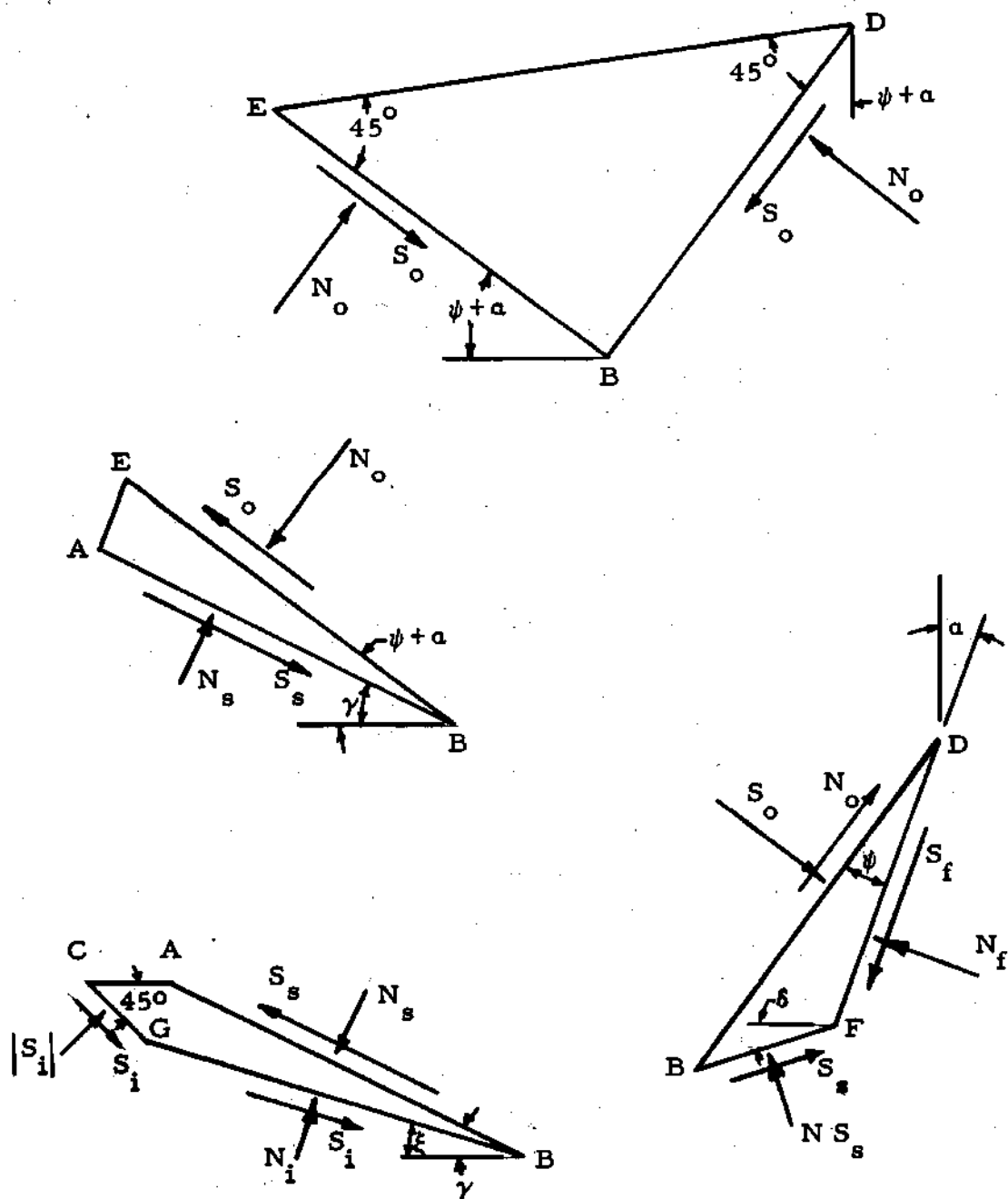


Figure 24: Individual Zones of Proposed Model

and will, therefore, vary slightly with rake angle and cutting speed. The quantitative value for  $S_s$  can be calculated from an equation of the form of Equation (24).

Once the material passes plane AB it is deformed at a rapidly decreasing strain rate until it approaches plane BE where the strain rate is very low. The plane BE approximates the upper boundary of the primary deformation zone and the shear stress on this plane (denoted by  $S_o$ ) will be lower than that on plane AB due to the decreased strain rate and slight increase in temperature at normal cutting speeds, having greater effect than that of the additional plastic strain occurring between planes AB and BE.

## 2. Zone BDE

Stresses are transmitted from the secondary deformation zone to the primary deformation zone through the zone BDE. It is assumed that no deformation takes place in the zone but that the material is stressed to its yield point. The material passing through the secondary deformation zone will arrive at plane BD in a workhardened state, similar to that of the material at plane BE. Thus, the magnitude of the shear stress on plane BD will be very close to the magnitude of the shear stress on plane BE.

It is reasonable to assume that the forces acting on the chip after it passes through the region BDE are negligible. Hence, the shear and normal stresses on plane DE will also be negligible and no forces will be transmitted across that plane. The planes BE and BD are planes of maximum shear stress and the shear stresses on them are equal. Therefore, the triangle BDE must be a right isosceles tri-

angle with the magnitude of the normal stresses,  $N_o$ , on planes BD and BE equal to  $S_o$  in order to maintain force equilibrium.

### 3. Secondary Deformation Zone - BDF

All planes of the zone BDF have normal and shear stresses acting on them. It has been shown previously that the shear and normal stresses acting on plane BD are of the same magnitude,  $S_o$ . The length of plane DF is defined to be the length of the chip tool interface over which sticking occurs. The shear and normal stresses on plane DF are designated as  $S_f$  and  $N_f$ , respectively;  $S_f$  may be greater or less than the stress  $S_o$ , depending on the deformation characteristics of the material. The stress conditions on the plane DF will be shown to control directly the geometry of the cutting process.

The position of the plane BF is defined by its deflection from the horizontal and its intersection with plane BD. It will be assumed that the shear stress on plane BF is of magnitude  $S_s$  and the normal stress is of equal magnitude. The magnitude of the shear stress on plane BF will lie somewhere near  $S_s$ , because of the high strains, strain rates, and the decreased temperatures (due to heat conduction into the workpiece) present. The entire model with stresses on the appropriate planes is shown in Figure 23.

### Model Analysis

The experimental model (Figures 22 and 23) can be used to develop expressions relating to the angles  $\psi$ ,  $\delta$ ,  $\gamma$ , and  $\xi$ , and the stresses  $S_i$ ,  $S_f$ ,  $N_f$ ,  $S_o$ ,  $S_s$ , and  $N_s$  to the tool forces and the cutting geometry. An additional expression is required relating the work performed in cutting

to that calculated as a function of the stresses present in the primary deformation zone.

The total energy absorbed in metal cutting is determined by the product of cutting speed and cutting force. It is composed of the work performed in the primary deformation zone and that performed in the secondary deformation zone. It is felt that it would be difficult to analyze the modes of deformation and the energy consumed on the secondary deformation zone because of the complex nature of the frictional and normal stresses and the sliding and sticking present at the chip tool interface. Hence, the "work of friction" (determined experimentally) will be subtracted from the total work in order to determine the work performed in the primary deformation zone.

The work performed in the primary deformation zone per unit time can be expressed analytically as a function of the stresses on, and deformation of an element passing through that zone. The amount of time required for this element to pass through the primary deformation zone is a function of the size of that zone. Thus, the total work performed on the element as it passes through the primary deformation zone occurs at a rate dependent upon the size of that zone. If this rate is to be consistent with the experimental results it must be equal in magnitude to the experimentally determined work rate. This constitutes an additional criterion which is applicable to the proposed model. Equations will now be derived relating the dimensionless stress ratios  $\frac{S_s}{S_o}$  and  $\frac{S_f}{S_o}$  and the angle parameters of the model.

Forces transmitted across planes EB and BF must be in equilibrium with the cutting and thrust forces as shown in the force polygon of

Figure 25. Resolving horizontally:

$$F_c = w S_o BE [\sin(\Psi+\alpha) + \cos(\Psi+\alpha)] + w S_s BF [\cos \delta - N \sin \delta] \quad (26)$$

and vertically

$$F_t = w S_o BE [\cos(\Psi+\alpha) - \sin(\Psi+\alpha)] + w S_s BF [\sin \delta + N \cos \delta] \quad (27)$$

Combining Equations (27) and (26) and substituting

$$\frac{BF}{BE} = \frac{\sin \Psi}{\cos(\alpha+\delta)} \quad , \quad (28)$$

then solving for  $\tan \delta$  gives

$$\tan \delta = \frac{Y \cos \alpha + \frac{F_t}{F_c} - N}{Y \sin \alpha + N \frac{F_t}{F_c} + 1} \quad , \quad (29)$$

where

$$Y = \frac{\left[ \frac{F_t}{F_c} - 1 \right] \cos(\alpha+\Psi) + \left[ \frac{F_t}{F_c} + 1 \right] \sin(\alpha+\Psi)}{\frac{S_s}{S_o} \sin \Psi} \quad (30)$$

A force polygon of triangle BDF is shown in Figure 26. Resolving parallel to the tool rake face for a unit width,  $w$ , gives

$$S_f DF = S_o BD \cos \Psi - N_o BD \sin \Psi + S_s BF [\sin(\alpha+\delta) + N \cos(\alpha+\delta)] \quad (31)$$

substituting

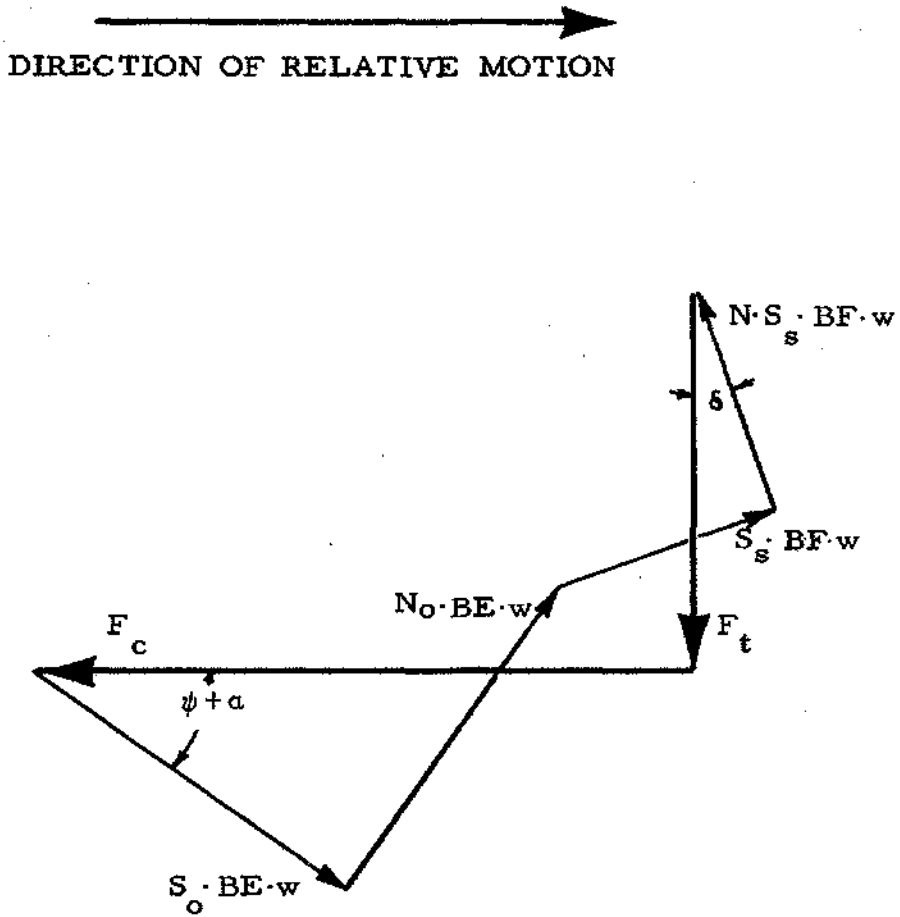


Figure 25: Force Polygon Across Surface EBF of Model

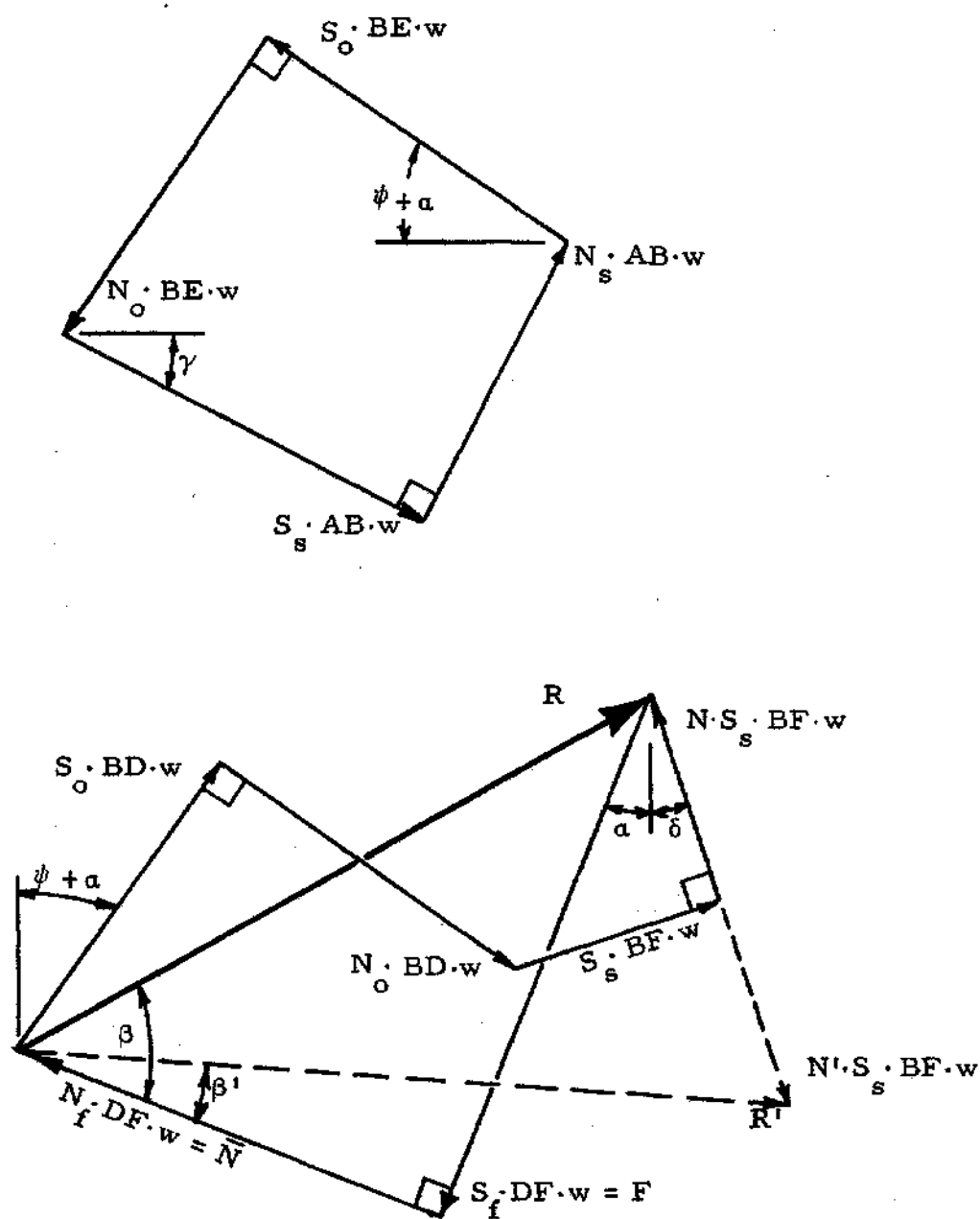


Figure 26. Force Polygons of Triangles BDF and ABE of Model



$$\frac{BD}{DF} = \frac{\cos(\alpha+\delta)}{\cos(\alpha+\delta+\Psi)} \quad (32)$$

and

$$\frac{BF}{DF} = \frac{\sin \Psi}{\cos(\alpha+\delta+\Psi)} \quad (33)$$

then simplifying, gives

$$\frac{S_f}{S_o} = \frac{1 + \tan \Psi + \frac{S}{S_o} \tan \Psi [\tan(\alpha+\delta) + N]}{1 - \tan \Psi \tan(\alpha+\delta)} \quad (34)$$

It can be shown from Figure 22 that the undeformed chip thickness,  $t_1$ , is given by

$$t_1 = AB \sin \gamma - BF \sin \delta \quad (35)$$

and the chip thickness,  $t_2$ , by

$$t_2 = BE \cos \Psi + BD \sin \Psi \quad (36)$$

Substituting

$$BE = BD \quad (37)$$

$$\frac{AB}{BE} = \frac{\cos \Psi}{\cos(\gamma-\alpha)} \quad (38)$$

and

$$\frac{BF}{BD} = \frac{\sin \Psi}{\cos(\alpha+\delta)} \quad (39)$$

and then solving for the cutting ratio,  $r_c$ , where  $r_c$  is defined by Equation (5), gives:

$$r_c = \frac{\cos \Psi \sin \gamma}{\cos(\gamma - \alpha) [\cos \Psi + \sin \Psi]} - \frac{\sin \Psi \sin \delta}{\cos(\alpha + \delta) [\cos \Psi + \sin \Psi]} \quad (40)$$

Rearranging Equation (40) gives

$$\tan \gamma = \frac{\Gamma \cos \alpha}{\left[ \frac{1}{(1 + \tan \Psi)} \right] - \Gamma \sin \alpha} \quad (41)$$

where

$$\Gamma = r_c + \frac{\tan \Psi \sin \delta}{\cos(\alpha + \delta) [1 + \tan \Psi]} \quad (42)$$

The force polygon for the triangle ABE is shown in Figure 27.

Resolving parallel to AB

$$S_s AB w = w BE S_o \{ \cos[\Psi - (\gamma - \alpha)] + \sin[\Psi - (\gamma - \alpha)] \} \quad (43)$$

Substituting

$$\frac{EB}{AB} = \frac{\cos(\gamma - \alpha)}{\cos \Psi} \quad (44)$$

gives

$$\frac{S_s}{S_o} = \{ [1 + \tan \Psi] \cos(\gamma - \alpha) - [1 - \tan \Psi] \sin(\gamma - \alpha) \} \cos(\gamma - \alpha) \quad (45)$$

The lengths of the planes of the proposed model can also be determined using the fact that BE and BD are of equal length. Rearranging Equation

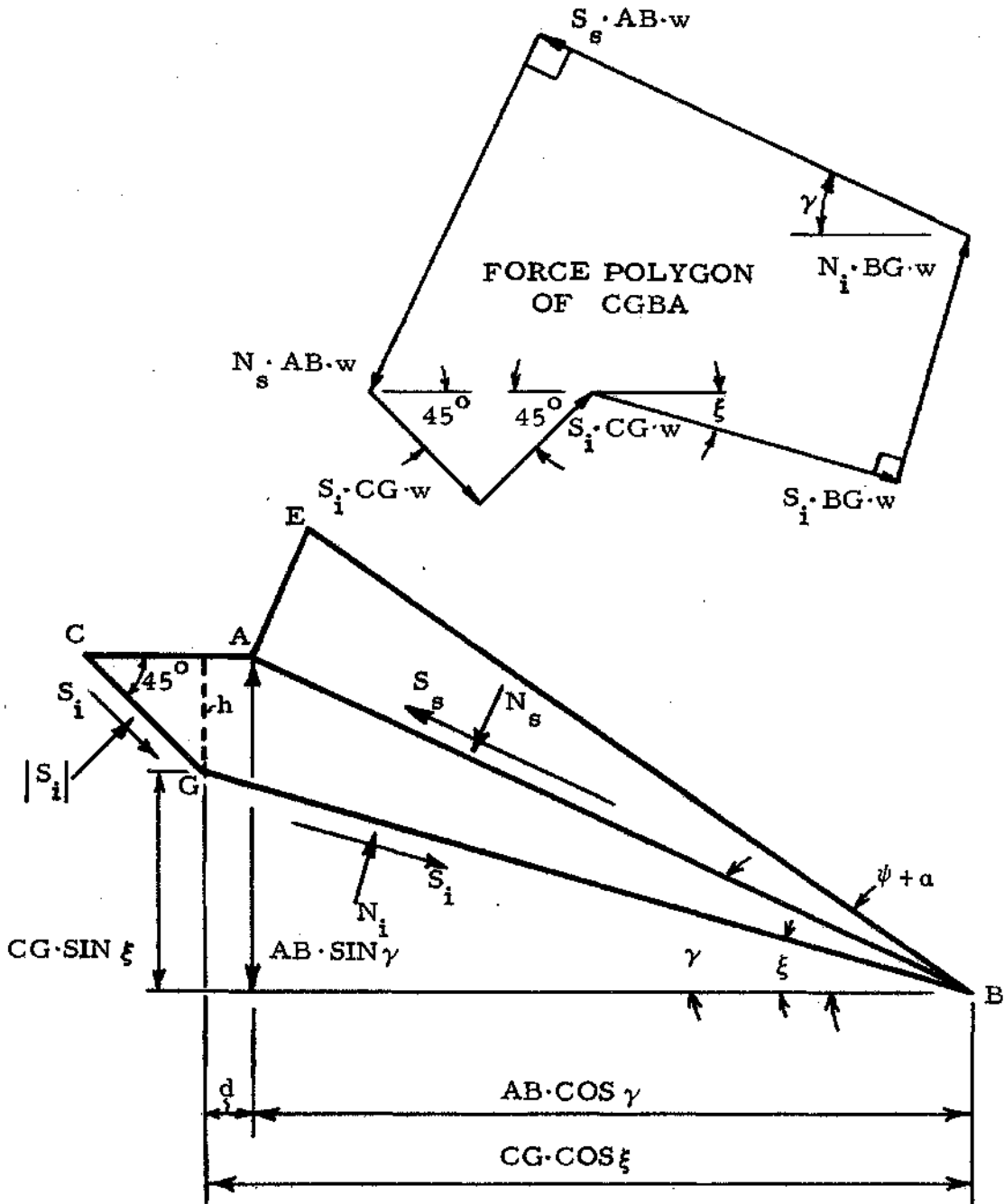


Figure 27. Primary Deformation Zone of Model

(36) gives:

$$BE = \frac{t_2}{(\cos \Psi + \sin \Psi)} \quad (46)$$

from triangle BDF:

$$BF = \frac{BD \sin \Psi}{\cos(\alpha + \delta)} \quad (47)$$

and

$$DF = \frac{BD \cos(\alpha + \Psi + \delta)}{\cos(\alpha + \delta)} \quad , \quad (48)$$

and from triangle ABE:

$$AB = \frac{BE \cos \Psi}{\cos(\gamma - \alpha)} \quad . \quad (49)$$

Rearranging Equation (26) gives:

$$S_o = \frac{F_c}{w \left\{ BE [\sin(\Psi + \alpha) + \cos(\Psi + \alpha)] + \frac{S_s}{S_o} BF [\cos \delta - N \sin \delta] \right\}} \quad . \quad (50)$$

An equilibrium diagram of the forces acting on tetrahedron CGBA is shown in Figure 27. Solving for the initial shear strength of the workpiece material,  $S_i$ , gives:

$$S_i = \frac{S_s \cos(\gamma - \xi) + N_s \sin(\gamma - \xi)}{1 + 2 \cos \xi [\sin \gamma - \sin \xi]} \quad , \quad (51)$$

where the normal stress on plane AB ( $N_s$ ) is obtained by resolving forces

acting on triangle ABE perpendicular to plane AB; that is,

$$N_s = S_o \frac{BE}{AB} [\cos(\Psi + \alpha - \gamma) - \sin(\Psi + \alpha - \gamma)] \quad , \quad (52)$$

and where the shear stress  $S_s$  is written as:

$$S_s = \left\{ \frac{S_s}{S_o} \right\} S_o \quad . \quad (53)$$

The angle  $\xi$  can be determined from Equation (51) for a given initial shear strength of the workpiece material,  $S_1$ , where ( $0 < \xi < \gamma$ ).

In order to compute the work performed in the primary deformation zone a value for the mean stress on that zone is required. The actual stress will be somewhat greater than  $S_1$  and less than  $S_s$ . (Preliminary computations showed that the stress was close to  $S_o$  over a wide range of cutting conditions and therefore this value was used in all subsequent calculations.)

The sum total of all work per unit time performed in the primary deformation zone in compression and shear is given by (see Appendix II):

$$W_{pt} = S_o w \left[ \frac{1 - r_c^2}{2 r_c} + \tan \nu \right] \frac{A_{pdz}}{T_{rq}} \quad , \quad (54)$$

where the average time required for an element to pass through this zone is given approximately by (see Appendix II):

$$T_{rq} = \frac{AB (\Psi + \alpha - \xi)}{V_c (1 + r_c)} \quad , \quad (55)$$

and where the area of primary deformation zone is approximately

$$A_{pdz} = \frac{1}{2} \{AB\}^2 (\Psi + \alpha - \xi) + \frac{1}{2} h AC \quad . \quad (56)$$

The angle  $(\Psi + \alpha - \xi)$  is expressed in radians, and the length of plane AC is given by:

$$AC = AB [\sin \gamma - \sin \xi + \cos \xi - \cos \gamma] \quad . \quad (57)$$

The perpendicular distance,  $h$ , from point G to plane AC (Figure 27) is

$$h = AB [\sin \gamma - \sin \xi] \quad . \quad (58)$$

The angle  $\nu$  is the angle through which a unit square element must be sheared to maintain continuity of material flow throughout deformation and is given by (see Appendix II):

$$\tan \nu = \frac{r_c \cos \phi - \sin(\alpha - \phi)}{\cos(\alpha - \phi)} \quad . \quad (59)$$

The total work rate performed during the cutting operation is given by:

$$W_{tl} = F_c V_c \quad . \quad (1)$$

The work rate performed by "friction" is given by:

$$W_{kf} = F V_c r_c \quad , \quad (60)$$

where the force parallel to the rake face of the tool is given by:

$$F = F_c \sin \alpha + F_t \cos \alpha \quad . \quad (61)$$

The work rate performed in the primary deformation zone (as determined experimentally) is then given by:

$$W_{pd} = W_{tl} - W_{kf} \quad . \quad (62)$$

Sufficient expressions have now been derived to analyze cutting test data. The analysis is performed in the following manner.

The basic material properties of mass density ( $\rho$ ), specific heat ( $C_p$ ), and thermal conductivity ( $k$ ), are obtained from standard tables. The initial shear strength of the work material ( $S_i$ ) is determined by a comparison of the initial microhardness of the workpiece and that listed in a materials handbook. A cutting test is performed with a fixed cutting speed ( $V_c$ ), rake angle ( $\alpha$ ), chip width ( $w$ ), and undeformed chip thickness ( $t_1$ ). The results of the cutting test yield the chip thickness ( $t_2$ ) the cutting force ( $F_c$ ), and the thrust force ( $F_t$ ).

Using an iterative procedure the angle  $\Psi$  is found which results in agreement between  $W_{pt}$  and  $W_{pd}$  with the desired degree of accuracy while maintaining the equality of the system of Equations (28) to (51) for the angles  $\delta$ ,  $\gamma$ ,  $\xi$ ,  $S_i$ , and the stress  $S_f$ . Although multiple solutions may exist for the angle  $\Psi$ , from the geometry one can observe that the range of interest will be such that

$$0 < \Psi < \frac{\pi}{2} \quad ,$$

and that  $\Psi$  will generally be small. The trivial case of no secondary

deformation zone existing occurs when  $\Psi$  is equal to 0. This solution completely defines the geometry of the model and the dimensionless stress ratios  $\frac{s}{s_0}$  and  $\frac{f}{s_0}$  for a given set of cutting conditions.



## CHAPTER V

## MODEL APPLICATION

The preceding chapter has shown how the proposed model can be used in the analysis of experimental results, given  $\alpha$ ,  $V_c$ ,  $t_1$ ,  $t_2$ ,  $F_c$ ,  $F_t$  for a particular metal cutting test. In order to test the complete validity of the model it must be capable of analyzing experimental data produced from a wide range of cutting conditions. The range of experimental cutting tests analyzed with the present model was limited at low cutting speeds and low rake angles by the formation of a built-up edge on the tool rake face and at high speeds by exceeding the power available to perform the cutting operation. The geometry of the dynamometer precluded using rake angles greater than 45 degrees.

The numerical values for the stresses  $S_s$ ,  $S_o$ , and  $S_f$ , the angles  $\delta$ ,  $\gamma$ ,  $\xi$ , and  $\Psi$ , and the stress ratio  $\frac{S_s}{S_o}$  for each test were determined by selecting the angle  $\Psi$  which gave agreement between the work performed in the primary deformation zone as determined by the experimentally measured tool forces and that determined from the stresses and the assumed mode of deformation in the primary deformation zone. These stress values are listed in Tables 3, 4, 5, and 6 in Appendix I. It is seen that the only stress which remains approximately constant is  $S_s$ , and a means of correlating the other stresses with the individual tests is required. Further analysis of the machining process must be made.

The stress required to deform any workhardened material depends

on its previous strain history, temperature, and the rate at which deformation is occurring. Hence, these quantities should be included in any analysis of the metal cutting process. In order to explain satisfactorily changes in  $S_f$ ,  $S_o$ ,  $S_s$ , and  $\frac{S}{S_o}$ , it is necessary to examine the strain, strain rate, and temperature conditions in both the primary and secondary deformation zones.

The shear strain associated with machining for a shear plane model of the cutting process (the use of this plane being justifiable because in this area the mode of deformation is not important) is given by:

$$\gamma_s = \cot \phi + \tan(\phi - \alpha) \quad (63)$$

after Merchant<sup>1,2</sup>, where  $\phi$  is the shear angle as defined by Equation (4).

The average rate of strain in the primary deformation zone which depends on the average size of that zone is given by (see Appendix II):

$$\dot{\gamma}_1 = 0.2 \gamma_s V_c [1 + r_c] / [AB(\Psi + \alpha - \xi)] \text{ sec}^{-1} \quad (64)$$

If a parabolic velocity distribution throughout the secondary deformation zone is assumed as being reasonable (see reference 15) then the strain rate is given by:

$$\dot{\gamma}_2 = \frac{0.4 V_c r_c}{l_o \tan \Psi} \text{ sec}^{-1} \quad (65)$$

where  $l_o$  is the chip tool length, i.e., plane DF of Figure 22.

Procedures for calculating the temperature in the primary and secondary deformation zones based on plane heat sources and a shear

plane model of the metal cutting process have been given by several workers<sup>45,49</sup>. These procedures have been shown to give results in good agreement with experimental data<sup>48</sup> and it is proposed to use them in the present work. Consequently, a mean or average temperature will be computed for the zones rather than the complete temperature distribution as it actually occurs.

The total amount of heat generated during the cutting process is given by

$$q_{tl} = \frac{F_c V_c}{1400} \frac{\text{CHU}}{\text{min}} \quad (66)$$

The amount of heat generated by forces parallel to the rake face of the tool is given by

$$q_f = \frac{F V_c r_c}{1400} \frac{\text{CHU}}{\text{min}} \quad (67)$$

where  $F$  is defined by Equation (61). The heat generated in the primary deformation zone due to deformation is approximately the difference of Equations (66) and (67), that is,

$$q_s = q_{tl} - q_f \frac{\text{CHU}}{\text{min}} \quad (68)$$

The percentage of this heat which is conducted into the workpiece is given by

$$\beta_s = 0.475 - 0.1498 \ln \theta \quad (69)$$

or

$$\beta_s = 0.10, \text{ if } \theta > 12, \quad (70)$$

after Weiner<sup>45</sup>, where  $\theta$  is the thermal number and is given by

$$\theta = 720 \left[ \frac{\rho c_p}{k} \right] V_c t_1 \tan \phi \quad (71)$$

The maximum possible uniform temperature rise of the chip due to the deformation in the primary deformation zone is given by

$$\theta_{ts} = \frac{q_s}{[12 \rho c_p V_c t_1 w]} \text{ } ^\circ\text{C} \quad (72)$$

Consideration of the heat transmitted to the workpiece gives an approximation to the average uniform temperature rise of the chip due to shear deformation in the primary deformation zone. This temperature rise is clearly

$$\theta_s = [1 - \beta_s] \theta_{ts} \text{ } ^\circ\text{C} \quad (73)$$

The average temperature rise of the chip due to "friction" at the chip tool interface is given by

$$\theta_f = \frac{q_f}{[12 \rho c_p V_c t_1 w]} \text{ } ^\circ\text{C} \quad (74)$$

and the maximum temperature rise at the chip tool interface by

$$\theta_{mx} = 0.72 B \left[ \left[ 0.856 \right] \left[ 0.4 B \left[ \frac{1}{t_2} \right] \tan \psi \right] \right] \theta_f \text{ } ^\circ\text{C} \quad (75)$$

after Boothroyd<sup>48,50</sup> where:

$$B = \left[ \frac{720 \left[ \frac{\rho_c c_p}{k} \right] v_c t_1}{\left[ \frac{l_o}{t_1} \right]} \right]^{\frac{1}{2}}, \quad (76)$$

and  $l_o$  is the chip tool contact length (plane DF of the present model). The maximum temperature rise of the chip at the chip tool interface is thus

$$\theta_{ma} = \theta_{mx} + \theta_s \quad ^\circ\text{C} \quad (77)$$

It is clear at this stage that equations relating the stress to the strain, strain rate, and temperature in the primary and secondary deformation zones are required, i.e., the functional relationship:

$$\tau_i = f_i(\gamma_s, \dot{\gamma}_i, T_i) \quad (78)$$

must be evaluated. In the present work it was decided to use an expression of the form

$$\tau_i = \sigma_o G^T \gamma_s^{(A+BT)} \dot{\gamma}_i^{(C+DT+F[\ln \gamma_s]T)} \quad (79)$$

where  $i$  is 1, 2, or 3 and refers to one of the stresses  $S_s$ ,  $S_o$ , or  $S_f$ ;  $\gamma_s$  is the shear strain;  $\dot{\gamma}_i$  is the shear strain rate;  $T$  is temperature in  $^\circ\text{C}$ ; and  $\sigma_o$ ,  $G$ ,  $A$ ,  $B$ ,  $C$ ,  $D$ , and  $F$  are constants. The constant  $C$  permits the use of an arbitrary point of reference for the temperature  $T$ . In this work the reference point was taken as the ambient temperature.

Equation (79) was used as it is slightly more general than that proposed by Lubahn<sup>21</sup>, and it gave slightly better results.

The results of cutting tests over a wide range of experimental conditions were substituted into Equation (79) and the constants of the functional relationships between the stresses, strains, strain rates, and temperatures determined. These equations were then used to predict  $S_f$ ,  $S_o$ , and  $\frac{S}{S_o}$ . The percentage error of the prediction of the quantities  $S_f$  and  $\frac{S}{S_o}$  are shown in Tables 5 and 6 in Appendix I. Errors in predicting  $S_s$  are of the order of one percent. It can be seen from Tables 5 and 6 that the percentage error for all predictions are extremely small, thus giving strong justifications of the validity of the present model.

## CHAPTER VI

### MODEL UTILIZATION

#### Introduction

The present model of the orthogonal metal cutting process differs from most others previously developed in that it can be used to predict qualitatively the effects of changes in cutting speed and rake angle on the tool forces and the geometry of the cutting process. The purpose of this chapter is to develop the functional relationships which make such predictions possible.

The functional relationships developed have been solved by a complex iterative computer procedure (see Appendix III). The results of this solution are compared with the experimental results in Figures 29 through 37 in Appendix I for the complete range of cutting speeds and rake angles used in the experimental investigation.

The multivalued characteristics of trigonometrical functions can lead in some cases to unrealistic solutions of an equation. The solutions of some trigonometric equations were obtained by an iterative procedure within a selected range of the angular variables which would give a realistic geometry. For example, it would seem intuitively obvious that the angle  $\Psi$  would lie in the range of  $0 < \Psi < (90 - \alpha)$ . Similar deductions can be made with respect to other angles (i.e.,  $0 < \gamma < (\Psi + \alpha)$ ,  $0 < \xi < \gamma$ , etc.).

The known input parameters are the undeformed chip thickness ( $t_1$ ),

the cutting speed ( $V_c$ ), the rake angle ( $\alpha$ ), the material properties ( $\rho$ ,  $C_p$ ,  $k$ ,  $S_i$ ), and the constants for the stress, strain, strain rate, and temperature equation (Equation (79)) describing the stresses  $S_o$ ,  $S_f$ , and  $S_s$ . These constants were determined from metal cutting tests since data concerning the properties of materials under the conditions of strain, strain rate, and temperature present during metal cutting are not currently available.

Given the seven input conditions, a solution to the problem of determining a unique geometry and the cutting forces may exist if the number of unknown dependent variables and associated equations does not exceed the numbers of known independent variables. The unknown variables are the angles  $\Psi$ ,  $\delta$ ,  $\gamma$ , and  $\xi$ , the cutting and thrust forces ( $F_c$  and  $F_t$ ) and the chip thickness ( $t_2$ ). Thus, it is at least possible for a solution to exist.

#### Utilization

The block diagram for the iterative procedure used is shown in Figure 28. The stress values for  $S_s$  and  $S_o$  lie within a relatively small range. Any initial estimate of their values will be only a relatively small amount in error. In order to begin the iterative process initial values of  $S_s$  and  $S_o$  are assumed. Trial values of the angles  $\Psi$  and  $\delta$  are also assumed. The angle  $\gamma$  is found by satisfying the previously derived relationship:

$$\frac{S_s}{S_o} = \{[1 + \tan \Psi] \cos(\gamma - \alpha) - [1 - \tan \Psi] \sin(\gamma - \alpha)\} \cos(\gamma - \alpha) \quad (45)$$



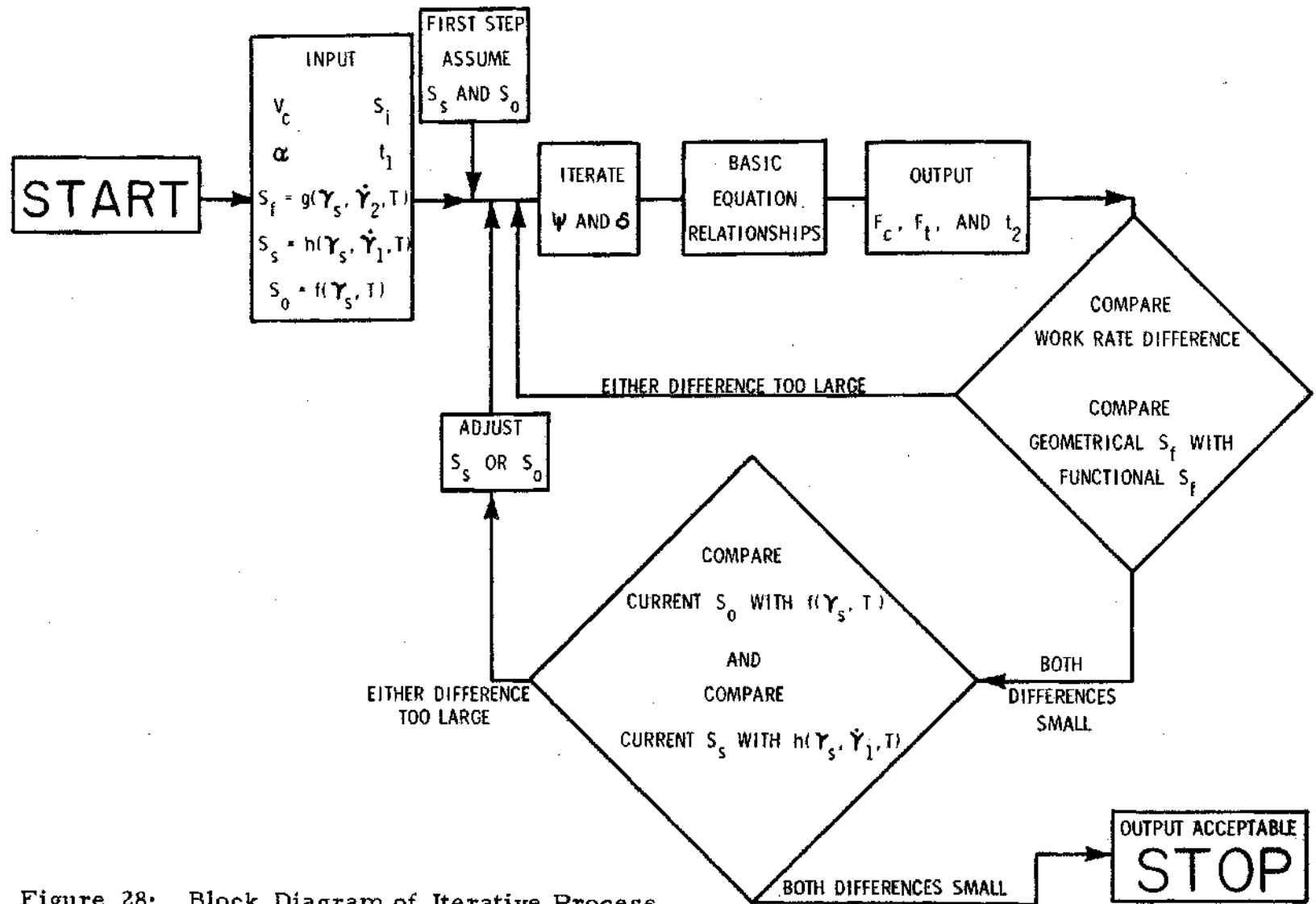


Figure 28: Block Diagram of Iterative Process

in the range  $0 < \gamma < (\Psi + \alpha)$ .

The cutting ratio  $r_c$  is then calculated from the expression:

$$r_c = \frac{\cos \Psi \sin \gamma}{\cos(\gamma - \alpha) [\cos \Psi + \sin \Psi]} - \frac{\sin \Psi \sin \delta}{\cos(\alpha + \delta) [\cos \Psi + \sin \Psi]}, \quad (40)$$

and the chip thickness from

$$t_2 = \frac{t_1}{r_c} \quad (80)$$

The cutting and thrust forces are obtained from

$$F_c = w S_o BE [\sin(\Psi + \alpha) + \cos(\Psi + \alpha)] + w S_s BF [\cos \delta - N \sin \delta] \quad (26)$$

and

$$F_t = w S_o BE [\cos(\Psi + \alpha) - \sin(\Psi + \alpha)] + w S_s BF [\sin \delta + N \cos \delta] \quad (27)$$

where

$$BE = \frac{t_2}{[\cos \Psi + \sin \Psi]} \quad (81)$$

and

$$BF = \frac{BD \sin \Psi}{\cos(\alpha + \delta)} \quad (47)$$

In order to maintain force equilibrium the stress  $S_f$  must satisfy the expression:

$$S_f = S_o \left[ \frac{S_f}{S_o} \right], \quad (82)$$

where  $\left[ \frac{S_f}{S_o} \right]$  is determined from Equation (34), and  $S_f$ , as a function of the strain, strain rate, and temperature (determined through Equation (63) to Equation (77)) of the secondary deformation zone, is calculated from Equation (79). A comparison of the two means of calculating the rate of work performed in the primary deformation zone (Equations (54) and (62)) is made. A satisfactory trial solution is found when this comparison and Equation (82) are both simultaneously satisfied.

The previously assumed values of the stresses  $S_s$  and  $S_o$  are now compared with those predicted through use of the general stress equation, Equation (78), or the specific one, Equation (79). If there is a significant difference, new values for  $S_s$ ,  $S_o$ ,  $\Psi$ , and  $\delta$  are taken and the procedure is repeated until all differences are sufficiently small.

The results of applying this process over the range of rake angles from 20 to 45 degrees and speeds of 80 to 480 surface feet per minute are plotted in Figures 29 through 37 in Appendix I. A discussion of the results and the assumptions necessary for the analysis follows in Chapter VII.

## CHAPTER VII

## DISCUSSION

Figure 29 is a plot of the shear angle ( $\phi$ ) versus the difference between the friction angle ( $\beta$ ) and rake angle ( $\alpha$ ). Many of the shear angle theories<sup>1,2,5,7,8, etc.</sup> and the experimental work upon which these workers base their statements indicate that this graph should be a straight line. It can be seen from Figure 29 that it could be possible to place a "best" straight line through the least means square average of the experimental data points with only a small amount of deviation. Furthermore, this straight line would be relatively close to another passed through the least means square average of the predicted data points. Thus, by the current standards of metal cutting analysis the model developed here is of acceptable quality.

The value of the model cannot be judged from an all-inclusive plot such as Figure 29. A more realistic judgment of the value of the model can be made through evaluation of Figures 30, 31, 32, and 33, in which the trends of the predicted friction angle and the predicted shear angle agree extremely well with the results of experimental cutting tests for both the variation resulting from changes in rake angle and the variation resulting from changes in cutting speed. Thus, a qualitative prediction of the effects of changing the cutting speed of orthogonal machining of aluminum has been made with extremely good accuracy.

The results of using the developed model to predict the effects

of the change of speed and rake angle on the chip thickness, Figures 34 and 35, and the cutting forces, Figures 36a, 36b, and 37a, 37b, are also excellent. It is extremely doubtful that a better approximation to the experimental data points shown for the two angle parameters or that a much better one for the forces of cutting and the chip geometry could be obtained over the entire range of speeds and rake angles. This qualitative agreement is the most significant indication of the value of the model developed.

The primary result of this research is the model of the metal cutting process and as such the assumptions used in its development are of prime importance. Overall justification of the sum total of all assumptions made can be effectively summarized in the fact that the model accurately predicts the effects of changes in cutting speed on the chip thickness and the forces of cutting. Specific justification of the individual assumptions will now be made.

#### Basic Assumptions

Justification of the basic assumptions of the metal cutting process is not exceptionally difficult. The analysis of non-plane strain conditions would be exceedingly and unnecessarily complex and would add a third dimension to the force, displacement, stress, and strain vectors obtained. The presence of a built-up edge at the chip-tool interface would most probably lead to non-steady state conditions during cutting. This would exceed the applicability of any model to be developed at this time.

A single phase material whose deformation characteristics can be

described by a single equation is theoretically possible; however, to date the development of that equation independently has not occurred in the range of high strains, strain rates, and temperatures inherent in the metal cutting process. This difficulty was overcome by the use of metal cutting tests to determine an applicable material property equation. In doing this if errors are introduced in using the experimental metal cutting tests to develop the constitutive equations for each stress, they preclude the use of that constitutive equation for any purpose other than the analysis of other metal cutting data. As such, the errors made in developing a constitutive equation will be self cancelling when that equation is used to show the functional relationship between stress, strain rate, and temperature for the appropriate material when deformed in a metal cutting test.

The use of a lubricant during the cutting process is precluded due to its indeterminate cooling properties and the questionable capability of generating an appropriate expression for the shear stress at the chip-tool interface.

A standard metal cutting analysis using the shear plane approach for determination of many metal cutting characteristics was necessary in order to satisfactorily complete the analysis. A new derivation for determining the strain, percentage of heat conducted to the workpiece, and temperature rise at the chip-tool interface would be beyond the scope of this analysis and would not add appreciably to the analysis.

### Model Geometry Assumptions

#### Primary Deformation Zone

The assumption that the initial shear strength of the work material can be represented as a constant shear stress along surface CGB is justifiable as being a mechanical property of the workpiece material. In order to maintain static equilibrium a surface does exist along which a shear stress of constant magnitude acts. Plasticity theory indicates that a surface of maximum shear stress intersects a free surface at 45 degrees and will have shear and normal stresses of equal magnitude acting thereon. Plane CG is defined as having the properties of being a plane of maximum shear stress and it intersects a free surface. Although it is not defined as being a slip line, the analogy is made that plane CG does intersect the free surface at 45 degrees and does have equal shear and normal stresses acting on it.

The assumption that plane BG and plane AB are of equal length is purely arbitrary. However, it is readily apparent that a small variation in the length of plane BG would result in only a slight variation in the quantitative results of analyzing an experimental cutting test (those quantitative results being the numerical values of the angles  $\Psi$  and  $\delta$ ). Preliminary computations showed that a consistent variation of 10 percent in the length of plane BG had very little effect on the results of analyzing and predicting the results of a series of metal cutting tests.

The plane AB is assumed to be the plane of maximum shear stress. A free body diagram of the Primary Deformation Zone with stresses acting on the appropriate planes will indicate that plane AB is the shortest

plane which will intersect the free surface CAE and pass through point B. Hence, in order to maintain static equilibrium the stress on plane AB will be a maximum.

### Secondary Deformation Zone

The shear stress on plane BD is assumed to be equal to that on plane BE. This assumption is reasonable in light of the fact that the material along plane BD will have been deformed to a large amount of strain, as will the material along plane BE. The material along plane BD will most probably have been strained slightly more than that along plane BE but it is most probably at a slightly higher temperature. Hence, these two factors will tend to offset each other and the assumption of equal stresses being present is not unreasonable. A plane will exist which intersects the free surface near the tool flank in a manner similar to the plane CG. This plane will be physically close to plane DF and will have equal shear and normal stresses acting on it. The magnitude of the stresses acting on plane DF is assumed to be equal to  $S_s$  because of the high strain to which the material has been subjected as it passed through the primary deformation zone and the cooling effects of the work-piece material. An intuitive case can be made to justify the direction of the normal stress on plane BF as being either tensile or compressive. However, in order to maintain static equilibrium of a reasonably shaped zone BDF with  $S_f$  being larger than  $N_f$ , it is apparent that the normal stress along plane BF must be compressive. A qualitative justification of this is shown in Figure 26 where, if a reasonable geometry of the cutting process is assumed, i.e., the angles  $\Psi$  and  $\delta$  are relatively small, the friction angle  $\beta$  would be of the magnitude shown as  $\beta'$  in Figure 26.



In most metal machining, the friction angle is much larger than this decreased angle,  $\theta'$ .

The tool nose forces have been neglected because their relative magnitude is small, while the static equilibrium of the chip requires that the tool nose forces be transmitted across surface CGRF and hence at least a large portion of the tool nose forces are inherent in the analysis of experimental data.

The determination of the strain rate of the secondary deformation zone is based on the assumption that the velocity distribution therein is parabolic. This may be in error but the error will be systematic throughout the analysis and hence will be self-cancelling in predicting metal cutting test results. A similar justification can be made for the development of the average strain rate in the primary deformation zone. This is acceptable in the present analysis because the comparison is qualitative.

Thus, individual basic assumptions inherent to this analysis are, at least in part, justifiable and the sum total of all errors associated with the assumptions do not result in large variation in the ability of the model to predict metal cutting results.

#### Independent Correlation

Zorev<sup>46</sup> found an area of sticking and an area of sliding between the chip and tool at the chip-tool interface. This has been verified analytically by Bailey and Boothroyd<sup>15</sup>. These works form the basis for neglecting the sliding region at the chip-tool interface in the present work.

In high speed hot machining of chromium-molybdenum steels, Sata<sup>40</sup> found the shear stress in the shear zone remained approximately constant with increased cutting speed but decreased with rising temperature of the workpiece. This is especially significant since an increase in speed yielded large increases in cutting temperature. The conclusion drawn by Sata was that the effects of an increase in strain rate were offset by the effects of an increased cutting temperature. Ostafiev and Kobayashi<sup>32</sup> found that the stress-strain curve obtained during metal cutting yielded a slightly higher stress for a given strain than that of a static compression test. The results of these two experimental investigations support the use of an equation of the form of Equation (79) to describe the deformation characteristics of a generalized material during metal cutting.

Shaw<sup>23</sup> has listed the important factors in the orthogonal metal cutting process in an approximate order of importance as follows.

- "1. Chips are produced by a shear process.
2. There is a strong interaction between the shear deformation occurring in the shear zone and that occurring on the tool face.
3. Most materials strain harden.
4. A built-up edge is usually present at low cutting speeds.
5. At high cutting speeds a secondary shear zone is present in the chip along the tool face.
6. Chips frequently curl and this in turn changes the chip-tool contact length.
7. The chip-tool contact length may be controlled by tool design.
8. Dull tools or tools cutting with a large BUE will have a rounded cutting edge." (BUE is an acronym for built-up edge.)

- "9. Forces exist on the relief face of a tool, especially when an appreciable wear land is present..

In addition to the steady-state problem there are several important problems associated with non-steady state input conditions, such as variable undeformed chip thickness ( $t$ ), speed ( $V$ ), rake angle ( $\alpha$ ), depth of cut ( $b$ ), or material properties. . . . Solutions that incorporate the important concepts of items 2, 4, and 5 seem to be missing."

The model as developed in the present work has included many of these phenomena noted by Shaw<sup>23</sup>. Of the five more important phenomena, only the built-up edge is excluded from this analysis. Variations of chip geometry and cutting forces with variable cutting speed are included.

## CHAPTER VIII

### CONCLUSIONS

The results of the development of a theoretical model of orthogonal machining are quite good in that (a) the change of chip geometry and cutting forces resulting from changes in rake angle are qualitatively predicted extremely well, and (b) the changes of chip geometry and cutting forces resulting from changes in cutting speed are also qualitatively predicted extremely well.

The model proposed in the present work is a significant advancement in the understanding of the orthogonal machining process.

## CHAPTER IX

### RECOMMENDATIONS

It is felt that further development of this work would be redundant with the exception of further study of the built-up edge. It is not felt that the extension of the present work to a built-up edge analysis would be feasible.

In order to prove the generality of the analysis, application of the model to other materials could be made in the future.

A great deal of work is required in order to understand the behavior of materials at high deformation rates and varying temperatures. Until advancements occur in this field further metal cutting analyses will be of limited value.

## APPENDIX I

## EXPERIMENTAL RESULTS

Table 1. Nominal and Actual Cutting Speeds and Rake Angles

Nominal Rake Angle (degrees)	Actual Rake Angle (degrees)	Nominal Cutting Speed (SFPM)	Actual Cutting Speed (SFPM)
20	18.5	80	78
25	25.3	120	117
30	29.6	160	156
35	34.3	240	235
40	40.0	320	310
45	45.0	480	470

Table 2. Experimental Cutting Test Results

Rake Angle (degrees)	Cutting Speed (SFPM)	Cutting Force (pounds)	Thrust Force (pounds)	Chip Thickness (inches)
20*	80	726.4	400.1	0.116
25	80	684.6	339.2	0.110
30	80	634.5	269.6	0.098
35	80	542.7	200.0	0.085
40	80	450.8	147.8	0.066
45	80	400.7	113.0	0.053
20*	120	684.6	382.7	0.110
25	120	642.9	313.1	0.102
30	120	584.4	243.5	0.091
35	120	500.9	182.6	0.078
40	120	425.8	139.1	0.063
45	120	384.0	104.3	0.052
20*	160	642.9	356.6	0.105
25	160	601.1	295.7	0.096
30	160	551.0	226.1	0.084
35	160	467.5	165.2	0.072
40	160	409.1	113.0	0.060
45	160	375.7	95.6	0.051
20*	240	617.8	313.1	0.101
25	240	576.1	260.9	0.091
30	240	526.0	208.7	0.079
35	240	450.8	147.8	0.067
40	240	400.7	104.3	0.057
45	240	367.3	86.9	0.050
20*	320	592.8	287.0	0.096
25	320	551.0	234.8	0.085
30	320	492.6	191.3	0.073
35	320	434.1	130.4	0.063
40	320	392.4	95.6	0.054
45	320	359.0	86.9	0.048
30	480	450.8	173.9	0.069
35	480	417.4	121.7	0.061
40	480	384.0	86.9	0.052
45	480	350.6	78.2	0.046

\* Data questionable due to built-up edge possibility.



Table 3. Stress  $S_s \times 10^{-3}$  in psi

Cutting Speed (SFPM)	Rake Angle (degrees)					
	20*	25	30	35	40	45
80	22.0	21.6	21.9	20.9	21.3	22.5
120	21.6	21.6	21.4	20.7	20.8	21.8
240	20.6	20.9	21.4	20.8	21.1	21.5
320	20.5	21.1	21.3	21.1	21.6	21.5
480	**	**	20.3	20.8	21.9	22.0

\* Data questionable due to built-up edge possibility.

\*\* Exceeded power of lathe.

Table 4. Stress Ratio  $\frac{S}{S_0}$

Cutting Speed (SFPM)	Rake Angle (degrees)					
	20 <sup>*</sup>	25	30	35	40	45
80	1.467	1.462	1.422	1.361	1.284	1.229
120	1.434	1.411	1.369	1.310	1.251	1.209
160	1.396	1.363	1.323	1.263	1.225	1.197
240	1.336	1.323	1.285	1.228	1.202	1.184
320	1.332	1.300	1.250	1.212	1.190	1.167
480	**	**	1.216	1.202	1.190	1.171

\* Data questionable due to built-up edge possibility.

\*\* Exceeded power of lathe.

Table 5. Stress  $S_o \times 10^{-3}$  in psi

Cutting Speed (SFPM)	Rake Angle (degrees)					
	20*	25	30	35	40	45
80	15.0	14.8	15.4	15.4	16.6	18.3
120	15.1	15.3	15.6	15.8	16.6	18.0
160	15.1	15.5	16.2	16.2	16.9	18.1
240	15.2	15.8	16.7	16.9	17.6	18.1
320	15.4	16.3	17.0	17.4	18.2	18.5
480	**	**	16.7	17.3	18.4	18.7

\* Data questionable due to built-up edge possibility.

\*\* Exceeded power of lathe.

Table 6. Stress  $S_f \times 10^{-3}$  in psi

Cutting Speed (SFPM)	Rake Angle (degrees)					
	20*	25	30	35	40	45
80	66.0	56.8	50.0	41.1	39.0	42.5
120	64.2	52.8	44.0	37.3	35.6	37.9
160	58.7	48.0	40.3	34.1	31.8	34.5
240	51.1	42.1	36.2	30.4	28.4	29.5
320	45.8	37.9	33.2	28.5	27.7	30.3
480	**	**	29.2	26.0	27.6	33.2

\* Data questionable due to built-up edge possibility.

\*\* Exceeded power of lathe.

Table 7. Percent Error in Predicting  $S_f$ 

Cutting Speed (SFPM)	Rake Angle (degrees)					
	20 <sup>*</sup>	25	30	35	40	45
80	+10.8	+0.1	+0.7	+0.7	-5.1	-0.2
120	+1.3	+0.3	+1.7	-0.4	-5.7	+0.5
160	-1.9	-6.2	-0.4	+2.0	+6.5	+1.3
240	+22.2	+5.4	-1.6	+2.6	+1.5	-3.8
320	+24.7	+6.4	-5.2	+4.7	+1.0	-4.6
480	**	**	-8.3	+0.3	+1.4	+1.7

\* Data questionable due to built-up edge possibility.

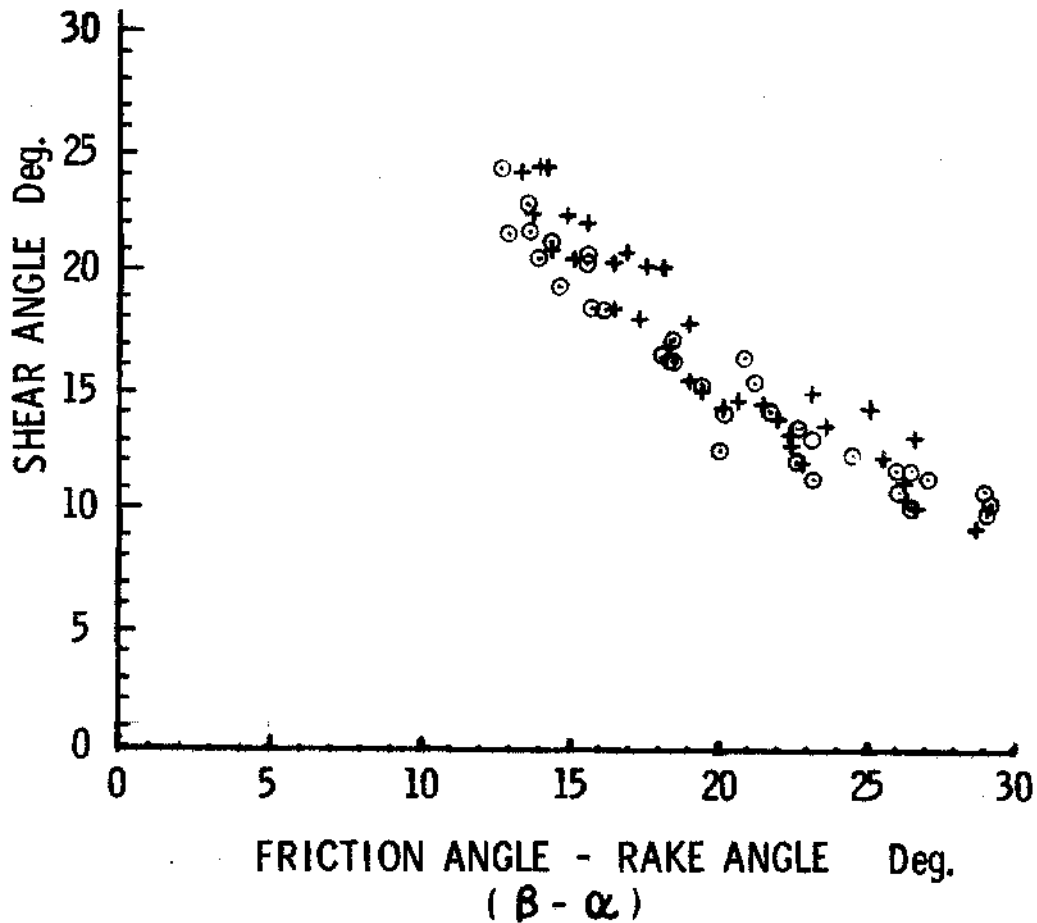
\*\* Exceeded power of lathe.

Table 8. Percent Error in Predicting  $\frac{S_s}{S_o}$

Cutting Speed (SFPM)	Rake Angle (degrees)					
	20*	25	30	35	40	45
80	-2.8	+1.0	+0.6	-0.3	-0.9	-0.4
120	+0.3	-0.1	-0.3	-0.5	-0.6	-0.1
160	-0.6	-0.4	-0.2	+0.3	+0.2	+0.2
240	-0.5	-0.1	-0.1	+0.9	+0.6	+0.3
320	-0.8	-0.4	-0.1	+0.7	+0.4	-0.6
480	**	**	-0.2	-0.1	-0.8	-0.7

\* Data questionable due to built-up edge possibility.

\*\* Exceeded power of lathe.

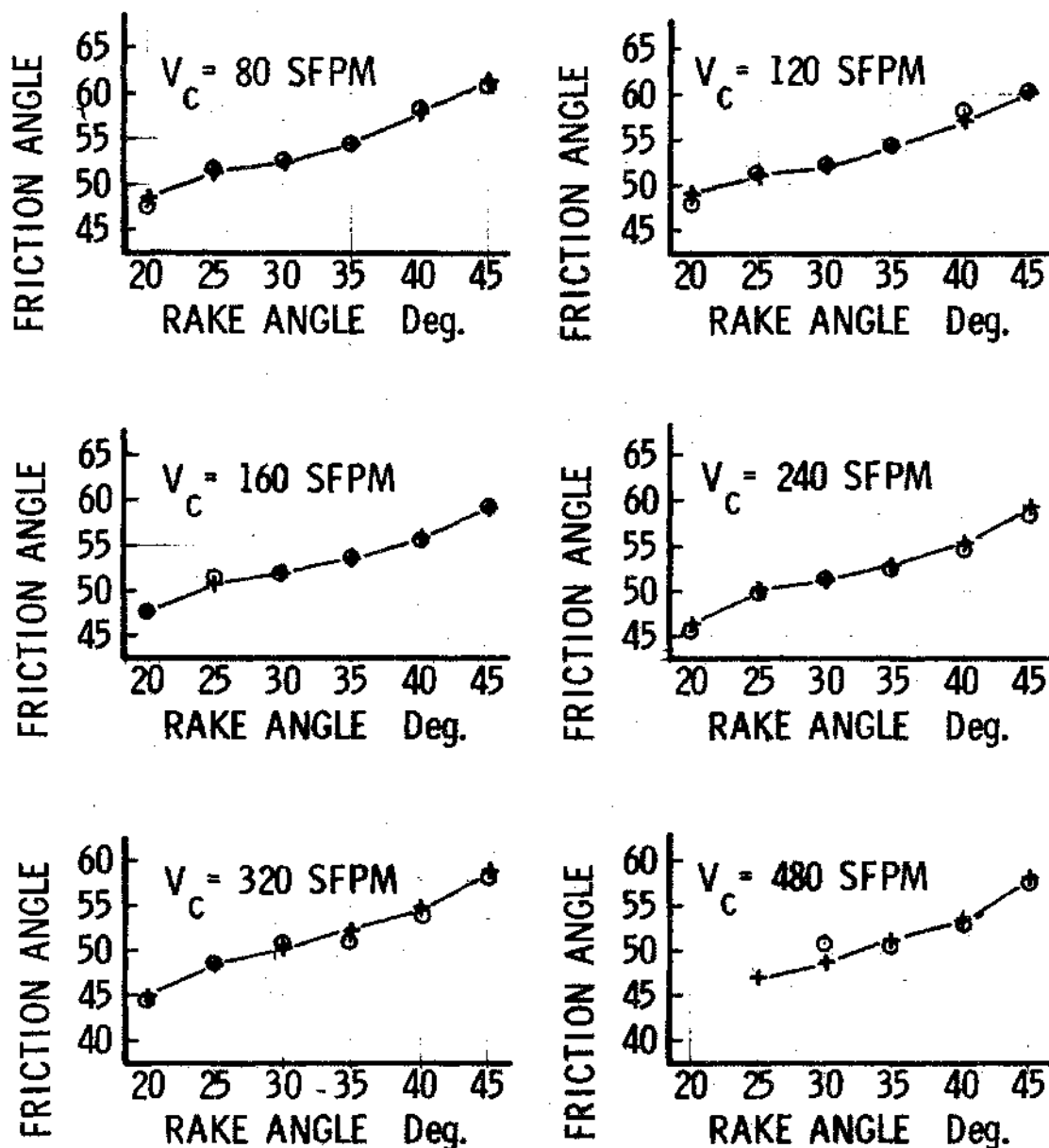


MATERIAL: 1100-O Al; TOOL MATERIAL: HSS

• EXPERIMENTAL DATA POINT

+ PREDICTED DATA POINT

FIGURE 29: SHEAR ANGLE vs. DIFFERENCE BETWEEN FRICTION ANGLE AND RAKE ANGLE

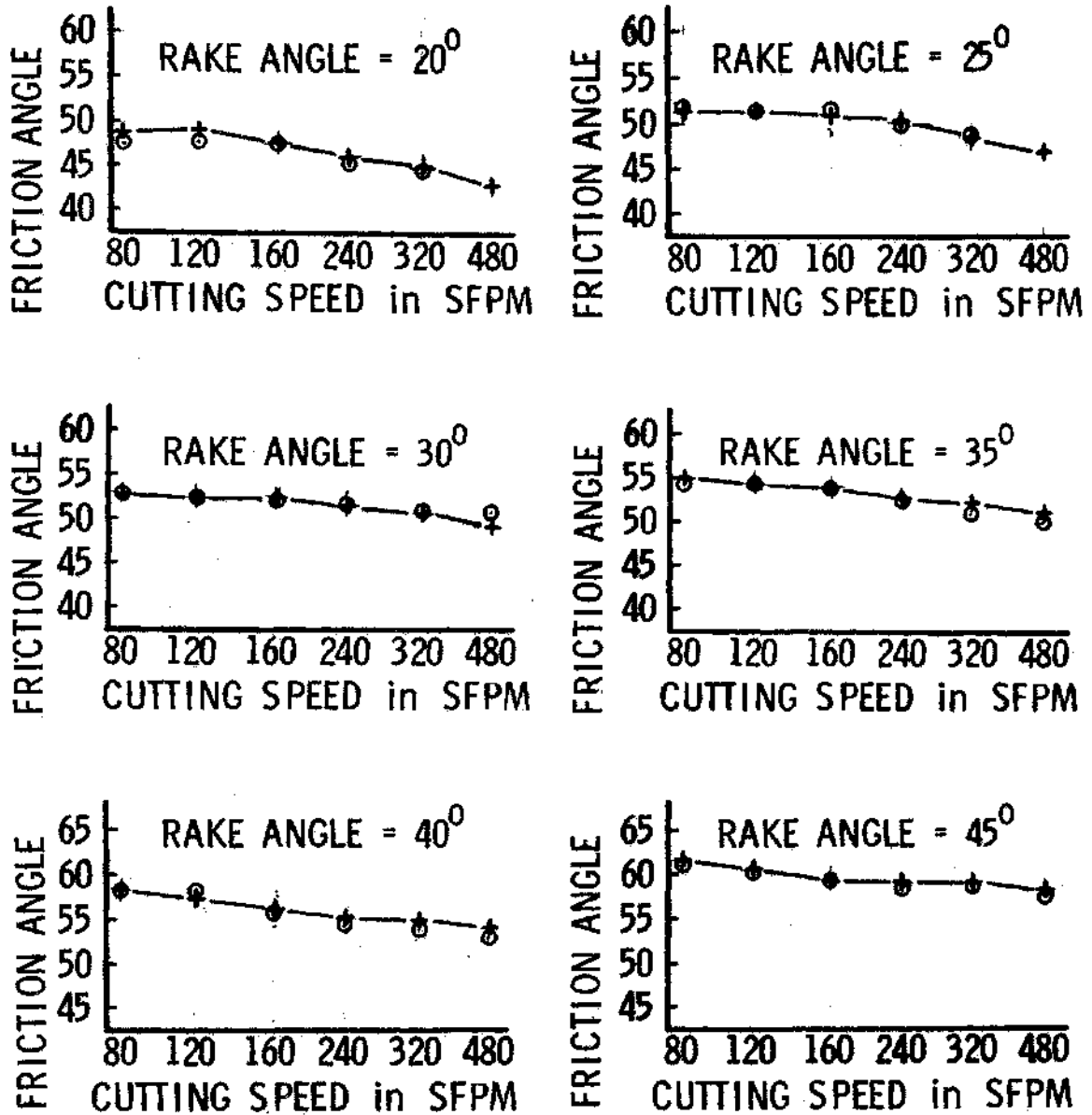


MATERIAL: 1100-O Al; TOOL MATERIAL: HSS;  $t_1 = 0.0202$  ins.

• EXPERIMENTAL DATA POINT; ✕ PREDICTED DATA POINT;

FIGURE 30: FRICTION ANGLE vs. RAKE ANGLE  
FOR VARIOUS CUTTING SPEEDS

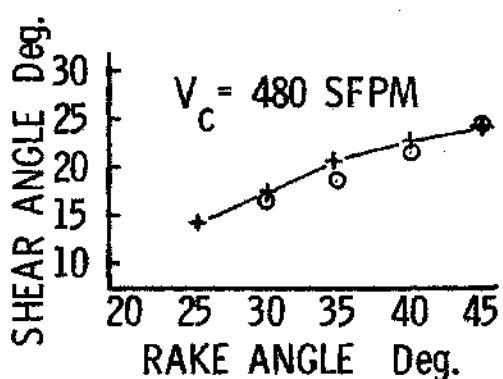
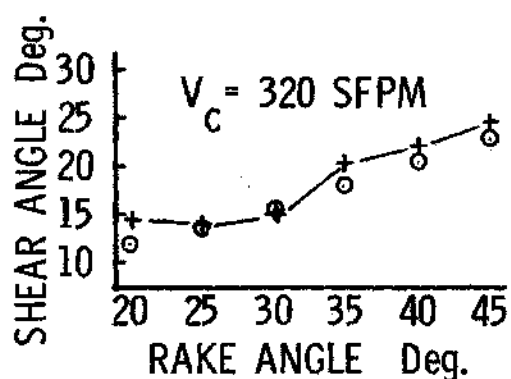
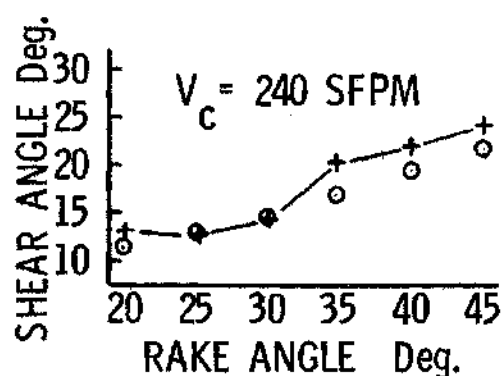
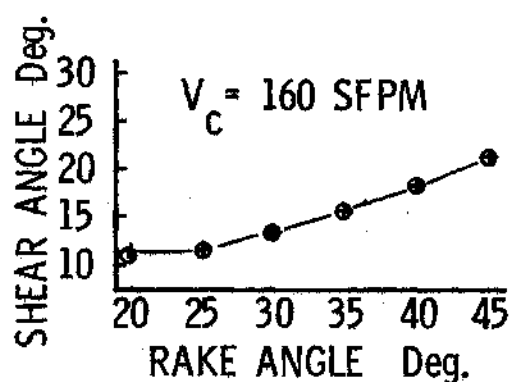
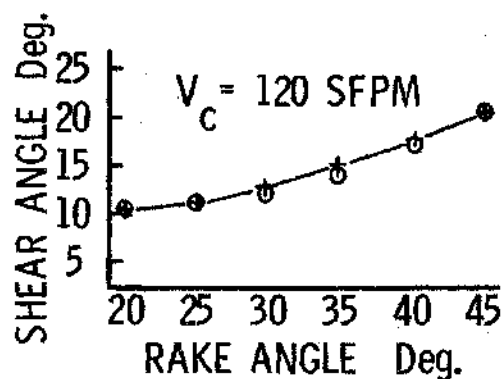
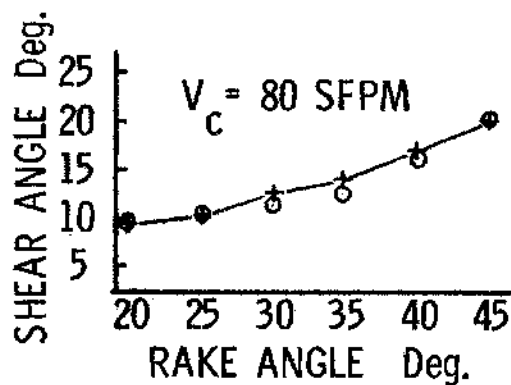




MATERIAL: 1100-O Al; TOOL MATERIAL: HSS;  $t_1 = 0.0202$  ins.

○ EXPERIMENTAL DATA POINT; + PREDICTED DATA POINT;

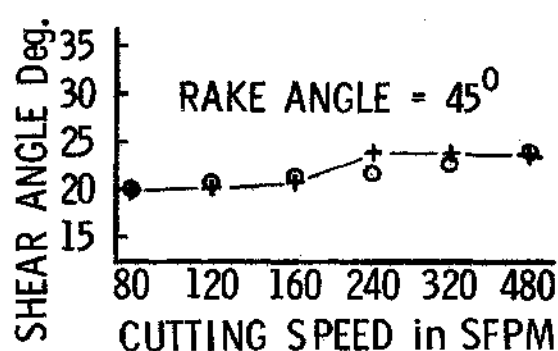
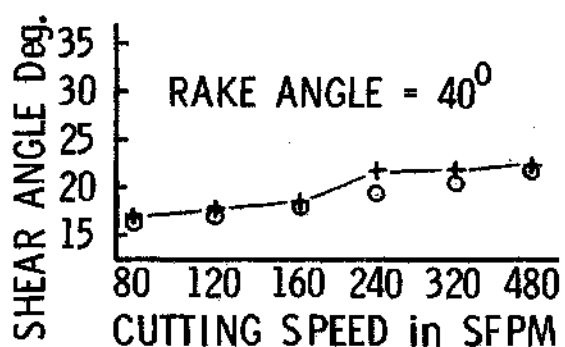
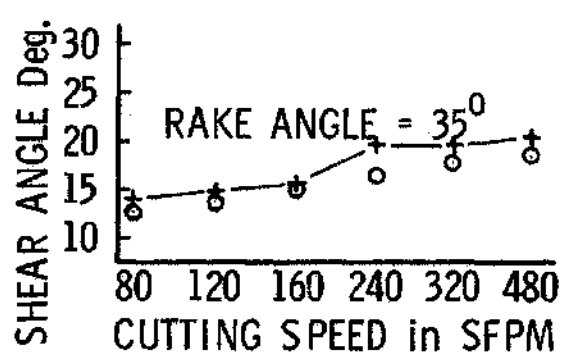
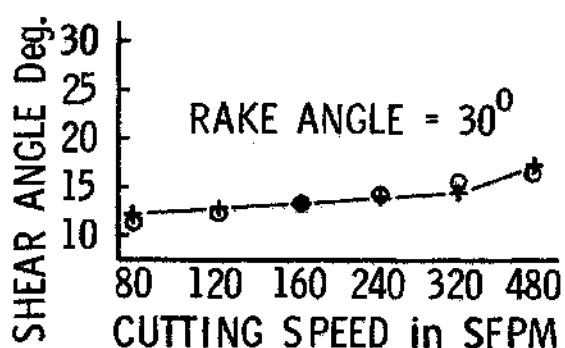
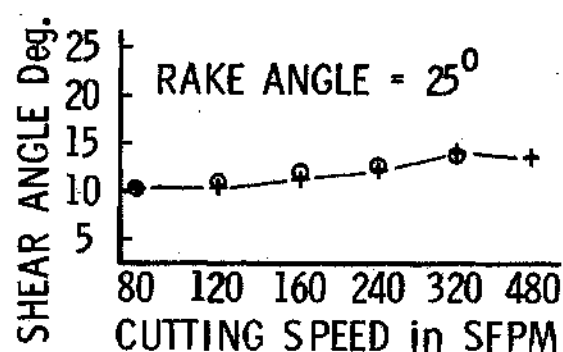
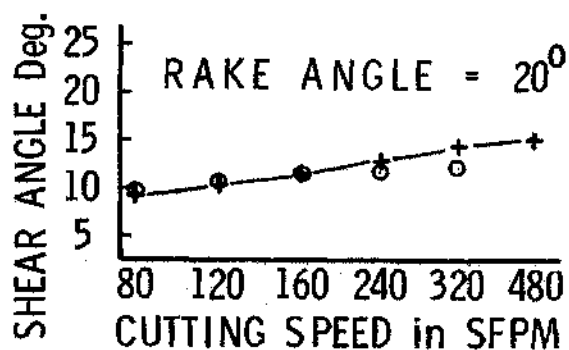
FIGURE 31: FRICTION ANGLE vs. CUTTING SPEED  
FOR VARIOUS RAKE ANGLES



MATERIAL: 1100-O Al; TOOL MATERIAL: HSS;  $t_1 = 0.0202$  ins.

○ EXPERIMENTAL DATA POINT; ✕ PREDICTED DATA POINT;

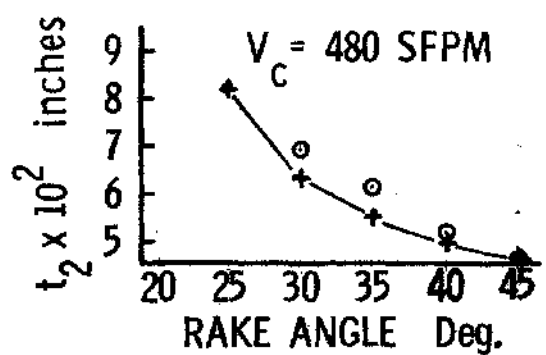
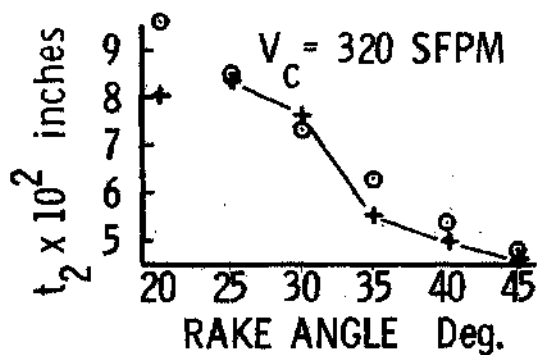
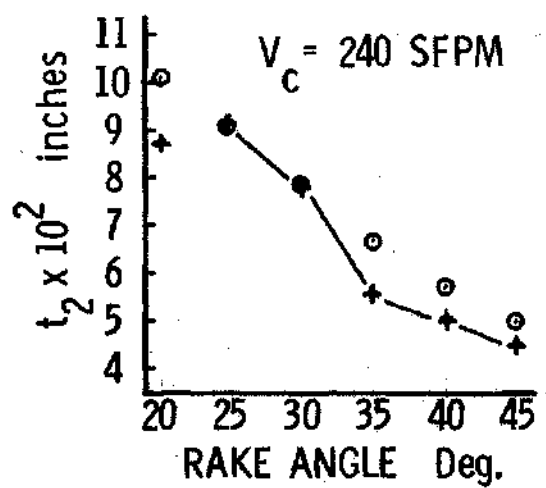
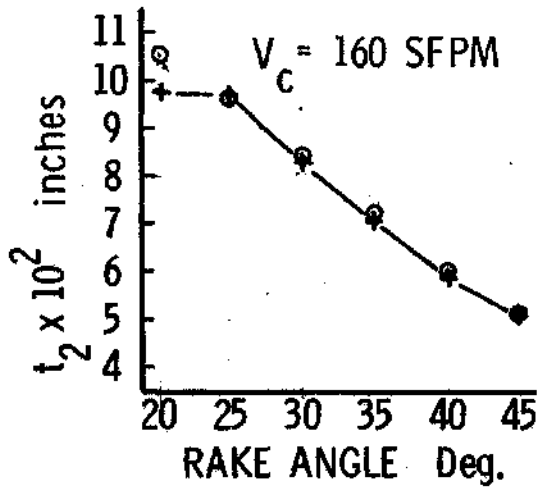
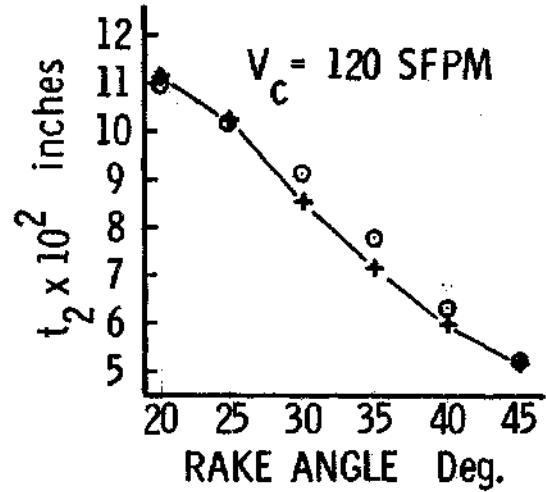
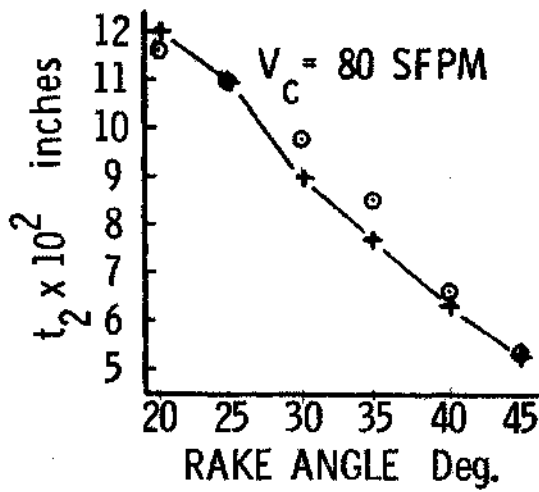
FIGURE 32: SHEAR ANGLE vs. RAKE ANGLE  
FOR VARIOUS CUTTING SPEEDS



MATERIAL: 1100-O Al; TOOL MATERIAL: HSS;  $t_1 = 0.0202$  ins.

◊ EXPERIMENTAL DATA POINT; —+— PREDICTED DATA POINT;

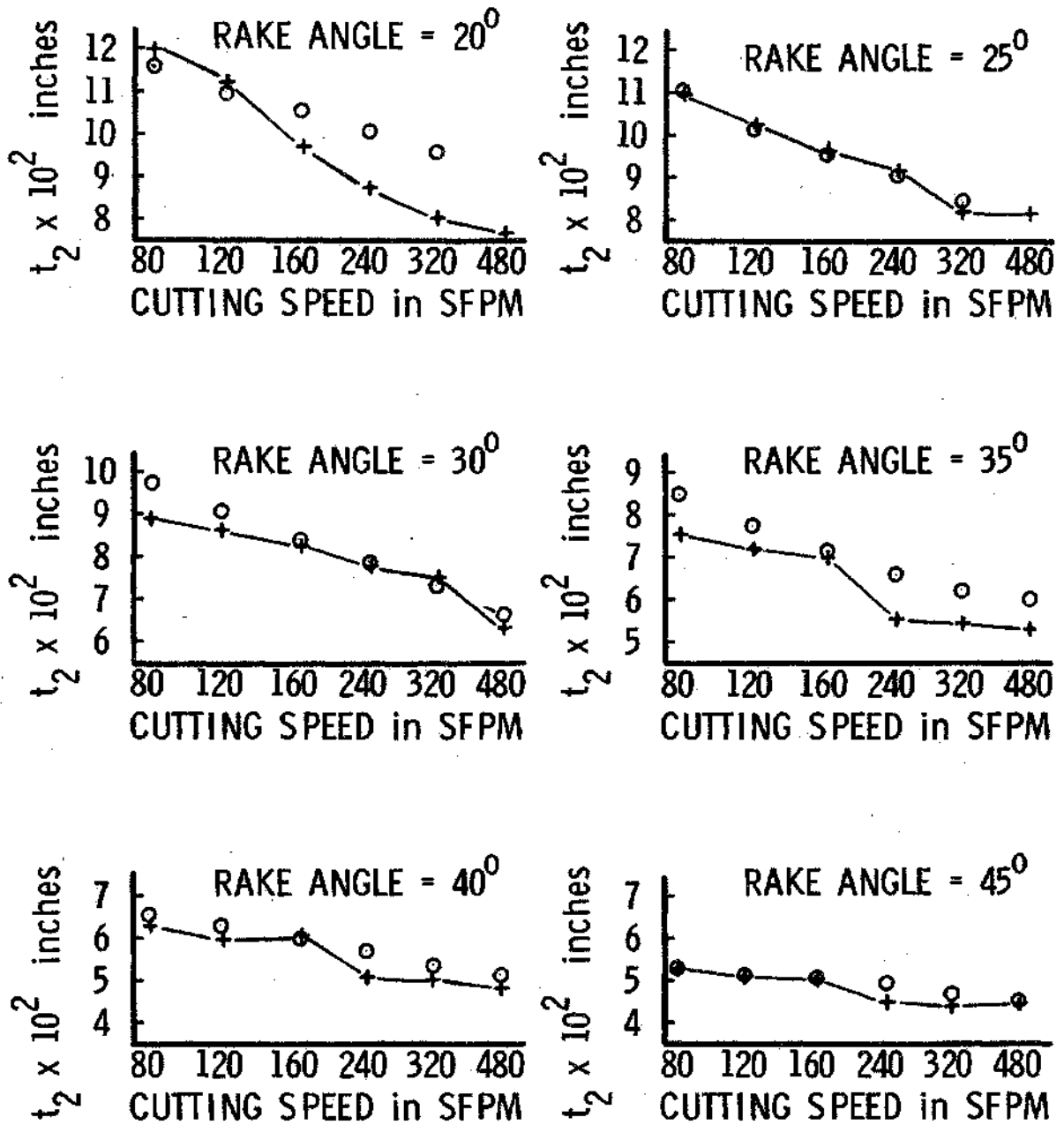
FIGURE 33: SHEAR ANGLE vs. CUTTING SPEED  
FOR VARIOUS RAKE ANGLES



MATERIAL: 1100-O Al; TOOL MATERIAL: HSS;  $t_1 = 0.0202$  ins.

◊ EXPERIMENTAL DATA POINT; + PREDICTED DATA POINT;

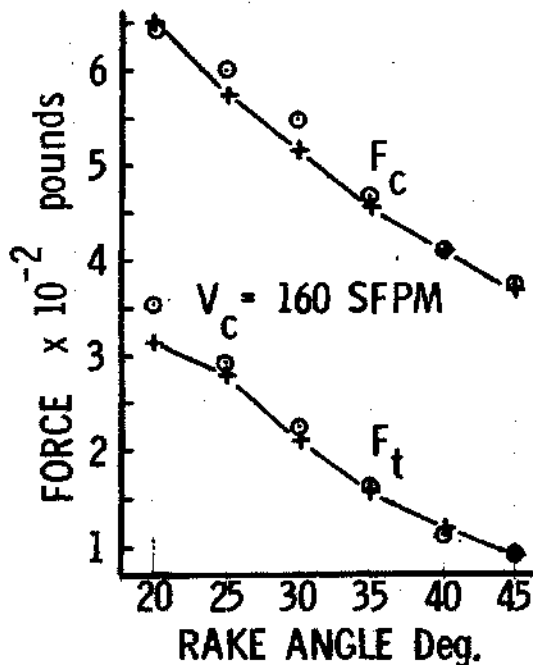
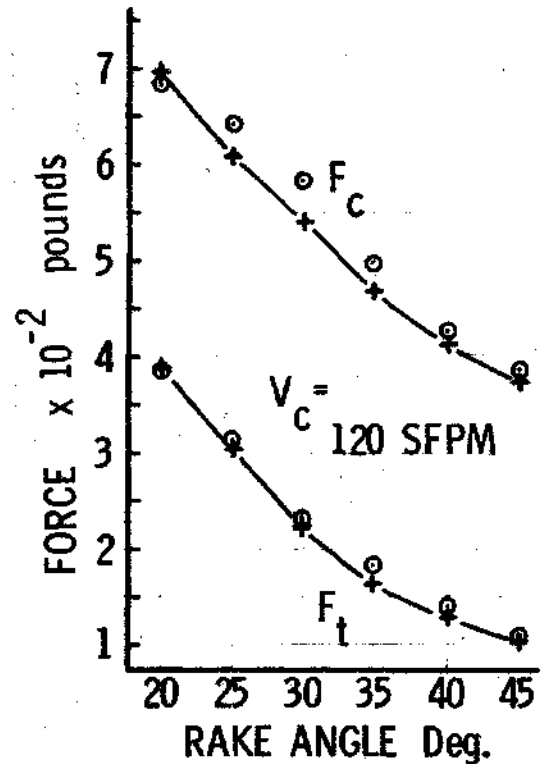
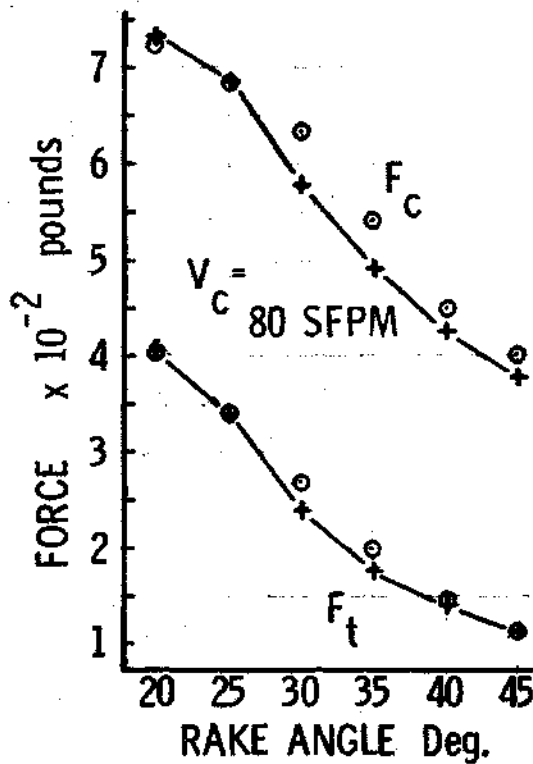
FIGURE 34: CHIP THICKNESS vs. RAKE ANGLE



MATERIAL: 1100-O Al; TOOL MATERIAL: HSS;  $t_1 = 0.0202$  ins.

○ EXPERIMENTAL DATA POINT; + PREDICTED DATA POINT;

FIGURE 35: CHIP THICKNESS vs. CUTTING SPEED



MATERIAL: 1100-O Al;  
 + PREDICTED DATA POINT;  
 o EXPERIMENTAL POINT;  
 $t_1 = 0.0202$  ins.  
 TOOL MATERIAL: HSS;

FIGURE 36a: CUTTING & THRUST FORCE vs. RAKE ANGLE  
 FOR VARIOUS CUTTING SPEEDS

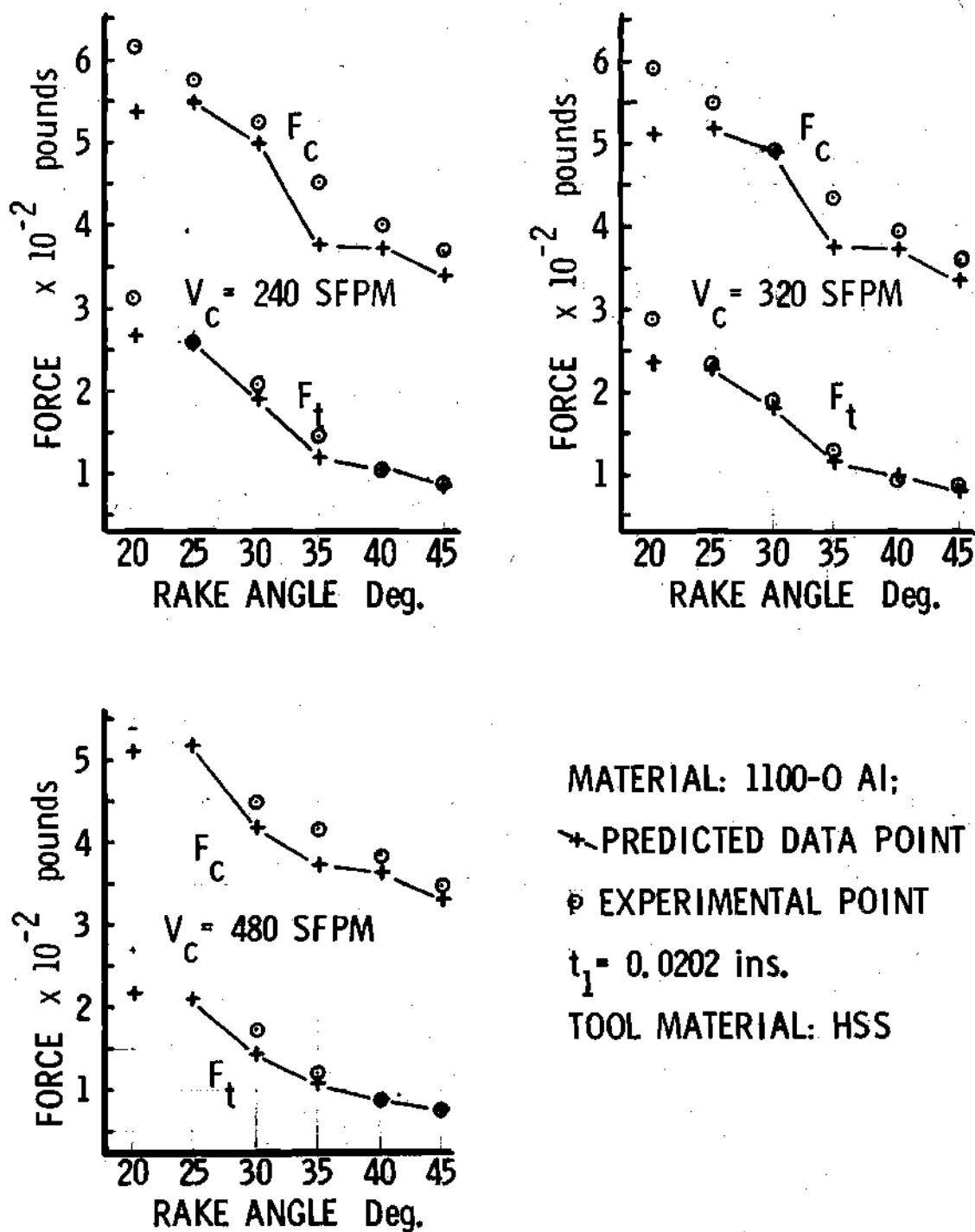
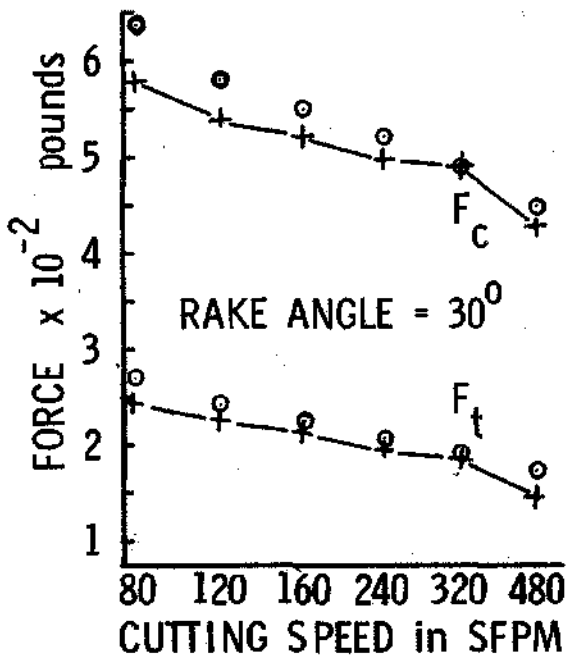
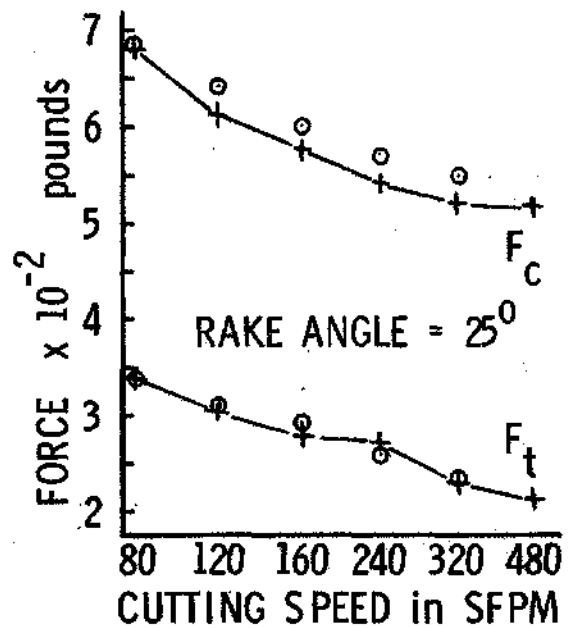
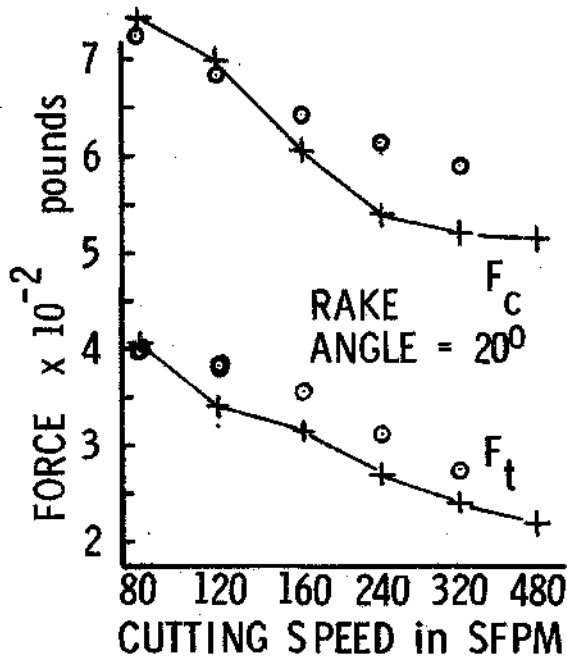


FIGURE 36b: CUTTING & THRUST FORCES vs. RAKE ANGLE FOR VARIOUS CUTTING SPEEDS



MATERIAL: 1100-O Al

+ PREDICTED DATA POINT

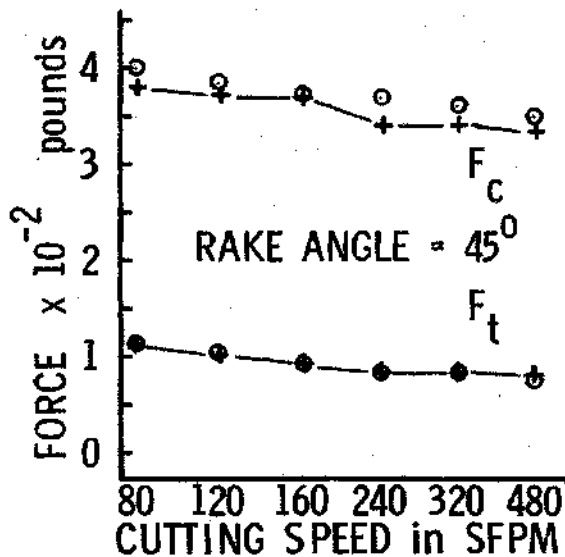
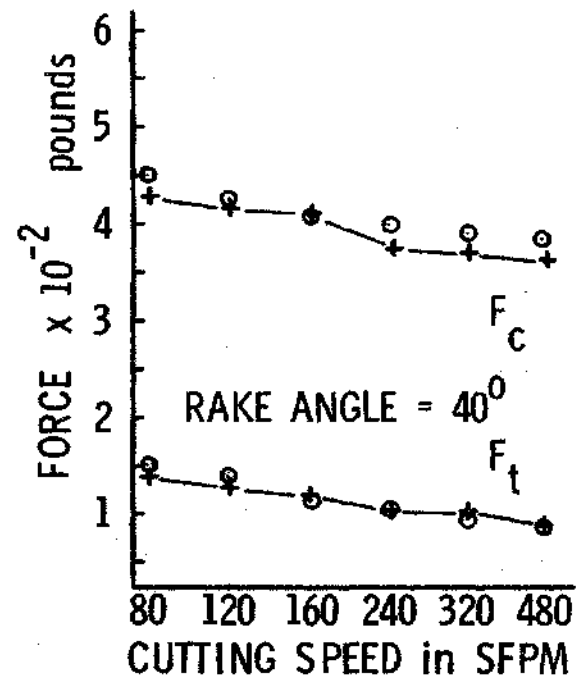
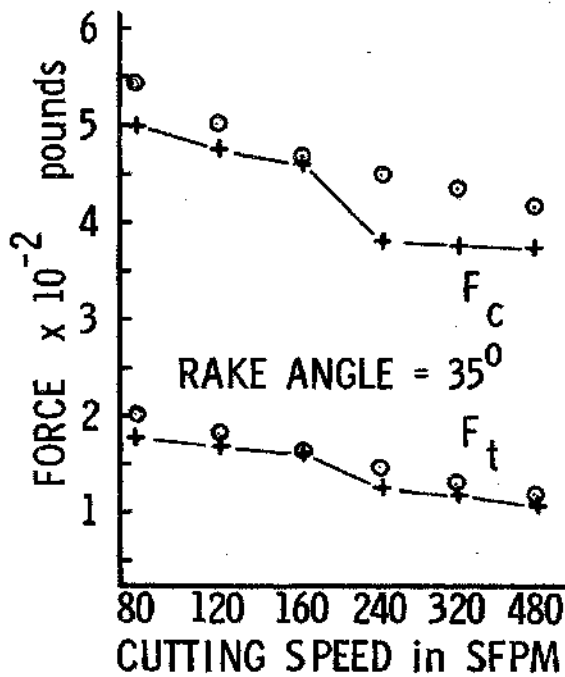
o EXPERIMENTAL POINT

$t_1 = 0.0202$  inches

TOOL MATERIAL: HSS

FIGURE 37a: CUTTING AND THRUST FORCES vs. CUTTING SPEED FOR VARIOUS RAKE ANGLES





MATERIAL: 1100-O Al

+ PREDICTED DATA POINT

o EXPERIMENTAL POINT

$t_1 = 0.0202$  inches

TOOL MATERIAL: HSS

FIGURE 37b: CUTTING AND THRUST FORCES vs. CUTTING SPEED FOR VARIOUS RAKE ANGLES

## APPENDIX II

## RATE OF WORK IN PRIMARY DEFORMATION ZONE

## APPENDIX II

### Introduction

An expression is to be derived which will relate the rate of work performed in the Primary Deformation Zone during metal cutting to the stresses and rate of deformation associated with the model of the metal cutting process which has been developed. The following analytical results are not unique in that other solutions may exist and, in fact, may be easily developed. The primary strength of the following analysis is that in use any small errors present when the model is used to investigate the results of a series of experimental tests will be systematic and in turn will be self correcting when the model is used to predict the qualitative results of a series of metal cutting tests.

### Development

The initial element is shown in Figure 38 at ABCD, as it would appear prior to deformation. After completely passing through the primary deformation zone the element can be represented by a parallelepiped of width  $w$ , height  $t_2$ , and base length EF. If ABCD is a rectangular parallelepiped of size  $t_1 \times t_1 \times w$ , then the length of EF is given by  $t_1 \times r_c$  and the deformation can be divided into two portions: (1) hypothetical pure compression from the element ABCD to an element of dimensions  $t_2 \times EF$ , i.e., a rectangular parallelepiped EFLJ; and, (2) shear deformation of this rectangular element through the angle  $\nu$  to the condition EFGH.

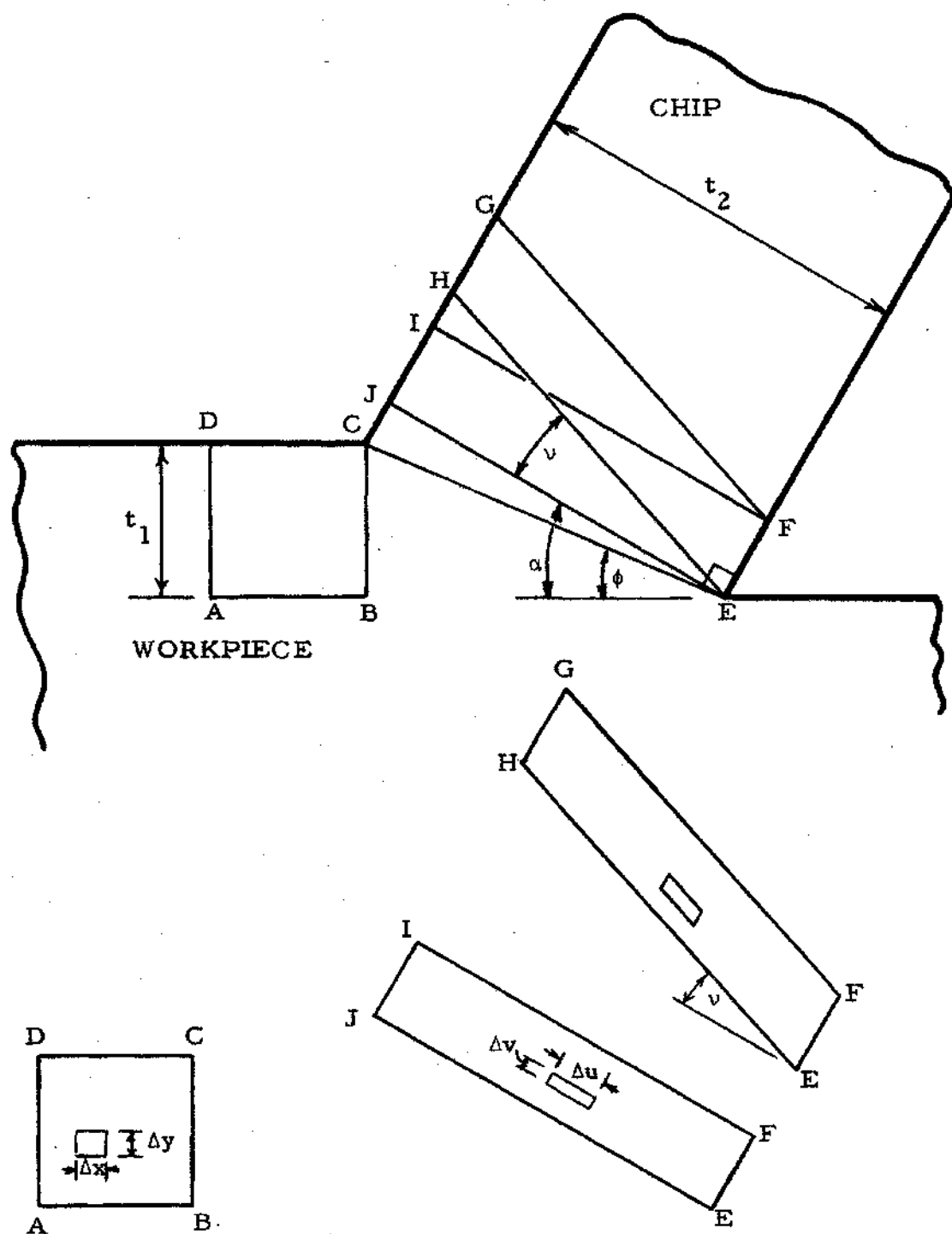


Figure 38: Shear Plane Model Used to Determine Deformation as a Function of Shear and Compression

The work performed in these two separated processes occurs simultaneously and comprises the total amount of work performed in the primary deformation zone. The pure compression deformation results in the chip segment being compressed from dimensions  $t_1 \times t_1$  to the dimensions  $t_2 \times (r_c \cdot t_1)$  where  $r_c$  is the cutting ratio. Figure 38 also shows a chip element before and after being subjected to pure compression. The average normal force on the single element will be

$$\Delta F_{av} = S_{av} w \frac{\Delta x + \Delta u}{2} , \quad (83)$$

where  $S_{av}$  is the average normal stress on the element, and  $\Delta x$  and  $\Delta u$  are defined in Figure 38.

The distance the force  $\Delta F_{av}$  moves is given by  $\Delta y - \Delta v$ . Thus, the incremental work performed is given by

$$\Delta W_c = S_{av} w \frac{(\Delta x + \Delta u)(\Delta y - \Delta v)}{2} . \quad (84)$$

No generality is lost if

$$\Delta y = \Delta x , \quad (85)$$

and since continuity of mass flow must occur, then

$$\Delta v = r_c \Delta y \quad (86)$$

and

$$\Delta u = \frac{\Delta x}{r_c} . \quad (87)$$

Substituting into Equation (83) yields

$$\Delta W_c = S_{av} w \Delta x \Delta y \left[ \frac{1 - r_c^2}{2 r_c} \right] , \quad (88)$$

and taking the limit as  $\Delta x$  and  $\Delta y \rightarrow 0$  yields

$$dW_c = S_{av} w \left[ \frac{1 - r_c^2}{2 r_c} \right] dA . \quad (89)$$

The amount of shear deformation of the element can be represented by the pure shear deformation from condition EFIJ to condition EFGH of Figure 38.

In order to find the amount of shear deformation it will temporarily be assumed that the primary deformation zone can be represented as a shear plane. No generality will be lost in this case because only the amount of shear deformation is of current interest. The mode of shear deformation will be incorporated further into the analysis.

In order to maintain continuity of material flow when an elementary particle travels (Figure 38) from point "D" to point "C" a particle that was at point "A" will have reached point "B." After crossing line CE a particle travels with velocity  $V_c r_c$ , while before it crosses line CE it travels with velocity  $V_c$ . Thus, while an element at point B travels from B to E, an element at point C travels from C to H and length CH is given by

$$CH = BE r_c , \quad (90)$$

where

$$BE = CE \cos \phi \quad . \quad (91)$$

The angle  $\nu$  can be found from

$$\tan \nu = \frac{JH}{t_2} \quad , \quad (92)$$

where

$$JH = CH - CJ \quad , \quad (93)$$

and CJ is given by

$$CJ = CE \sin(\alpha - \phi) \quad ; \quad (94)$$

and finally,

$$\cos(\alpha - \phi) = \frac{t_2}{CE} \quad . \quad (95)$$

Substituting for JH and CH in Equation (92) and simplifying gives:

$$\tan \nu = \frac{r_c \cos \phi - \sin(\alpha - \phi)}{\cos(\alpha - \phi)} \quad . \quad (59)$$

If the shear stress of deformation of the element of Figure 38 is assumed to be equal to  $S_{av}$ , then the elemental work performed will be

$$\Delta W_s = S_{av} w \Delta u \Delta v \tan \nu \quad , \quad (96)$$

and taking the limit as the element size approaches zero yields

$$dW_p = S_{av} w \left[ \frac{1 - r_c^2}{2 r_c} + \tan \nu \right] dA, \quad (97)$$

where

$$dW_p = dW_c + dW_s. \quad (98)$$

The average velocity of an element in passing through the primary deformation zone is given as

$$V_{av} = \frac{V_c (1+r_c)}{2}; \quad (99)$$

the average distance an element travels as it passes through the primary deformation zone (Figure 27) is approximately

$$D = \frac{1}{2} AB (\psi + \alpha - \xi), \quad (100)$$

where  $(\psi + \alpha - \xi)$  is expressed in radians. Thus, the average time required for an element to pass through the primary deformation zone is given as the distance divided by the velocity, or

$$T_{rq} = \frac{AB (\psi + \alpha - \xi)}{V_c (1+r_c)}. \quad (55)$$

If the elementary work is summed over the entire area of the primary deformation zone and it occurs at a rate dependent on the average time required to pass through that zone, then the work per unit time occurring in the primary deformation zone is given as:



$$W_{pt} = S_o w \left[ \frac{1 - r_c^2}{2 r_c} + \tan \nu \right] \frac{A_{pdz}}{T_{rq}}, \quad (54)$$

where the average stress of the primary deformation zone is assumed to be  $S_o$ .

## APPENDIX III

## LIST OF SYMBOLS USED

## APPENDIX III

## LISTING OF ALPHABETICAL SYMBOLS USED

$A_o$	cross-sectional area of undeformed chip
$A_{pdz}$	area of primary deformation zone
$dA$	incremental area
AB	Plane AB, length of that plane
BD	Plane BD, length of that plane
BE	Plane BE, length of that plane
BF	Plane BF, length of that plane
BG	Plane BG, length of that plane
BGC	lower boundary of Primary Deformation Zone
C	machining constant
CE	Plane CE, length of that plane
CG	Plane CG, length of that plane
CH	Plane CH, length of that plane
CJ	Plane CJ, length of that plane
d	small length of Primary Deformation Zone, Figure 27
D	average distance through Primary Deformation Zone
DF	Plane DF, length of that plane
$F_c$	cutting force component of resultant forces of cutting
$F_n$	normal force on shear plane
$F_t$	thrust force component of resultant forces of cutting

$G$	a dimensionless constant
$h$	small length of Primary Deformation Zone, Figure 27
$JH$	Plane JH, length of that plane
$K$	slope of shear stress versus normal stress curve
$k$	thermal conductivity of workpiece material
$k$	yield shear stress
$l_s$	length of shear plane
$l_o$	chip-tool contact length
$\bar{N}$	component of resultant cutting force acting normal to tool face
$N$	a dimensionless constant, the ratio of normal to shear stress acting on Plane BF; equal to 1
$N_f$	normal stress acting on chip-tool contact area
$N_o$	normal stress acting on Planes BE and BD
$N_s$	normal stress acting on Plane AB
$P$	tool nose force
$P_A$	hydrostatic stress at point A
$P_B$	hydrostatic stress at point B
$P_s$	specific cutting pressure
$q_f$	heat generated through "friction" at chip-tool interface
$q_s$	heat generated through shearing in Primary Deformation Zone
$q_{tl}$	total heat generated during metal cutting
$r_c$	cutting ratio
$R$	resultant tool force

$S$	shear stress on shear plane
$S_{av}$	average stress acting on element during deformation
$S_o$	shear stress intercept with zero normal stress on shear plane
$S_o$	shear stress on Planes BD and BE
$S_n$	normal stress on shear plane
$S_i$	initial shear strength of workpiece material
$S_f$	shear stress at chip-tool interface
$S_s$	shear stress along Plane AB and Plane BF of proposed model
$T$	temperature
$T_{rq}$	average time required for an element to pass through the Primary Deformation Zone
$t_1$	undeformed chip thickness
$t_2$	chip thickness
$V_c$	cutting speed
$w$	width of chip and workpiece
$W_{kf}$	work per unit time performed through "friction" forces
$W_{pd}$	work per unit time performed in Primary Deformation Zone as a function of the forces of cutting and the cutting velocity
$W_{pt}$	work per unit time performed in Primary Deformation Zone as a function of the stresses and deformation of that zone
$W_{tl}$	total work per unit time performed during cutting

#### Listing of Greek Symbols Used

$\alpha$	rake angle
$\beta$	friction angle

$\beta_s$	fraction of heat generated in Primary Deformation Zone that is transmitted to workpiece
$\delta$	angle parameter of proposed model
$\Delta u$	incremental length
$\Delta v$	incremental length
$\Delta W_c$	incremental work performed by compression
$\Delta W_s$	incremental work performed by shear
$\Delta x$	incremental length
$\Delta y$	incremental length
$\epsilon$	strain
$\dot{\epsilon}$	strain rate
$\eta$	angle between shear plane and direction of maximum shear stress after Shaw, et al. <sup>9</sup>
$\Gamma$	dimensionless constant
$\gamma$	shear angle parameter of proposed model
$\dot{\gamma}_i$	generalized shear strain rate
$\gamma_s$	shear strain in metal cutting
$\dot{\gamma}_1$	average strain rate of Primary Deformation Zone
$\dot{\gamma}_2$	average strain rate of Secondary Deformation Zone
$\mu$	coefficient of friction
$\omega$	an angle parameter after Huck <sup>8</sup>
$\phi$	shear angle
$\psi$	angle parameter of proposed model
$\rho$	density of workpiece material
$\sigma$	stress

$\sigma_o$	a stress constant
$\tau$	shear stress
$\tau_i$	individual shear stress
$\theta$	angle parameter after Palmer and Oxley <sup>18</sup>
$\theta$	thermal number
$\theta_f$	average temperature rise of the chip due to "friction" at the chip-tool interface
$\theta_{ma}$	maximum temperature rise of the chip above ambient temperature at the chip-tool interface
$\theta_{mx}$	maximum temperature rise of the chip due to "friction" at the chip-tool interface
$\theta_s$	average temperature rise of the chip as a result of shear deformation in the Primary Deformation Zone
$\theta_{ts}$	maximum possible average temperature rise of the chip due to deformation in the Primary Deformation Zone
$\nu$	angle of shear deformation required to maintain mass flow continuity
$\xi$	angle parameter of proposed model

## APPENDIX IV

## COMPUTER PROGRAMS



## APPENDIX IV

### Introduction

The following computer programs were used to determine the applicability of the model, analyze experimental results, and then predict the trends inherent to the metal cutting process.

The first program, called PR 6 PROCEDURE OPTIONS (MAIN), reads experimental metal cutting data from a single test in step number 38. The model is then used to analyze this data and, after determination of an applicable geometry is made, the output is printed in steps 311 to 319. This process is repeated until no data is found in the data storage and the condition **END FILE** exists. Computation then terminates.

The second program, called PR 4 PROCEDURE OPTIONS (MAIN), has several subroutines in it. One of these subroutines, called FNCTN, beginning in step number 405 defines the model developed in this work. The preceding 400 steps are required to define the problem and provide a complex iterative procedure required to select the proper geometry which will satisfy all of the constraints of the system.

The third program, called PR 2 PROCEDURE OPTIONS (MAIN), is used to determine the appropriate constants for Equation (79). Several equations are tried of the forms proposed by various workers<sup>15,24,21</sup>, and that proposed by Lubahn<sup>21</sup> was found to approximate closely the final conditions. Slight modification of this equation resulted in Equation (79).

## PR6: PROCEDURE OPTIONS (MAIN)

```

1      PR6: PROCEDURE OPTIONS (MAIN)
2      ON ENDFILE (SYSIN) GO TO LBL
3      ON ZERO DIVIDE GO TO LBL1
4      DECLARE I DECIMAL (8) , K DECIMAL , LAB DECIMAL , LBE DECIMAL (9) ,
5              LBF DECIMAL (9) , LO DECIMAL (9) , LT1R DECIMAL , LT2R DECIMAL
6              , NOSO DECIMAL , NS DECIMAL (10) , KE1 DECIMAL , KE2 DECIMAL :
7      DECLARE ( LBC , WI , KSP , H
8              ) DECIMAL :
9      DECLARE ZH(30) , HQ(35) , H1(35) , LBH DECIMAL
10     DECLARE ( HH,GG,TT,V,JJ,KK,CT
11             ) BINARY FIXED
12     DECLARE R0(25) , CH(25)
13     DECLARE AR1(50,10) , AR2(50,10) , P0(45) , P1(45) , P2(25) , PS(45) , G0(25)
14     DECLARE R1(25)
15     DECLARE DL(20) , BS(20) , G1(25)
16     PMTCK: FORMAT ( 12 F(10,4) )
17     PMT01: FORMAT ( 2F(9,1) , F(9,3) , 2F(9,4) , 2F(9,1) , 2F(9,2) , 4F(9,0) , A(3) )
18     PMT02: FORMAT ( 3F(10,3) , 3F(10,3) , 5F(10,1) , F(10,4) )
19     PMT03: FORMAT ( 4F(10,4) , 2F(10,0) , F(10,2) , 2F(10,2) , 4F(10,0) )
20     DTA2:  FORMAT ( X(1) , F(7,1) , X(2) , F(6,2) , X(2) , F(6,3) , X(2) ,
21             F(6,4) , X(2) , F(7,5) , X(2) , F(6,4) , X(2) , 2(F(5,2) , X(2)) , F(15,5) )
22     DTA3:  FORMAT ( X(1) , F(7,1) , X(2) , F(6,2) , X(2) , F(6,3) , X(2) , X(48) ,
23             F(6,4) , X(2) , F(7,5) , X(2) , F(6,4) , X(2) , 2(F(5,2) , X(2)) , F(7,5) )
24
25     L = 0 ;
26     SSN = 25000
27     SOW = 25000
28     SSSON = 2 ; PSIDN = 45 ;
29     PI = 3.1415926536
30     DTR = PI/180.0
31     RTD = 180.0/PI
32     P = 0.0975
33     K = 10.81
34     CP = 0.243
35     SII = 15000
36     NOSO = 1.0
37     TT = 0
38     C34 = 1.0
39
40     LBL0:
41     IF MOD(L,5) = 0 THEN
42     PUT EDIT ('.') (PAGE , X(119) , A(1) )
43     L = L + 1 ;
44     GET EDIT ( I,VC,ALPD,W,T1,T2,RCH,RTH,CLO ) ( R(DTA2)
45     PSID = 0.0005
46     JC = 10
47     J = 0
48     GG = 0
49     CT = 0
50     HH = 1
51     ALPD = ALPD
52     IF ALPD < 26 THEN PSID = 10.005
53     ALFR = ALPD * DTR
54     PT = 17.4*RTH
55     PC = 16.7*RCH
56     RC = T1/T2
57     FIT = (RC * COS(ALFR))/( 1 - RC*SIN(ALFR))

```

## PR6: PROCEDURE OPTIONS (MAIN)

```

53      PFIR= ATAN(PIT) ; PFID = PFIR*RTD ;
55      QF = VC*RC*(PC*SIN(ALFR) + PT*COS(ALFR))/1400 ;
56      THF = QF/(12*P*CP*VC*T1*W) ;
57      QS = PC*VC/1400 - QF ;
58      R = 720*P*CP*VC*T1/K ;
59      THNB = R*FIT ; THNB = ABS(THNB) ;
61      IF THNB > 12.0 THEN BETA = 0.10; ELSE BETA = 0.475 - 0.1498*LOG(THNB) ;
64      THS = QS*(1-BETA)/(12*P*CP*VC*T1*W) ;
65      THRS= THS/(1-BETA) ;
66      BER = ALFR + ATAN(PT/PC) ; BED = BER*RTD ;
68      F = PC*SIN(ALFR) + PT*COS(ALFR) ;
69      FN = PC*COS(ALFR) - PT*SIN(ALFR) ;
70      WTL = PC*VC ;
71      WKF = P*VC*RC ;
72      WPD = WTL - WKF ;
73      THT = ATAN((RC*COS(PFIR) - SIN(ALFR-PFIR))/(COS(ALFR-PFIR))) ;
74      THT = ATAN((RC*COS(PFIR) - SIN(ALFR-PFIR))/(COS(ALFR-PFIR))) ;
75      TTHT= ((RC*COS(PFIR) - SIN(ALFR-PFIR))/(COS(ALFR-PFIR))) ;
76      TTHT = ABS(TTHT) ;
77      THTD= THT*RTD ;
78      SSSO= 1.40 ;
79      LB3:
80      IF J > JC THEN GO TO LB5 ;
81      CT = CT + 1 ;
82      IF CT > 51 THEN GO TO LB1 ;
84      IF TT > 40 THEN GO TO LBL ;
86      SSSOH= SSSO ;
87      PSIR = PSID*DTR ;
88      Y = ((PT/PC-1)*COS(ALFR+PSIR) + (PT/PC+1)*SIN(ALFR+PSIR))/(SSSO*
      SIN(PSIR)) ;
89      DELR = ATAN((Y*COS(ALFR) + PT/PC - WOSO)/(Y*SIN(ALFR)+WOSO*PT/PC+1)) ;
90      DELD = DELR*RTD ;
91      PSYD = PSID ;
92      SSSO= SSSOH ;
93      PP = 1.0 + (SIN(PSIR))/(COS(PSIR)) ;
94      PM = 1.0 - (SIN(PSIR))/(COS(PSIR)) ;
95      CPPS= COS(PSIR) + SIN(PSIR) ;
96      ZZ = RC + (((SIN(PSIR))*SIN(DELR)))/(COS(DELR+ALFR)*CPPS)) ;
97      GNT = (ZZ*(COS(ALFR))/(1.0/PP) - ZZ*(SIN(ALFR))) ;
98      GNR = ATAN(GNT) ; GND = GNR*RTD ;
100     SSSO= (PP*COS(GNR-ALFR) - PM*SIN(GNR-ALFR))*COS(GNR-ALFR) ;
101     IF CT = 1 THEN GO TO LB3 ;
103     LT2R= COS(PSIR+ALFR+DELR)/(CPPS*COS(ALFR+DELR)) ;
104     LT1R= LT2R/RC ;
105     LO = LT1R*T1 ;
106     LBE = T2/PPS ;
107     LBF = (LBE*(SIN(PSIR)))/(COS(ALFR+DELR)) ;
108     LAB = LBE*(COS(PSIR))/(COS(GNR-ALFR)) ;
109     RCAB = (SIN(GNR))/(SIN(2*GNR-ALFR-PSIR)) ;
110     LBC = LAB*RCAB ;
111     SSSOH=SSSO ;
112     SO = PC/((W*(LBE*(SIN(PSIR+ALFR) + COS(PSIR+ALFR)) +
      SSSO*LRF*(COS(DELR) - WOSO*(SIN(DELR)))))) ;

```

## PR6: PROCEDURE OPTIONS (MAIN)

```

113      SP50= (PM/(PP-1) + SSSO*(SIN(ALPB+DELR)/COS(ALPB+DELR) + NOSO))/
114      (1/(PP-1) - SIN(ALPB+DELR)/COS(ALPB+DELR))
115      SSSO=SSSOH
116      SFT1= SP50*SO
117      SS = SO*SSSO
118      E = (SIN(PFIR-ALPB))/(COS(PFIR-ALPB)) + (COS(PFIR))/(SIN(PFIR))
119      B = SORT(ABS(R/LT2R))
120      THMX= 0.72*THP*B*(0.856*(B*LT2R*(PP-1)/2.5))
121      THMA= THMX + THS
122      PS = P/(LO*N)
123      NS = (COS(PSIR+ALPB-GMR)-SIN(PSIR+ALPB-GMR))*SO*LBE/LAB
124      ET1 = 0.1*E*VC*(1 + RC)/(LBE*(PSIR+ALPB-GMR))
125      ET2 = 0.4*VC*RC/(LO*(PP-1))
126      IF ET2 < 0.0001 THEN ET2 = 1.0
127      SFT2= 477*(E**1.577)*(ET2**0.290)
128      N = 1
129      CH(1) = 15.0
130      CH(2) = 20.0
131      LB6:
132      IF CH(N) > GMD THEN CH(N) = 10
133      IF CH(N) < 0.01 THEN CH(N) = 2
134      CHID = CH(N)
135      CHIR = CHID*DTR
136      AA = (2*COS(CHIR))*(SIN(GMR) - SIN(CHIR)) + 1.0
137      DD = SS*COS(GMR-CHIR) + NS*SIN(GMR-CHIR)
138      SI = DD/AA
139      RO(N) = SI - SII
140      IF N = 1 THEN DO ; N = 2 ; GO TO LB6 ; END
141      IF ABS(RO(N)) > 1.0 THEN DO
142      R1(N) = (RO(N)-RO(N-1))/(CH(N) - CH(N-1))
143      CH(N+1) = CH(N) - RO(N)/R1(N)
144      N = N + 1
145      IF N > 25 THEN GO TO LB1
146      GO TO LB6
147      END /* IF RO(N) > 1.0 */
148      H = LAB*(SIN(GMR) - SIN(CHIR))
149      D = LAB*(COS(CHIR) - COS(GMR))
150      CC = NS*COS(GMR-CHIR) - SS*SIN(GMR-CHIR)
151      NI = CC
152      APDZ = (LAB**2)*(PSIR+ALPB-CHIR)/2 + H*(H+D)/2
153      TRQ = LAB*(PSIR+ALPB-CHIR)/(VC*(1+RC))
154      WPT = SO*N*((1-RC**2)/(2*RC) + TTHT)*APDZ/TRQ
155      REZ = WPD - WPT
156      IF GG > 0 THEN DO
157      FO(J) = WPD - WPT
158      IF ABS(FO(J)) < WPD/5000 THEN GO TO LB5
159      END
160      IF J > 2 THEN F1(J) = (FO(J) - FO(J-1))/(PS(J) - PS(J-1))
161      IF GG = 5 THEN GO TO LB5
162      IF GG = 0 THEN DO
163      IF WPT<WPD THEN DO
164      IF J = 0 THEN DO
165      J = 1

```

## PR6; PROCEDURE OPTIONS (MAIN)

```

180          GG = 1
181          PS(1) = PSID + 1
182          DO N = 1 TO 16
183             PS(N) = PS(1) + 1 - N
184          END
185          END
186          JC = J + N
187          END
188          END
189          IF GG = 0 THEN DO
190             IF PSID < 45 THEN DO : PSID = PSID + 5 : GO TO LB3 :END
191             IF J = 0 THEN GO TO LB1
192          END
193          IF GG = 1 THEN DO
194             IF WPT > WPD THEN DO
195                GG = 2
196                DO N = 1 TO 14
197                   PS(J+N) = PS(J) - 0.4 + N/5
198                END
199                JC = J + N
200                END
201                J = J + 1
202                PSID = PS(J)
203                GO TO LB3
204            END
205            IF GG = 2 THEN DO
206                IF WPT < WPD THEN DO
207                   DO N = 1 TO 15
208                      PS(J+N) = PS(J) + 0.12 - 0.04*N
209                   GG = 3
210                END
211                JC = J + N
212                END
213                J = J + 1
214                PSID = PS(J)
215                GO TO LB3
216            END
217            IF GG = 3 THEN DO
218                IF WPT > WPD THEN DO
219                   DO N = 1 TO 14
220                      PS(J+N) = PS(J) - 0.02 + 0.005*N
221                   GG = 4
222                END
223                JC = J + N
224                END
225                J = J + 1
226                PSID = PS(J)
227                IF ABS(F0(J-1)) > 10.0 THEN GO TO LB3
228            END
229            IF GG = 4 THEN DO
230                IF WPT < WPD THEN DO
231                   PS(J+1) = PS(J) - F0(J)/F1(J)
232                   GG = 5

```

## PR6: PROCEDURE OPTIONS (MAIN)

```

248         END
249         J = J + 1
250         PSID = PS(J)
251         GO TO LB3
252     END
253 LB5:
254     RR = (H + D + LAB * COS(GMR) - LBE * COS(PSIR + ALPR)) / COS(ALPR)
255     N = 1
256     ZH(1) = 10.0 ; ZH(2) = 15.0
257 LB2:
258     IF ZH(N) > (90.0 - ALFD) THEN ZH(N) = 40
259     IF ZH(N) < 0.01 THEN ZH(N) = 2.0
260     ZHID = ZH(N)
261     ZHIR = ZHID * DTR
262     AG = COS(ALPR) / COS(GMR) - SIN(ALPR) / SIN(GMR) +
263         LBE * (COS(PSIR + ALPR) / COS(GMR) - SIN(PSIR + ALPR) / SIN(GMR)) / PR
264     HO(N) = SIN(ZHIR) / COS(ZHIR) - COS(ZHIR) / SIN(GMR) - AG
265     IF N = 1 THEN DO ; N = 2 ; GO TO LB2 ; END
266     IF ABS(HO(N)) > 0.0001 THEN DO
267         H1(N) = (HO(N) - HO(N-1)) / (ZH(N) - ZH(N-1))
268         ZH(N+1) = ZH(N) - HO(N) / H1(N)
269         N = N + 1
270         IF N > 25 THEN GO TO LB4
271         GO TO LB2
272     END /* IF HO(N) > 0.0001 */
273 LB1:
274     LBH = (H + D + LAB * COS(GMR) - RR * SIN(ZHIR)) / COS(GMR)
275     TSS = LAB * SS / LBH
276 LB4:
277     SK0 = 1.12033 ; GK = 6.08377 ; T = THHS / 1000 ; AA = -0.0123976 ;
278     BR = 0.340303 ; CC = -0.16177 ;
279     SSSOP = SK0 * (GK ** T) * (R ** (AA + BR * T)) * (ET1 ** (CC * T))
280     SSK = 15830 ; GSK = 8305.47 ; AAS = -0.492552 ; BRS = -2.16237 ;
281     CCS = -0.120091 ;
282     SSP = SSK * (GSK ** T) * (R ** (AAS + BRS * T)) * (ET1 ** (CCS * T))
283     SOP = SSP / SSSOP ;
284     T = THHA / 1000 ;
285     SPO = EXP(14.1042) ;
286     GK = EXP(-13.2560) ;
287     AA = -1.84670 ;
288     BB = 15.7909 ;
289     CC = -0.246249 ;
290     DD = 1.19791 - 1.36858 * (LOG(R)) ;
291     SPE1 = SPO * (GK ** T) * (R ** (AA + BB * T)) * (ET2 ** (CC + DD * T)) ;
292     SPT2 = SPE1 ;
293     SPT3 = SPT2 * SOP / SO
294     SFSOP = SPT1 / SOP
295     ESOP = 100 * (SOP - SO) / SO
296     ESSP = 100 * (SSP - SS) / SS
297     ESSSOP = 100 * (SSSOP - SSSO) / SSSO
298     ESPT2 = 100 * (SPT2 - SPT1) / SPT1 ; ESPT3 = 100 * (SPT3 - SPT1) / SPT1
299     PUT EDIT ( ' ITERATIONS ON TEST NUMBER ', I, ' ARE COMPLETE WITH ', J,
300             ' ITERATIONS AND A WORK DIFFERENCE OF ', RE2, ' PT-LB/MIN' )
301

```

## PR6: PROCEDURE OPTIONS (MAIN)

```

312      (SKIP(3), A(27), P(6), A(19), P(3), A(36), X(8), P(11,3), A(10) );
PUT EDIT ('.....VC.....ALPD.....W.....T1.....T2.....PC.....',
          'FT.....PFID.....BED.....WTL.....WPD.....THS.....THMA')
          (A(56), X(6), A(58) );
313 PUT EDIT ('VC,ALPD,W,T1,T2,PC,FT,PFID,BED,WTL,WPD,THS,THMA','...')
          ( R(PMT01) )
314 PUT EDIT ('      LO      LBR      LBP      LAB      ET1      ET2'
          , '      F      WSD      NOSO      WPT      WKP      SPT2'
          , '      A(60), A(60) )
315 PUT EDIT ('LO,LBR,LBP,LAB,ET1,ET2,F,WSD,NOSO,WPT,WKP,SPT2') (R(PMT03));
316 PUT EDIT ('      PSYD      GND      DELD      RC      LT1R      LT2R'
          , '      SPT1      FS      SO      SS      NS      SSSO'
          , '      A(59), X(1), A(60) )
317 PUT EDIT ('PSYD,GND,DELD,RC,LT1R,LT2R,SPT1,FS,SO,SS,NS,SSSO') (R(PMT02));
318 PUT DATA ( THS, SOP, PSOP, BSSP, SSP, BSSSOP, SSSOP )
319 PUT DATA ( SPT2, ESPT2, CHID )
320 SOT = SOT + SO
321 SST = SST + SS
322 IF SO < SON THEN SON = SO
323 IF SS < SSN THEN SSN = SS
324 IF SO > SOX THEN SOX = SO
325 IF SS > SSX THEN SSX = SS
326 SSSOS = SSSOS + SSSO
327 IF SSSO > SSSOX THEN SSSOX = SSSO ; IF SSSO < SSSON THEN SSSON = SSSO
328 IF PSID < PSIDN THEN PSIDN = PSID
329 IF PSID > PSIDX THEN PSIDX = PSID
330 TT = TT + 1
331 GO TO L80
332 LBL:
333 PUT EDIT ('.' ) ( SKIP(1), A(1) )
334 PUT EDIT ('.....' ) ( PAGE,X(95), A(25) )
335 SOA = (SOT-SON-SOX)/(TT - 2 )
336 SSA = (SST-SSX-SSN)/(TT-2)
337 SSSOA = (SSSOS-SSSOX-SSSON)/(TT-2)
338 VSO = (SOX-SON)/SOA
339 VSS = (SSX-SSN)/SSA
340 VSSSO = (SSSOX-SSSON)/SSSOA
341 PUT DATA ( VSO, SOA, SON, SOX, VSS, SSA, SSN, SSX, TT )
342 PUT DATA ( PSIDX, PSIDN, SSSOX, SSSON, SSSOA, VSSSO )
343 END PR6

```







ITERATIONS ON TEST NUMBER 43169 ARE COMPLETE WITH 21 ITERATIONS AND A WORK DIFFERENCE OF -6.171 FT-LB/MIN

VC	ALPD	W	T1	T2	FC	FT	PFID	BED	WTL	WPD	THS	THMA
156.0	45.0	0.284	0.0201	0.0509	375.7	95.6	21.25	59.28	58616	38018	66	178...
LO	LBE	LBP	LAB	BT1	BT2	E	WSD	NOSO	WPT	WKP	SPT2	
0.0343	0.0480	0.0139	0.0487	3906	11157	2.13	0.00	1.00	38025	20598	34502	
PSYD	GMD	DELD	RC	LT1R	LT2R	SPT1	FS	SO	SS	NS	SSSO	
3.690	34.515	32.168	0.396	1.700	0.673	34059.7	34059.6	18064.4	21616.6	12899.0	1.1966	
TTSS= 1.06355E+02	SOP= 1.79605E+04	ESOP= -5.75132E-01	BSSP= -3.91192E-01	SSP= 2.15320E+00	SSSOP= 1.84974E-01	SSSOP= 1.19845E+00;	SPT2= 3.45026E+04	ESPT2= 1.30827E+00	CHID= 1.33156E+01;			

ITERATIONS ON TEST NUMBER 43168 ARE COMPLETE WITH 24 ITERATIONS AND A WORK DIFFERENCE OF -5.832 FT-LB/MIN

VC	ALPD	W	T1	T2	FC	FT	PFID	BED	WTL	WPD	THS	THMA
156.0	40.0	0.284	0.0201	0.0599	409.1	113.0	18.20	55.53	63827	45846	76	174...
LO	LBE	LBP	LAB	BT1	BT2	E	WSD	NOSO	WPT	WKP	SPT2	
0.0410	0.0549	0.0146	0.0556	3503	5273	2.63	0.00	1.00	45452	18380	31827	
PSYD	GMD	DELD	RC	LT1R	LT2R	SPT1	FS	SO	SS	NS	SSSO	
5.539	29.243	28.638	0.336	2.033	0.684	29894.6	29894.3	16921.1	20727.6	11312.2	1.2249	
TTSS= 1.27134E+02	SOP= 1.70237E+04	ESOP= 6.06329E-01	BSSP= 8.45471E-01	SSP= 2.09028E+04	BSSSOP= 2.37687E-01	SSSOP= 1.22786E+00;	SPT2= 3.18270E+04	ESPT2= 6.46392E+00	CHID= 1.21891E+01;			

ITERATIONS ON TEST NUMBER 43167 ARE COMPLETE WITH 21 ITERATIONS AND A WORK DIFFERENCE OF 1.156 FT-LB/MIN

VC	ALPD	W	T1	T2	FC	FT	PFID	BED	WTL	WPD	THS	THMA
156.0	34.3	0.284	0.0201	0.0719	467.5	165.2	15.38	53.78	72945	55431	88	189...
LO	LBE	LBP	LAB	BT1	BT2	E	WSD	NOSO	WPT	WKP	SPT2	
0.0420	0.0615	0.0217	0.0607	3635	2171	3.29	0.00	1.00	55430	17513	34055	
PSYD	GMD	DELD	RC	LT1R	LT2R	SPT1	FS	SO	SS	NS	SSSO	
10.847	28.329	23.435	0.280	2.082	0.584	33371.9	33375.5	16205.2	20459.7	10953.2	1.2625	
TTSS= 1.55066E+02	SOP= 1.62275E+04	ESOP= 1.37517E-01	BSSP= 4.29750E-01	SSP= 2.05476E+04	BSSSOP= 2.91797E-01	SSSOP= 1.26621E+00;	SPT2= 3.40557E+04	ESPT2= 2.04902E+00	CHID= 1.22472E+01;			

ITERATIONS ON TEST NUMBER 43166 ARE COMPLETE WITH 23 ITERATIONS AND A WORK DIFFERENCE OF -12.062 FT-LB/MIN

VC	ALPD	W	T1	T2	FC	FT	PFID	BED	WTL	WPD	THS	THMA
156.0	29.6	0.284	0.0201	0.0839	551.0	226.1	13.34	51.96	85971	68369	105	215...
LO	LBE	LBP	LAB	BT1	BT2	E	WSD	NOSO	WPT	WKP	SPT2	
0.0406	0.0671	0.0307	0.0640	3541	1187	3.92	0.00	1.00	69381	17602	40322	
PSYD	GMD	DELD	RC	LT1R	LT2R	SPT1	FS	SO	SS	NS	SSSO	
17.261	28.608	19.960	0.240	2.013	0.484	40471.5	40470.8	16224.0	21861.4	10792.5	1.322E	
TTSS= 1.91258E+02	SOP= 1.61760E+04	ESOP= -2.95832E-01	BSSP= -4.58252E-01	SSP= 2.13631E+04	BSSSOP= -1.62932E-01	SSSOP= 1.32066E+00;	SPT2= 4.03229E+04	ESPT2= -3.67204E-01	CHID= 1.04906E+01;			

ITERATIONS ON TEST NUMBER 43165 ARE COMPLETE WITH 36 ITERATIONS AND A WORK DIFFERENCE OF -7.687 FT-LB/MIN

VC	ALPD	W	T1	T2	FC	FT	PFID	BED	WTL	WPD	THS	THMA
156.0	25.3	0.284	0.0201	0.0959	601.1	295.7	11.80	51.57	93787	76556	113	235...
LO	LBE	LBP	LAB	BT1	BT2	E	WSD	NOSO	WPT	WKP	SPT2	
0.0359	0.0727	0.0424	0.0669	3865	826	4.54	0.00	1.00	76563	17231	48047	
PSYD	GMD	DELD	RC	LT1R	LT2R	SPT1	FS	SO	SS	NS	SSSO	
23.851	31.757	25.759	0.210	1.779	0.374	51245.2	51243.9	15481.1	21096.7	10994.6	1.3627	
TTSS= 2.14160E+02	SOP= 1.53293E+04	ESOP= -9.80377E-01	BSSP= -1.35408E+10	SSP= 2.08110E+04	BSSSOP= -3.77413E-01	SSSOP= 1.35759E+00;	SPT2= 4.80477E+04	ESPT2= -6.23965E+00	CHID= 1.36390E+01;			







ITERATIONS ON TEST NUMBER 43124 ARE COMPLETE WITH 41 ITERATIONS AND A WORK DIFFERENCE OF -12.812 FT-LB/MIN

VC	ALPD	W	T1	T2	PC	PT	PFID	RED	WTL	WPD	THS	THMA
117.0	18.5	0.284	0.0201	0.1099	684.6	382.7	10.47	47.77	80109	67628	118	233...
LO	LBE	LBP	LAB	ET1	ET2	P	WSD	NOSO	WPT	WKF	SPT2	
0.0321	0.0795	0.0553	0.0693	3061	411	5.26	0.03	1.00	67641	12481	64183	
PSYD	GMD	DELD	RC	LT1P	LT2R	SPT1	PS	SO	SS	NS	SSSO	
32.977	34.382	20.016	0.183	1.592	0.292	63155.3	63153.0	15092.8	21648.7	11430.7	1.4343	
THS= 2.52247E+02	SOP= 1.49864E+04	ESOP= -7.35061E-01	ESSP= -4.21954E-01	SSP= 2.15573E+04	CHID= 1.42571E+01							
BSSSOP= 2.85098E-01	SSSOP= 1.43845E+00	SPT2= 6.41815E+04	ESPT2= 1.30727E+00									

ITERATIONS ON TEST NUMBER 43164 ARE COMPLETE WITH 29 ITERATIONS AND A WORK DIFFERENCE OF 10.000 FT-LB/MIN

VC	ALPD	W	T1	T2	PC	PT	PFID	RED	WTL	WPD	THS	THMA
156.0	18.5	0.284	0.0201	0.1099	642.9	356.6	10.99	47.59	100300	84807	122	248...
LO	LBE	LBP	LAB	ET1	ET2	P	WSD	NOSO	WPT	WKF	SPT2	
0.0318	0.0762	0.0520	0.0673	4460	604	5.01	0.00	1.00	83997	16292	58660	
PSYD	GMD	DELD	RC	LT1P	LT2R	SPT1	PS	SO	SS	NS	SSSO	
31.973	34.821	20.543	0.192	1.576	0.303	59415.3	59832.5	15061.7	21327.1	11789.1	1.3960	
THS= 2.35004E+02	SOP= 1.40499E+04	ESOP= -7.88792E-01	ESSP= -1.36270E+00	SSP= 2.07406E+04	CHID= 1.55835E+01							
BSSSOP= -6.18562E-01	SSSOP= 1.38742E+00	SPT2= 5.86605E+04	ESPT2= -1.93064E+00									

ITERATIONS ON TEST NUMBER 43244 ARE COMPLETE WITH 20 ITERATIONS AND A WORK DIFFERENCE OF 2.687 FT-LB/MIN

VC	ALPD	W	T1	T2	PC	PT	PFID	RED	WTL	WPD	THS	THMA
235.0	18.5	0.284	0.0201	0.1099	617.8	313.1	11.44	45.44	145206	122003	133	258...
LO	LBE	LBP	LAB	ET1	ET2	P	WSD	NOSO	WPT	WKF	SPT2	
0.0414	0.0751	0.0425	0.0682	6512	896	4.81	0.03	1.00	122001	23202	51121	
PSYD	GMD	DELD	RC	LT1P	LT2R	SPT1	PS	SO	SS	NS	SSSO	
26.851	29.531	18.460	0.200	2.051	0.410	41786.0	41795.0	15180.6	20640.1	11492.7	1.3596	
THS= 2.26563E+02	SOP= 1.61983E+04	ESOP= 1.16976E-01	ESSP= -3.51424E-01	SSP= 2.05677E+04	CHID= 1.24911E+01							
BSSSOP= -4.66864E-01	SSSOP= 1.35328E+00	SPT2= 5.11214E+04	ESPT2= 2.23407E+01									

ITERATIONS ON TEST NUMBER 43324 ARE COMPLETE WITH 32 ITERATIONS AND A WORK DIFFERENCE OF -21.912 FT-LB/MIN

VC	ALPD	W	T1	T2	PC	PT	PFID	RED	WTL	WPD	THS	THMA
310.0	18.5	0.284	0.0201	0.0959	592.8	287.0	12.06	44.40	183783	153715	137	270...
LO	LBE	LBP	LAB	ET1	ET2	P	WSD	NOSO	WPT	WKF	SPT2	
0.0443	0.0724	0.0372	0.0667	9998	1294	4.66	0.03	1.00	153737	30067	45789	
PSYD	GMD	DELD	RC	LT1P	LT2R	SPT1	PS	SO	SS	NS	SSSO	
24.597	27.944	17.319	0.212	2.180	0.458	36726.4	36725.6	15416.2	20533.7	11748.9	1.3319	
THS= 2.16392E+02	SOP= 1.55087E+04	ESOP= 5.97508E-01	ESSP= -1.70641E-01	SSP= 2.04987E+04	CHID= 1.12609E+01							
BSSSOP= -7.63607E-01	SSSOP= 1.32178E+00	SPT2= 4.57893E+04	ESPT2= 2.46769E+01									

VSO= 2.37912E-01	SOA= 1.65755E+04	SON= 1.47997E+04	SOX= 1.87432E+04	VSS= 1.05491E-01
SSA= 2.12556E+04	SSN= 2.25730E+04	SSX= 2.24953E+04	TT= 30;	PSIDY= 3.29778E+01
PSIDN= 2.06123E+00	SSSOX= 1.46655E+00	SSSON= 1.16747E+00	SSSOA= 1.28595E+00	VSSSO= 2.32575E-01;

## PR4: PROCEDURE OPTIONS (MAIN)

```

1      PR4: PROCEDURE OPTIONS (MAIN)
2      CALL NPR
3      NPR: PROCEDURE
4      DCL C(2) , D(2) , G(2) , AN(7,30) , B(30)
5      DCL Z(2) , GT(2)
6      DCL R(7,30)
7      FT1 = 400 ; TTMS = 100 ;
8      KLL = 0
9
10     DO VC = 480 , 320 , 240 , 160 , 120 , 80 ;
11     PUT EDIT ('.') ( PAGE , A(1) ) ;
12     DO ALPD = 45 , 40 , 35 , 30 , 25 , 20
13     LSTTM:
14     SS = 22500 ;
15     IF ALPD = 45 THEN DO ; PSN=2 ; PSX=7 ; PSS=1 ; DLN=26 ; DLX=36;DLS=2 ;
22     SRN = 1.16 ; SRX = 1.23 ; /* 45 DEGREES */
24     SR = 1.17 ; SO = 18800 ; E = 1.9 ;
28     IF ALPD = 40 THEN DO ; PSN=3 ; PSX=11; PSS=1 ; DLN=23 ; DLX=33;DLS=2 ;
36     SRN = 1.19 ; SRX = 1.29 ; /* 40 DEGREES */
38     SR = 1.19 ; SO = 18500 ; E = 2.2 ;
42     IF ALPD=35 THEN DO ; PSN=5 ; PSX = 16;PSS=2 ; DLN=17 ; DLX=23;DLS=1.5;
50     SRN = 1.20 ; SRX = 1.36 ; /* 35 DEGREES */
52     SR = 1.20 ; SO = 17200 ; E = 2.7 ;
56     IF ALPD = 30 THEN DO ; PSN=12; PSX=22; PSS=2 ; DLN=17 ; DLX=23;DLS=1 ;
64     SRN = 1.21 ; SRX = 1.37 ; /* 30 DEGREES */
66     SR = 1.22 ; SO = 17000 ; E = 3.2 ;
70     IF ALPD=25 THEN DO ; PSN=18;PSX=28;DLN=17;DLX=22;DLS=1 ; PSS=2
78     SRN = 1.28 ; SRX = 1.47 ; /* 25 DEGREES */
80     SR = 1.29 ; SO = 16250 ; E = 4.0 ;
84     IF ALPD = 20 THEN DO ; SRN = 1.27 ; SRX=1.5 ; SR = 1.4 ; PSX=32;
90     DLN = 13 ; SO = 16000 ;
92     PSNH = PSN ; PSXH = PSX ; PSSH = PSS ; DLNH=DLN;DLXH=DLX;DLSH=DLS
94     KL = 0 ;
96     LLL = 0 ;
98     D(*) = 0.1000001 ;
100    C(1) = (PSN+PSX)/2 ; C(2) = (DLN+DLX)/2 ;
102    LABEL:
104    SPSO = 10**75
106    DEL1 = 200.0 ; DEL2 = 0.001 ;
108    DEL3 = 12000 ;
110    HIJ = 20 ;
112    CALL TAYLOR (NN,MM,C,D,G,HIJ,DEL1,DEL2,XY,SPSO,FK,PXTI,B,B,VC,ALPD,SR,
114    F,FT1,TTMS,SO,SS
116    CALL STS ;
118    STS: PROCEDURE
119    IF E > 6.0 THEN E = 6.0 ; IF E < 1.6 THEN E = 1.6 ;
121    IF TTMS > 300 THEN TTMS = 300 ; IF TTMS < 80 THEN TTMS = 80 ;
123    IF FT1 > 50000 THEN FT1 = 50000 ; IF FT1 < 300 THEN FT1 = 300 ;
125    SKO = 1.12033 ; GK = 6.08377 ; T = TTMS/1000 ; AA = -.0123976 ;
127    BB = 0.340303 ; CC = -.016177 ;
129    SSSOP = SKO*(GK**T)*(**{(AA+BB*T)}*(FT1**{(CC*T)}
131    SSK = 15830 ; GSK = 8305.47 ; AAS = -.0492552 ; BBS = -2.16237 ;
133    CCS = -.0120691 ;
135    SSP = SSK*(GSK**T)*(**{(AAS+BBS*T)}*(FT1**{(CCS*T)}
136

```

## PR4: PROCEDURE OPTIONS (MAIN)

```

137      IF SSP > 22200 THEN SSP = 22200 ; IF SSP< 20100 THEN SSP = 20400 ;
141      IF SSSOP < SRN THEN SSSOP = SRN ; IF SSSOP > SRX THEN SSSOP = SRX ;
145      SOP = SSP/SSSOP ;
146      END STS ;
147      SSSO = SR ;
148      KL = KL + 1 ;
149      IF KL > 20 THEN GO TO THE_END ;
151      IF KK=-1 | ABS(SO-SOP)>300 | SSSO>(SSSOP+C.002) | SSSO<(SSSOP-0.001)
152                                     THEN DO ;
153          SSSO = SSSOP ; SR = SSSOP ; SO = SOP ; SS = SSP ;
154          JKJ = 0 ;
155          IF KK = -1 THEN DO ; SOH = 10**75 ;
156      STP:
157          DO Z(1) = PSN TO PSX BY PSS ; DO Z(2) = DLN TO DLX BY DLS ;
158          LK = -3 ;
159          CALL FNCTN (Z,G,AR,B,LK ,VC,ALPD,SR,P , ET1,THS,SO,SS ) ;
160          SQM = SQM(G(*)**2) ;
161          IF SQM < SOH THEN DO : SQM = SQM/C(*) = Z(*) ; CALL STS ;      END :
162          END : END ;
163          PSN = C(1) - PSS ; PSX = C(1) + PSS ; PSS = PSS/4 ;
164          DLN = C(2) - DLS ; DLX = C(2) + DLS ; DLS = DLS/4 ;
165          JKJ = JKJ + 1 ;
166          IF JKJ < 2 THEN GO TO STP ;
167          DLS=DLSH ; DLX=DLXH ; DLN=DLNH ; PSS=PSSH ; PSX=PSXH ; PSN = PSNH ;
168          CALL STS ;
169          END :
170          LK = 0 ;
171          GO TO LABEL ;
172      END :
173      THE_END:
174      LK = 3 ;
175      CALL FNCTN (C,G,AR,B,LK ,VC,ALPD,SR,E , ET1,THS,SO,SS ) ;
176      END : END : /* DO RANGE OF OSPREDS & FEEDS */
177      END MPR
178      /*
179      /*
180      TAYLOR: PROCEDURE (JJJ,LLL,X,N,P,ITMAX,EPS1,*PS2,DEF,S,KENN,EXIT,AR,BH,
181              VEL,ALF,SRH,FTT,ET1TT,TTHSTT,SOIT,SSIT
182              DCL X(2) , P(2) , H(2) , PP(2) , PM(2) , R(2) , DX(2) , DDX(2,2) ,
183              AA(2,2) , AR(7,30) , BH(2)
184              DCL Z BINARY FIXED
185              ON ERROR GO TO LR ;
186              SR = SRH ;
187              AL = ALF ;
188              HS = S ;
189              N = 2 ; M = 2 ;
190              JX = 0 ;
191              Z = 0 ;
192              KENN = 0 ;
193      ITERATION:
194          Z = Z + 1 ;
195          IF Z > ITMAX THEN DO ;
196              KENN = 1 ;

```



## PR4: PROCEDURE OPTIONS (MAIN)

```

216          GO TO ENDE
217          END /* IF Z > ITMAX */
218          L = 0
219          HL = 1.0
220          DAMP:
221              L = L + 1
222              IF KPNM = 0 & L > 16 THEN DO ;
223                  KPNM = 3 ; HL = 1.0 ; L = 0 ; DX(*) = -DX(*) ;
224                  L = 16 ; DX(*) = 0 ; /* THIS CARD PREVENTS 15 EQUAL STEPS */
225              END ;
226              IF KPNM = 3 & L = 16 THEN DO ; KPNM=-1 ; X(*) = X(*)-DX(*) ; GOTO ENDE ;
227              END ;
228          LBI:
229              IF X(1) < 1.0 THEN DO ; KPNM=-1 ; GOTO ENDE ; END ;
230              CALL FNCTN ( X , F , AP , BH , JK , VEL , AL , SR , ETT,ETITT,THSTT,
231                          SOTT,SSTT
232                          ) ;
233              N = 2 ; M = 2
234              HF = 0
235              DO I = 1 TO N ; HF = HF + F(I)*F(I) ; END
236              IF HF > (HS*(1.0 - 0.2*HL)) THEN DO
237                  IF KPNM = 0 THEN HL = HL/2 ; ELSE HL = 1/15 ;
238                  DO K = 1 TO N ; X(K) = X(K) + HL*DX(K) ; END
239                  GO TO DAMP
240              END /* IF HF > (HS*(1.0-0.2*HL)) */
241              HS = HF
242              IF HS < EPS1 THEN GO TO ENDE
243              IF HS < 3000 THEN H(*) = 0.01 ; IF HS < 300 THEN H(*) = 0.001
244              M = 2 ; N = 2
245              DO I = 1 TO N ; HF = H(I) ; HZ = 2.0*HF
246          LBI:
247              X(I) = X(I) + HF
248              CALL FNCTN ( X , FP , AR , BH , JK , VEL , AL , SR , ETT,ETITT,THSTT,
249                          SOTT,SSTT
250                          ) ;
251              X(I) = X(I) - HF ;
252              DO K = 1 TO N ; DFDX(K,I) = (FP(K)-F(K))/HF ; END
253          END /* I = 1 TO N */
254          LBI:
255              M = 2 ; N = 2
256              IF M = N THEN DO ; CALL GAUSS (N,DFDX,F,DX,EXIT) ; END
257              ELSE DO
258                  LBI:
259                      DO I = 1 TO N ;
260                          HF = 0
261                          DO K = 1 TO N ; HF = HF + (DFDX(K,I))*F(K) ; END
262                          B(I) = HF
263                      DO K = 1 TO N
264                          HF = 0
265                          DO J = 1 TO N ; HF = HF + (DFDX(J,I))*(DFDX(J,K)) ; END
266                          AA(I,K) = HF
267                      AA(K,I) = HF
268                  END /* DO K = 1 TO N */
269                  END /* DO I = 1 TO N */
270              CALL GAUSS ( N , AA , B , DX , EXIT )
271

```

## PR4: PROCEDURE OPTIONS (MAIN)

```

301      END /* ELSE DO FOR IF N = N */
302      HZ = 0
303      HF = 0
304      DO I = 1 TO N
305      IF (X(I) - DX(I)) < 1.0 THEN DX(I) = X(I) - 1.0 ;
306      IF (X(I) - DX(I)) > 40 THEN DX(I) = X(I) - 40 ;
307      X(I) = X(I) - DX(I)
308      LBM:
309      HZ = HZ + ABS(X(I))
310      HF = HF + ABS(DX(I))
311      END /* DO I = 1 TO N */
312      IF HF >= EPS2*HZ THEN GO TO ITERATION
313      ENDR:
314      IF KENN = 0 THEN JK = 2 ; ELSE JK = KENN ;
315      CALL FNCTN ( X , F , AR , DH , JK , VEL , AL , SR , ETT,ETITT,THSTT,
316      SOTT,SSTT ) ;
317      LR:
318      S = A
319      ITMAX = 7
320      DO I = 1 TO N ; S = S + F(I)*P(I) ; FND
321      RETURN
322      END TAYLOR
323      /*
324      /*
325      /*
326      GAUSS: PROCEDURE ( MM , AR , B , X , EXIT )
327      DCL X(7) , AR(7,30)
328      DCL A(4) , B(2) , BR(2) , AR(4)
329      ON ERROR GO TO LL4
330      NN = 0
331      L0:
332      DO L = 1 TO MM ; DO M = 1 TO MM ; NM = NM+1 ; A(NM) = AR(M,L);END:END;
333      L1:
334      N = MM
335      L2:
336      BR(1) = B(1) ; BR(2) = B(2)
337      TOL = 0.0001
338      KS = 0
339      JJ = -N
340      DO J = 1 TO N
341      JY = J+1
342      JJ = JJ+N+1
343      L3:
344      BIGA = 0.0
345      IT = JJ-J
346      /* SEARCH FOR MAX COEFFICIENT IN COLUMN */
347      DO I = J TO N
348      IJ = IT+I
349      IF ( ABS(BIGA) - ABS(A(IJ)) ) < 0.0 THEN DO
350      BIGA = A(IJ)
351      IMAX = I
352      END /* (ABS(BIGA) - ABS(A(IJ))) < 0.0 */
353
354
355

```

## PR4: PROCEDURE OPTIONS (MAIN)

```

356      END /* I = J TO N */
      /* TEST FOR PIVOT LESS THAN TO L */
      /* INTERCHANGE ROWS IF NECESSARY */
357      L5:
      I1 = J+N*(J-2)
      IT = IMAX-J
      DO K = J TO N
      I1 = I1+N
      I2 = I1 + IT
358      L6:
359      SAVE = A(I1)
360      L7:
361      A(I1) = A(I2)
362      A(I2) = SAVE
      /* DIVIDE EQUATION BY LEADING COEFFICIENT */
      A(I1) = A(I1)/BIGA
363      END /* IF ( ABS(DO K = J TO N */
364      SAVE = B(IMAX)
365      L8:
366      BH(1) = B(1) ; BH(2) = B(2)
367      B(IMAX) = B(J)
368      B(J) = SAVE/BIGA
369      L9:
370      BH(1) = B(1) ; BH(2) = B(2)
371      IF J = N THEN GO TO BKSOL
      /* ELIMINATE NEXT VARIABLE */
372      IQS = N*(J-1)
373      DO IX = JY TO N
374      IXJ = IQS + IX
      IT = J - IX
      DO JX = JY TO N
      IXJX = N*(JX-1) + IX
      JJX = IXJX + IT
      A(IXJX) = A(IXJX) - (A(IXJ))*A(JJX)
      END /* DO JX = JY TO N */
      B(IX) = B(IX) - (B(J))*A(IXJ)
      END /* DO IX = JY TO N */
      END /* J = 1 TO N */
      BKSOL: /* BACK SOLUTION */
      NY = N-1
      IT = N*N
      DO J = 1 TO NY
      IA = IT - J
      IB = N - J
      IC = N
      DO K = 1 TO J
      B(IB) = B(IB) - (A(IA))*B(IC)
      IA = IA - N
      IC = IC - 1
      END /* DO K = 1 TO J */
      END /* DO J = 1 TO NY */
      LL8:
      DO LL = 1 TO N ; X(LL) = B(LL) ; END
375
376
377
378
379
380
381
382
383
384
385
386
387
388
389
390
391
392
393
394
395
396
397
398
399
400
401

```

## PR4: PROCEDURE OPTIONS (MAIN)

```

403      RETURN ;
404      END GAUSS ;
      /* */
      /* */
      /* */
405      FNCTN: PROCEDURE ( C , G , RB , FL , TST , VEL , ALP , SSSOR ,
                        ET,RT1T,TTHST,SOT,SST ) ;
406          DCL C(2) , G(2) , RB(7,30) , FL(30) ;
407          DECLARE ( HH,GG,TST,I ) BINARY FIXED (31,C) ;
408          DECLARE ( K , LAB , LRB , LRF , LD , LTR , LTR2 , NOSO , NS )
                        DECIMAL ;
409          DECLARE GR(55) , DR0(35) , DR1(55) , CH(55) , RC(25) , R1(25) ;
410          DECLARE PS(201) , DL(101) , TS(101) ;
411          ON ERROR GO TO L2 ;
412          PMT01:
413          FORMAT (SKIP, 2 P(9,1), P(9,3), 2 P(9,4), 2 P(9,1), 2 P(9,2), 4 P(9), A(3)) ;
414          PMT02: FORMAT (3 P(10,2), 3 P(10,3), 5 P(10,1), P(10,4)) ;
415          PMT03: FORMAT ( 4 P(10,4) , 2 P(10,^), 2 P(10,2) , 4 P(10,0) ) ;
416          SSSO = SSSOR ;
417          PSID = C(1) ; DELD = C(2) ;
418          DL(L) = DELD ;
419          VC = VEL ; ALPD = ALP ;
420          STI = 15000 ;
421          PI = 3.1415926536 ;
422          DTR = PI/180.0 ;
423          RTD = 180/PI ;
424          P = 0.0975 ;
425          K = 10.81 ;
426          CP = 0.243 ;
427          W = 0.280 ;
428          T1 = 0.0202 ;
429          NOSO = 1.00 ;
430          L0:
431          I = 43000 + VC + ALPD/5 ;
432          J = 1 ;
433          L3:
434          III = III + 1 ;
435          PSIR= PSID*DTR ;
436          DELR= DELD*DTR ;
437          ALPR= ALPD*DTR ;
438          PP = 1.0 + SIN(PSIR)/COS(PSIR) ;
439          PM = 1.0 - SIN(PSIR)/COS(PSIR) ;
440          NN = 0 ;
441          CH = -2.0 ; GR(1) = PSID + ALPD ; GR(2) = PSID + ALPD -2 ;
442          L5:
443          NN = NN + 1 ;
444          IF NN > 15 THEN DO ;PUT DATA ( NN) ; RE1 = 100000 ; GO TO L2 ; END ;
445          N = 1 ;
446          CN = -1.0 ;
447          SSSOH = 0.0 ;
448          L5:
449          GMD = GR(N) ; GMR = GMD*DTR ;
450          SSSO = (PP*COS(GMR-ALPR) - PM*SIN(GMR-ALPR)) *COS(GMR-ALPR) ;

```

## PRQ: PROCEDURE OPTIONS (MAIN)

```

457      IF SSS0 > SSS0H THEN DO ; SSS0H = SSS0 ; GMDH = GR(N) ; END ;
462      IF SSS0 > SSS0 THEN TS(N) = 2 ; ELSE TS(N) = 1 ;
465      IF N = 1 THEN DO ; N = 2 ; GO TO L5 ; END ;
470      IF N>54 | (ABS(SSS0-SSS0) < 0.00001) THEN DO ;
472      GO TO L6 ;
473      END /* IF N>49 | SSS0=SSS0+-0.0001 */ ;
474      IK = 0 ;
475      IF TS(N) = TS(N-1) THEN DO ; IK = 1 ; CN = -CN/4 ; END ;
480      GR(N+1) = GR(N) + CN ;
481      N = N + 1 ;
482      GO TO L5 ;
483
484      L6:
485      IF N>54 & (ABS(SSS0-SSS0) > 0.00002) THEN DO ;
486      SSS0 = SSS0H ;
487      GMD = GMDH ; GMR = GMD*DTR ; PUT DATA ( GMD , SSS0 , SSS0 ) ; END ;
490      CPPS= COS(PSIR) + SIN(PSIR) ;
491      GNT = SIN(GMR)/COS(GMR) ;
492      RC = (SIN(GMR))/(PP*COS(GMR-ALFR)) - (TAN(PSIR))*(SIN(DELR))/(PP*COS(ALFR+DELR)) ;
493      T2 = T1/RC ;
494      PIT = RC*COS(ALFR)/(1 - RC*SIN(ALFR)) ;
495      PFIR= ATAN(PIT) ;
496      E = SIN(PFIR-ALFR)/COS(PFIR-ALFR) + COS(PFIR)/SIN(PFIR) ;
497      LT2R= COS(PSIR+ALFR+DELR)/(CPPS*COS(ALFR+DELR)) ;
498      LT1R= LT2R/RC ;
499      LO = LT1R*T1 ;
500      LBP = T2/PPS ;
501      LBF = LBR*SIN(PSIR)/COS(ALFR+DELR) ;
502      ET1 = 0.1*E*VC*(1+RC)/(LBP*(PSIR+ALFR-GMR)) ;
503      LAB = LBE*COS(PSIR)/COS(GMR-ALFR) ;
504      L7:
505      SSS0H= SSS0 ;
506      PC = SO*W*(LBE*(SIN(PSIR+ALFR) + COS(PSIR+ALFR)) +
507      SSS0*LBF*(COS(DELR) - NOS0*SIN(DELR))) ;
508      PT = SO*W*(LBE*(COS(PSIR+ALFR) - SIN(PSIR+ALFR)) +
509      SSS0*LBF*(SIN(DELR) + NOS0*COS(DELR))) ;
510      OP = VC*RC*(PC*SIN(ALFR) + PT*COS(ALFR))/1400 ;
511      THF = OP/(12*P*CP*VC*T1*W) ;
512      OS = PC*VC/1400 - OP ;
513      R = 720*P*CP*VC*T1/K ;
514      THNB= R*FIT ;
515      R = SQRT(ABS(R/LT2R)) ;
516      THNB = ABS(THNB) ;
517      IF THNB > 12.0 THEN BETA = 0.10; ELSE BETA = 0.475 - 0.1449*LOG(THNB) ;
518      THS = OS*(1-BETA)/(12*P*CP*VC*T1*W) ;
519      THSX= THS/(1-BETA) ;
520      THMX= 0.72*THF*B*(0.856*(B*LT2R*(PP-1)/2.5)) ;
521      THMA= THMX + THS ;
522      THTR= ATAN((RC*COS(PFIR)-SIN(ALFR-PFIR))/COS(ALFR-PFIR)) ;
523      THTR= ABS(THTR) ;
524      THTD= THTR*BTD ;
525      THNT= ((RC*COS(PFIR) - SIN(ALFR-PFIR))/(COS(ALFR-PFIR))) ;
526      THNT = ABS(THNT) ;

```

## PR4: PROCEDURE OPTIONS (MAIN)

```

526      PFID = PFIR*RTD ; BBD = ALPD + ATAND(PT/PC) ;
528      WKP = 1400*OP ;
529      WTL = PC*VC ;
530      WPD = WTL - WKP ;
531      WS = (COS(PSIR+ALPR-GMR)-SIN(PSIR+ALPR-GMR))*SO*LBE/LAB ;
532      N = 1 ; CH(1) = 0.0 ; CN = 2.0 ;
533
534      L8:
535      CHID = CH(N) ; CHIR = CHID*DTR ;
536      AA = 1.0 + (2*COS(CHIR))*(SIN(GMR) - SIN(CHIR)) ;
537      DD = SS*COS(GMR-CHIR) + WS*SIN(GMR-CHIR) ;
538      SI = DD/AA ;
539
540      IF SI > SII THEN TS(N) = 1 ; ELSE TS(N) = 2 ;
541      IF N = 1 THEN DO ; N = 2 ; CH(N) = 2.0 ; GO TO L8 ; END ;
542      IF N > 35 THEN DO ; PUT DATA ( N,CHID,SI) ; GO TO L9 ; FND ;
543      IF ABS(SII-SI) > 1.0 THEN DO ;
544      IF TS(N) = TS(N-1) THEN DO ;
545      CH(N+1) = CH(N) + CN ;
546      N = N + 1 ;
547      GO TO L8 ;
548      ELSE /* TS(N) = TS(N-1) ? */
549      CN = -CN/4 ;
550      CH(N+1) = CH(N) + CN ;
551      N = N + 1 ;
552      GO TO L8 ;
553      FND /* ELSE DO */
554      END /* ABS(SI-SII) > 1.0 */
555
556      L9:
557      H = LAB*(SIN(GMR) - SIN(CHIR)) ;
558      D = LAB*(COS(CHIR) - COS(GMR)) ;
559      APDZ = (LAB**2)*(PSIR+ALPR-CHIR)/2 + H*(H+D)/2 ;
560      TRQ = LAB*(PSIR+ALPR-CHIR)/(VC*(1+PC)) ;
561      WPT = SO**((1-RC**2)/(2*RC) + TTPT)*APDZ/TRQ ;
562      SPSO = (PM/(TAN(PSIR)) + SSSO*(TAN(ALPR+DELR) + NOSO))/
563      ((1/(TAN(PSIR))) - TAN(ALPR+DELR)) ;
564
565      SPT1 = SPSO*SO ;
566      IF ABS(LO) < 0.0001 THEN LO = 0.01 ;
567      IF ABS(PP-1) < 0.0001 THEN PP = 1.01 ;
568      ET2 = 0.4*VC*RC/(LO*(PP-1)) ;
569      IF E > 5.3 THEN E = 5.3 ; IF E < 1.8 THEN E = 1.8 ;
570      IF ET1 > 45000 THEN ET2 = 45000 ; IF ET2 < 300 THEN ET2 = 300 ;
571      IF THMA > 270 THEN THMA = 270 ; IF THMA < 150 THEN THMA = 150 ;
572      SPO = EXP(14.1042) ;
573      T = THMA/1000 ;
574      GK = EXP(-13.2560) ;
575      AA = -1.84670 ;
576      BB = 15.7909 ;
577      CC = -0.246249 ;
578      DD = 1.19791 - 1.36858*(LOG(E)) ;
579      SFE1 = SPO*(GK**T)*(E**(AA+BB*T))*(ET2**(CC+DD*T)) ;
580      SPT2 = SFE1 ;
581      RE1 = SPT1 - SFE1 ;
582      RE2 = WPT - WPD ;

```

## PR4: PROCEDURE OPTIONS (MAIN)

```

604       IF TST = 3 THEN DO ;
605       PUT EDIT ( '.....VC.....ALFD.....W.....T1.....T2.....FC.....',
                  'PT.....PFID.....BED.....WTL.....WPD.....THS.....THMA' ) ;
        { SKIP(2) , A(55) , A(58) , A(6) } ;
607       PUT EDIT (VC,ALFD,W,T1,T2,FC,PT,PFID,BED,WTL,WPD,THS,THMA,'...')
                  ( R(PMT01) ) ;
608       PUT EDIT ( '      LO      LBE      LBP      LAB      ET1      FT2'
                  '      F      WSD      NOSO      SPT      WKP      SFT2 '
                  ' [ A(60) , A(60) ] ) ;
609       PUT EDIT (LO,LBE,LBP,LAB,ET1,ET2,F,WSD,NOSO,SPT,WKP,SFT2) (R(PMT03)) ;
610       PUT EDIT ( '      PSID      GMD      DELD      RC      LT1R      LT2R'
                  '      SFT1      CHID      SO      SS      NS      SSSO'
                  ' ( A(59) , X(1) , A(60) ) ) ;
611       PUT EDIT (PSID,GMD,DELD,RC,LT1R,LT2R,SFT1,CHID,SO,SS,NS,SSSO) (R(PMT02)) ;
612       PUT EDIT ( 'ITERATIONS ON TEST NUMBER ', I, ' ARE COMPLETE WHERE ' ,
                  ' THE CUTTING SPEED = ', VC, ' THE RAKE ANGLE = ', ALFD,
                  ' THE UNDEFORMED CHIP THICKNESS = ', T1 ) (A(26),F(5),A(20),
                  A(20),F(5,1),A(18), F(5,2), A(33), F(7,5) ) ;
613       PUT DATA ( SOT , SSSOT , T2 , RC ) ;
614       KILL = KILL + 1 ;
615       END ;
616       G(1) = RF1 ; G(2) = RF2*RC/VC ;
618       ET = E ; ET1 = ET1 ; TTST = TTHS ; SOT = SO ; SST = SS ;
623       L2:
        RETURN ;
624       END PNCIN ;
625       END /* PR4 */ ;

```

....VC.....ALPD.....W.....T1.....T2.....FC.....FT.....PFID.....BED.....WTL.....WPD.....THS.....THMA  
 480.0 45.0 0.279 0.0201 0.0459 336.6 79.8 24.27 58.34 161615 99460 74 266...  
 LO LBE LBF LAB ET1 ET2 E WSD NOSO WPT WKP SPT2  
 0.0321 0.0436 0.0117 0.0440 15472 48956 1.83 0.00 1 99617 62154 32837  
 PSID GMD DELD RC LT1R LT2R SPT1 CHID SO SS NS SSSO  
 3.07 37.29 33.48 0.439 1.590 0.699 32747.1 18.6 18355.1 21299.5 14489.7 1.1604  
 ITERATIONS ON TEST NUMBER 43489 ARE COMPLETE WHERE THE CUTTING SPEED = 480.0 THE RAKE ANGLE = 45.00 THE UNDEFORMED CHIP  
 THICKNESS = 0.02019 SOP= 1.84730E+04 SSSOP= 1.15999E+00 T2= 4.59489E-02 RC= 4.39618E-01;

....VC.....ALPD.....W.....T1.....T2.....FC.....FT.....PFID.....BED.....WTL.....WPD.....THS.....THMA  
 480.0 40.0 0.279 0.0201 0.0499 365.2 91.0 22.72 51.96 175793 116532 86 269...  
 LO LBE LBF LAB ET1 ET2 E WSD NOSO WPT WKP SPT2  
 0.0339 0.0451 0.0120 0.0451 14566 29399 2.07 0.00 1 116574 59260 32132  
 PSID GMD DELD RC LT1R LT2R SPT1 CHID SO SS NS SSSO  
 6.40 34.21 25.33 0.404 1.678 0.679 32140.8 10.2 18500.0 22500.0 14192.4 1.1899  
 ITERATIONS ON TEST NUMBER 43488 ARE COMPLETE WHERE THE CUTTING SPEED = 480.0 THE RAKE ANGLE = 40.00 THE UNDEFORMED CHIP  
 THICKNESS = 0.02019 SOP= 1.82964E+04 SSSOP= 1.18999E+00 T2= 4.99293E-02 RC= 4.04571E-01;

....VC.....ALPD.....W.....T1.....T2.....FC.....FT.....PFID.....BED.....WTL.....WPD.....THS.....THMA  
 480.0 35.0 0.279 0.0201 0.0550 372.1 109.9 20.85 51.46 178621 125140 91 260...  
 LO LBE LBF LAB ET1 ET2 E WSD NOSO WPT WKP SPT2  
 0.0351 0.0477 0.0143 0.0471 15718 11935 2.37 0.01 1 125365 53480 30796  
 PSID GMD DELD RC LT1R LT2R SPT1 CHID SO SS NS SSSO  
 9.52 32.64 21.47 0.367 1.741 0.639 30807.8 9.7 17200.0 22500.0 13464.9 1.1999  
 ITERATIONS ON TEST NUMBER 43487 ARE COMPLETE WHERE THE CUTTING SPEED = 480.0 THE RAKE ANGLE = 35.00 THE UNDEFORMED CHIP  
 THICKNESS = 0.02019 SOP= 1.72557E+04 SSSOP= 1.19999E+00 T2= 5.50298E-02 RC= 3.67073E-01;

....VC.....ALPD.....W.....T1.....T2.....FC.....FT.....PFID.....BED.....WTL.....WPD.....THS.....THMA  
 480.0 30.0 0.279 0.0201 0.0644 427.7 147.0 17.83 48.96 205330 154026 108 268...  
 LO LBE LBF LAB ET1 ET2 E WSD NOSO WPT WKP SPT2  
 0.0423 0.0553 0.0157 0.0544 15303 7699 2.89 0.03 1 154025 51304 28794  
 PSID GMD DELD RC LT1R LT2R SPT1 CHID SO SS NS SSSO  
 10.45 28.12 20.34 0.313 2.094 0.656 28799.4 9.9 17111.6 20705.0 13274.6 1.2099  
 ITERATIONS ON TEST NUMBER 43486 ARE COMPLETE WHERE THE CUTTING SPEED = 480.0 THE RAKE ANGLE = 30.00 THE UNDEFORMED CHIP  
 THICKNESS = 0.02019 SOP= 1.71493E+04 SSSOP= 1.20999E+00 T2= 6.44866E-02 RC= 3.13243E-01;

....VC.....ALPD.....W.....T1.....T2.....FC.....FT.....PFID.....BED.....WTL.....WPD.....THS.....THMA  
 480.0 25.0 0.279 0.0201 0.0824 523.6 212.4 13.90 47.08 251355 202715 135 270...  
 LO LBE LBF LAB ET1 ET2 E WSD NOSO WPT WKP SPT2  
 0.0471 0.0666 0.0250 0.0640 12799 3460 3.84 0.07 1 202850 48639 31374  
 PSID GMD DELD RC LT1R LT2R SPT1 CHID SO SS NS SSSO  
 16.08 25.65 17.49 0.244 2.332 0.571 31366.3 8.6 16264.0 20823.1 11815.9 1.2799  
 ITERATIONS ON TEST NUMBER 43485 ARE COMPLETE WHERE THE CUTTING SPEED = 480.0 THE RAKE ANGLE = 25.00 THE UNDEFORMED CHIP  
 THICKNESS = 0.02019 SOP= 1.62090E+04 SSSOP= 1.27999E+00 T2= 8.24977E-02 RC= 2.44854E-01;

....VC.....ALPD.....W.....T1.....T2.....FC.....FT.....PFID.....BED.....WTL.....WPD.....THS.....THMA  
 480.0 20.0 0.279 0.0201 0.0768 515.1 219.1 15.19 43.04 247250 199322 135 270...  
 LO LBE LBF LAB ET1 ET2 E WSD NOSO WPT WKP SPT2  
 0.0405 0.0593 0.0261 0.0558 16489 3195 3.59 0.03 1 199039 48227 33673  
 PSID GMD DELD RC LT1R LT2R SPT1 CHID SO SS NS SSSO  
 21.30 28.52 14.38 0.262 2.005 0.527 33679.9 7.8 17097.5 21713.8 13684.9 1.2699  
 ITERATIONS ON TEST NUMBER 43484 ARE COMPLETE WHERE THE CUTTING SPEED = 480.0 THE RAKE ANGLE = 20.00 THE UNDEFORMED CHIP  
 THICKNESS = 0.02019 SOP= 1.69374E+04 SSSOP= 1.26999E+00 T2= 7.69128E-02 RC= 2.62976E-01;



....VC.....ALFD.....W.....T1.....T2.....PC.....PT.....PFID.....BED.....WTL.....WPD.....THS.....THMA  
 320.0 45.0 0.279 0.0201 0.0453 340.3 84.8 24.69 59.00 108927 66057 69 240...  
 LO LBE LBP LAB BT1 BT2 E WSD NOSO WPT WFP SPT2  
 0.0280 0.0415 0.0138 0.0415 11126 21087 1.80 0.00 1 65791 42870 38177  
 PSID GND DELD RC LT1R LT2R SPT1 CHID SO SS NS SSSO  
 5.49 40.15 24.29 0.445 1.390 0.619 38232.6 15.2 18688.6 21762.8 15044.8 1.1644  
 ITERATIONS ON TEST NUMBER 43329 ARE COMPLETE WHERE THE CUTTING SPEED = 320.0 THE RAKE ANGLE = 45.00 THE UNDEFORMED CHIP  
 THICKNESS = 0.02019 SOP= 1.86704E+04 SSSOP= 1.16425E+00 T2= 4.53431E-02 RC= 4.45492E-01;

....VC.....ALFD.....W.....T1.....T2.....PC.....PT.....PFID.....BED.....WTL.....WPD.....THS.....THMA  
 320.0 40.0 0.279 0.0201 0.0506 371.8 99.1 22.31 54.93 118980 78809 80 237...  
 LO LBE LBP LAB BT1 BT2 E WSD NOSO WPT WFP SPT2  
 0.0327 0.0454 0.0135 0.0452 10007 12556 2.11 0.00 1 74818 40171 34326  
 PSID GND DELD RC LT1R LT2R SPT1 CHID SO SS NS SSSO  
 7.06 35.12 25.58 0.398 1.622 0.646 34314.9 10.8 18500.0 22500.0 14329.3 1.1899  
 ITERATIONS ON TEST NUMBER 43328 ARE COMPLETE WHERE THE CUTTING SPEED = 320.0 THE RAKE ANGLE = 40.00 THE UNDEFORMED CHIP  
 THICKNESS = 0.02019 SOP= 1.83069E+04 SSSOP= 1.18999E+00 T2= 5.05802E-02 RC= 3.98577E-01;

....VC.....ALFD.....W.....T1.....T2.....PC.....PT.....PFID.....BED.....WTL.....WPD.....THS.....THMA  
 320.0 35.0 0.279 0.0201 0.0557 376.5 118.3 20.55 52.45 120508 84198 84 230...  
 LO LBE LBP LAB BT1 BT2 E WSD NOSO WPT WFP SPT2  
 0.0333 0.0477 0.0161 0.0469 10925 7443 2.40 0.00 1 84379 36309 33476  
 PSID GND DELD RC LT1R LT2R SPT1 CHID SO SS NS SSSO  
 10.57 34.04 22.13 0.362 1.652 0.599 33488.9 10.6 17200.0 22500.0 13643.1 1.1999  
 ITERATIONS ON TEST NUMBER 43327 ARE COMPLETE WHERE THE CUTTING SPEED = 320.0 THE RAKE ANGLE = 35.00 THE UNDEFORMED CHIP  
 THICKNESS = 0.02019 SOP= 1.72610E+04 SSSOP= 1.19999E+00 T2= 5.57173E-02 RC= 3.62544E-01;

....VC.....ALFD.....W.....T1.....T2.....PC.....PT.....PFID.....BED.....WTL.....WPD.....THS.....THMA  
 320.0 30.0 0.279 0.0201 0.0762 491.1 185.4 14.80 50.68 157181 122754 114 252...  
 LO LBE LBP LAB BT1 BT2 E WSD NOSO WPT WFP SPT2  
 0.0454 0.0640 0.0219 0.0627 8176 3420 3.51 0.00 1 122747 34426 31919  
 PSID GND DELD RC LT1R LT2R SPT1 CHID SO SS NS SSSO  
 12.29 26.76 21.50 0.264 2.250 0.595 31918.5 9.6 16533.8 20803.5 11751.8 1.2582  
 ITERATIONS ON TEST NUMBER 43326 ARE COMPLETE WHERE THE CUTTING SPEED = 320.0 THE RAKE ANGLE = 30.00 THE UNDEFORMED CHIP  
 THICKNESS = 0.02019 SOP= 1.65054E+04 SSSOP= 1.25887E+00 T2= 7.62756E-02 RC= 2.64828E-01;

....VC.....ALFD.....W.....T1.....T2.....PC.....PT.....PFID.....BED.....WTL.....WPD.....THS.....THMA  
 320.0 25.0 0.279 0.0201 0.0828 522.1 230.1 13.83 48.79 167084 133598 122 267...  
 LO LBE LBP LAB BT1 BT2 E WSD NOSO WPT WFP SPT2  
 0.0412 0.0654 0.0294 0.0622 9353 2259 3.86 0.00 1 133668 33485 37157  
 PSID GND DELD RC LT1R LT2R SPT1 CHID SO SS NS SSSO  
 18.49 29.10 20.06 0.283 2.043 0.498 37137.3 11.3 16213.7 20753.5 12282.5 1.2799  
 ITERATIONS ON TEST NUMBER 43325 ARE COMPLETE WHERE THE CUTTING SPEED = 320.0 THE RAKE ANGLE = 25.00 THE UNDEFORMED CHIP  
 THICKNESS = 0.02019 SOP= 1.60780E+04 SSSOP= 1.27999E+00 T2= 8.28694E-02 RC= 2.43756E-01;

....VC.....ALFD.....W.....T1.....T2.....PC.....PT.....PFID.....BED.....WTL.....WPD.....THS.....THMA  
 320.0 20.0 0.279 0.0201 0.0805 513.4 239.9 14.45 45.34 164312 132118 122 267...  
 LO LBE LBP LAB BT1 BT2 E WSD NOSO WPT WFP SPT2  
 0.0363 0.0610 0.0314 0.0570 11797 1987 3.78 0.00 1 132146 32193 39427  
 PSID GND DELD RC LT1R LT2R SPT1 CHID SO SS NS SSSO  
 23.86 31.81 18.29 0.250 1.798 0.451 39421.5 12.4 16414.9 20846.9 13516.9 1.2699  
 ITERATIONS ON TEST NUMBER 43324 ARE COMPLETE WHERE THE CUTTING SPEED = 320.0 THE RAKE ANGLE = 20.00 THE UNDEFORMED CHIP  
 THICKNESS = 0.02019 SOP= 1.62629E+04 SSSOP= 1.26999E+00 T2= 8.05258E-02 RC= 2.50850E-01;

....VC.....ALFD.....W.....T1.....T2.....PC.....PT.....PFID.....BED.....WTL.....WPD.....THS.....THNA  
 240.0 45.0 0.279 0.0201 0.0454 343.8 87.2 24.65 59.24 82532 49980 65 219...  
 LO LBE LBF LAB BT1 BT2 E WSD NOSO WPT WKP SPT2  
 0.0267 0.0410 0.0147 0.0408 8343 14030 1.80 0.00 1 49980 32552 80701  
 PSID GMD DELD RC LT1R LT2R SPT1 CHID SO SS WS SSSO  
 6.48 40.98 26.66 0.444 1.326 0.590 40639.2 14.2 18800.0 22500.0 15121.9 1.1699  
 ITERATIONS ON TEST NUMBER 43249 ARE COMPLETE WHERE THE CUTTING SPEED = 240.0 THE RAKE ANGLE = 45.00 THE UNDEFORMED CHIP  
 THICKNESS = 0.02019 SOP= 1.87163E+04 SSSOP= 1.16980E+00 T2= 4.54063E-02 RC= 4.44872E-01;

....VC.....ALFD.....W.....T1.....T2.....PC.....PT.....PFID.....BED.....WTL.....WPD.....THS.....THNA  
 240.0 40.0 0.279 0.0201 0.0512 376.1 105.3 22.01 55.65 90278 59777 76 216...  
 LO LBE LBF LAB BT1 BT2 E WSD NOSO WPT WKP SPT2  
 0.0319 0.0456 0.0146 0.0453 7677 8913 2.14 0.00 1 59769 30500 36113  
 PSID GMD DELD RC LT1R LT2R SPT1 CHID SO SS WS SSSO  
 7.57 35.82 25.71 0.394 1.579 0.622 36102.0 11.2 18500.0 22500.0 14430.5 1.1899  
 ITERATIONS ON TEST NUMBER 43248 ARE COMPLETE WHERE THE CUTTING SPEED = 240.0 THE RAKE ANGLE = 40.00 THE UNDEFORMED CHIP  
 THICKNESS = 0.02019 SOP= 1.83147E+04 SSSOP= 1.18999E+00 T2= 5.12635E-02 RC= 3.94042E-01;

....VC.....ALFD.....W.....T1.....T2.....PC.....PT.....PFID.....BED.....WTL.....WPD.....THS.....THNA  
 240.0 35.0 0.279 0.0201 0.0559 378.0 123.2 20.46 53.05 90734 63179 79 211...  
 LO LBE LBF LAB BT1 BT2 E WSD NOSO WPT WKP SPT2  
 0.0317 0.0474 0.0174 0.0464 8491 5363 2.41 0.00 1 63191 27554 35744  
 PSID GMD DELD RC LT1R LT2R SPT1 CHID SO SS WS SSSO  
 11.50 35.25 22.24 0.361 1.572 0.567 35743.4 11.4 17200.0 22500.0 13790.7 1.1999  
 ITERATIONS ON TEST NUMBER 43247 ARE COMPLETE WHERE THE CUTTING SPEED = 240.0 THE RAKE ANGLE = 35.00 THE UNDEFORMED CHIP  
 THICKNESS = 0.02019 SOP= 1.72723E+04 SSSOP= 1.19999E+00 T2= 5.59160E-02 RC= 3.61255E-01;

....VC.....ALFD.....W.....T1.....T2.....PC.....PT.....PFID.....BED.....WTL.....WPD.....THS.....THNA  
 240.0 30.0 0.279 0.0201 0.0786 500.5 196.9 14.31 51.47 120140 94207 109 233...  
 LO LBE LBF LAB BT1 BT2 E WSD NOSO WPT WKP SPT2  
 0.0434 0.0649 0.0250 0.0631 5994 2292 3.63 0.00 1 94206 25933 34605  
 PSID GMD DELD RC LT1R LT2R SPT1 CHID SO SS WS SSSO  
 13.90 27.75 21.49 0.256 2.150 0.552 34605.4 10.8 16269.4 20745.2 11429.0 1.2751  
 ITERATIONS ON TEST NUMBER 43246 ARE COMPLETE WHERE THE CUTTING SPEED = 240.0 THE RAKE ANGLE = 30.00 THE UNDEFORMED CHIP  
 THICKNESS = 0.02019 SOP= 1.62210E+04 SSSOP= 1.27599E+00 T2= 7.86705E-02 RC= 2.56766E-01;

....VC.....ALFD.....W.....T1.....T2.....PC.....PT.....PFID.....BED.....WTL.....WPD.....THS.....THNA  
 240.0 25.0 0.279 0.0201 0.0919 552.0 262.6 12.37 50.43 132502 107651 120 252...  
 LO LBE LBF LAB BT1 BT2 E WSD NOSO WPT WKP SPT2  
 0.0404 0.0714 0.0364 0.0671 6512 1388 4.33 0.00 1 107650 24851 41588  
 PSID GMD DELD RC LT1R LT2R SPT1 CHID SO SS WS SSSO  
 20.57 29.95 21.42 0.219 2.003 0.440 41592.3 13.8 15406.0 20204.3 11372.9 1.3114  
 ITERATIONS ON TEST NUMBER 43245 ARE COMPLETE WHERE THE CUTTING SPEED = 240.0 THE RAKE ANGLE = 25.00 THE UNDEFORMED CHIP  
 THICKNESS = 0.02019 SOP= 1.55485E+04 SSSOP= 1.31202E+00 T2= 9.19494E-02 RC= 2.19685E-01;

....VC.....ALFD.....W.....T1.....T2.....PC.....PT.....PFID.....BED.....WTL.....WPD.....THS.....THNA  
 240.0 20.0 0.279 0.0201 0.0884 539.0 268.8 13.10 46.50 129379 105823 119 250...  
 LO LBE LBF LAB BT1 BT2 E WSD NOSO WPT WKP SPT2  
 0.0360 0.0663 0.0372 0.0613 8205 1281 4.17 0.00 1 105825 23955 43361  
 PSID GMD DELD RC LT1R LT2R SPT1 CHID SO SS WS SSSO  
 25.41 32.46 20.05 0.228 1.782 0.407 43353.0 14.5 15700.3 20343.7 12738.7 1.2957  
 ITERATIONS ON TEST NUMBER 43244 ARE COMPLETE WHERE THE CUTTING SPEED = 240.0 THE RAKE ANGLE = 20.00 THE UNDEFORMED CHIP  
 THICKNESS = 0.02019 SOP= 1.55845E+04 SSSOP= 1.29514E+00 T2= 9.84367E-02 RC= 2.28411E-01;

....VC.....ALPD.....W.....T1.....T2.....FC.....PT.....PFID.....BED.....WTL.....WPD.....THS.....THNA  
 160.0 45.0 0.279 0.0201 0.0514 370.5 94.9 21.03 59.37 59290 38604 67 180...  
 LO LBE LBP LAB ET1 ET2 E WSD NOSO WPT WKP SPT2  
 0.0342 0.0482 0.0142 0.0489 3929 10608 2.15 0.00 1 38613 20685 38365  
 PSID GMD DELD RC LT1R LT2R SPT1 CHID SO SS WS SSSO  
 3.96 34.43 31.51 0.392 1.693 0.665 34366.0 13.5 17963.2 21572.0 12691.5 1.2010  
 ITERATIONS ON TEST NUMBER 43169 ARE COMPLETE WHERE THE CUTTING SPEED = 160.0 THE RAKE ANGLE = 45.00 THE UNDEFORMED CHIP  
 THICKNESS = 0.02019 SOP= 1.78834E+04 SSSOP= 1.19979E+00 T2= 5.14347E-02 RC= 3.92730E-01;

....VC.....ALPD.....W.....T1.....T2.....FC.....PT.....PFID.....BED.....WTL.....WPD.....THS.....THNA  
 160.0 40.0 0.279 0.0201 0.0593 410.0 120.2 18.44 56.34 65602 46247 77 185...  
 LO LBE LBP LAB ET1 ET2 E WSD NOSO WPT WKP SPT2  
 0.0382 0.0535 0.0162 0.0538 3809 4900 2.60 0.00 1 46267 19355 33265  
 PSID GMD DELD RC LT1R LT2R SPT1 CHID SO SS WS SSSO  
 6.63 30.95 27.57 0.340 1.891 0.643 33239.1 11.8 17405.6 21337.3 11984.4 1.2258  
 ITERATIONS ON TEST NUMBER 43168 ARE COMPLETE WHERE THE CUTTING SPEED = 160.0 THE RAKE ANGLE = 40.00 THE UNDEFORMED CHIP  
 THICKNESS = 0.02019 SOP= 1.73282E+04 SSSOP= 1.22647E+00 T2= 5.93859E-02 RC= 3.40147E-01;

....VC.....ALPD.....W.....T1.....T2.....FC.....PT.....PFID.....BED.....WTL.....WPD.....THS.....THNA  
 160.0 35.0 0.279 0.0201 0.0704 459.8 158.6 15.71 54.32 73580 55507 89 193...  
 LO LBE LBP LAB ET1 ET2 E WSD NOSO WPT WKP SPT2  
 0.0411 0.0602 0.0212 0.0595 3686 2361 3.20 0.00 1 55514 18073 34201  
 PSID GMD DELD RC LT1R LT2R SPT1 CHID SO SS WS SSSO  
 10.71 28.68 23.24 0.246 2.035 0.583 34199.0 11.5 16539.7 20895.6 11100.4 1.2633  
 ITERATIONS ON TEST NUMBER 43167 ARE COMPLETE WHERE THE CUTTING SPEED = 160.0 THE RAKE ANGLE = 35.00 THE UNDEFORMED CHIP  
 THICKNESS = 0.02019 SOP= 1.65288E+04 SSSOP= 1.26336E+00 T2= 7.04065E-02 RC= 2.86904E-01;

....VC.....ALPD.....W.....T1.....T2.....FC.....PT.....PFID.....BED.....WTL.....WPD.....THS.....THNA  
 160.0 30.0 0.279 0.0201 0.0831 520.3 213.6 13.46 52.32 83260 65959 101 209...  
 LO LBE LBP LAB ET1 ET2 E WSD NOSO WPT WKP SPT2  
 0.0413 0.0671 0.0296 0.0644 3730 1292 3.88 0.00 1 65960 17300 38412  
 PSID GMD DELD RC LT1R LT2R SPT1 CHID SO SS WS SSSO  
 16.19 28.54 20.91 0.242 2.049 0.497 38412.2 12.0 15843.5 20718.8 10713.8 1.3077  
 ITERATIONS ON TEST NUMBER 43166 ARE COMPLETE WHERE THE CUTTING SPEED = 160.0 THE RAKE ANGLE = 30.00 THE UNDEFORMED CHIP  
 THICKNESS = 0.02019 SOP= 1.58091E+04 SSSOP= 1.30775E+00 T2= 8.31716E-02 RC= 2.42871E-01;

....VC.....ALPD.....W.....T1.....T2.....FC.....PT.....PFID.....BED.....WTL.....WPD.....THS.....THNA  
 160.0 25.0 0.279 0.0201 0.0977 576.8 282.7 11.59 51.11 92296 75761 111 225...  
 LO LBE LBP LAB ET1 ET2 E WSD NOSO WPT WKP SPT2  
 0.0387 0.0746 0.0416 0.0690 3972 809 4.63 0.00 1 75761 16535 46026  
 PSID GMD DELD RC LT1R LT2R SPT1 CHID SO SS WS SSSO  
 22.84 30.54 20.97 0.206 1.920 0.396 46028.7 14.8 14944.1 20208.5 10612.0 1.3522  
 ITERATIONS ON TEST NUMBER 43165 ARE COMPLETE WHERE THE CUTTING SPEED = 160.0 THE RAKE ANGLE = 25.00 THE UNDEFORMED CHIP  
 THICKNESS = 0.02019 SOP= 1.50798E+04 SSSOP= 1.35280E+00 T2= 9.77389E-02 RC= 2.06672E-01;

....VC.....ALPD.....W.....T1.....T2.....FC.....PT.....PFID.....BED.....WTL.....WPD.....THS.....THNA  
 160.0 20.0 0.279 0.0201 0.0981 605.1 317.0 11.75 47.65 96831 80201 118 240...  
 LO LBE LBP LAB ET1 ET2 E WSD NOSO WPT WKP SPT2  
 0.0342 0.0723 0.0453 0.0652 4633 703 4.66 0.00 1 80207 16630 52618  
 PSID GMD DELD RC LT1R LT2R SPT1 CHID SO SS WS SSSO  
 28.64 33.26 20.09 0.205 1.696 0.349 52611.0 13.8 15564.9 21221.7 12066.9 1.3634  
 ITERATIONS ON TEST NUMBER 43164 ARE COMPLETE WHERE THE CUTTING SPEED = 160.0 THE RAKE ANGLE = 20.00 THE UNDEFORMED CHIP  
 THICKNESS = 0.02019 SOP= 1.54435E+04 SSSOP= 1.36228E+00 T2= 9.81341E-02 RC= 2.05840E-01;

....VC.....ALPD.....W.....T1.....T2.....FC.....FT.....PFID.....BED.....WTL.....WPD.....THS.....THMA  
 120.0 45.0 0.279 0.0201 0.0521 372.4 102.8 20.68 60.44 44689 29056 62 165...  
 LO LBE LBF LAB ET1 ET2 E WSD NOSO WPT WKF SPT2  
 0.0322 0.0480 0.0161 0.0485 3024 6545 2.19 0.00 1 29024 15633 37265  
 PSID GMD DELD RC LT1R LT2R SPT1 CHID SO SS NS SSSO  
 5.03 35.62 24.89 0.387 1.596 0.618 37218.2 14.7 17751.7 21435.1 12653.8 1.2058  
 ITERATIONS ON TEST NUMBER 43129 ARE COMPLETE WHERE THE CUTTING SPEED = 120.0 THE RAKE ANGLE = 45.00 THE UNDEFORMED CHIP  
 THICKNESS = 0.02019 SOP= 1.76550E+04 SSSOP= 1.20613E+00 T2= 5.21115E-02 RC= 3.87629E-01;

....VC.....ALPD.....W.....T1.....T2.....FC.....FT.....PFID.....BED.....WTL.....WPD.....THS.....THMA  
 120.0 40.0 0.279 0.0201 0.0607 415.4 128.2 17.94 57.15 49858 35282 72 169...  
 LO LBE LBF LAB ET1 ET2 E WSD NOSO WPT WKF SPT2  
 0.0366 0.0539 0.0183 0.0539 2827 3177 2.68 0.00 1 35302 14576 35665  
 PSID GMD DELD RC LT1R LT2R SPT1 CHID SO SS NS SSSO  
 7.80 31.69 26.44 0.332 1.812 0.602 35631.9 12.7 17178.6 21245.6 11720.9 1.2367  
 ITERATIONS ON TEST NUMBER 43128 ARE COMPLETE WHERE THE CUTTING SPEED = 120.0 THE RAKE ANGLE = 40.00 THE UNDEFORMED CHIP  
 THICKNESS = 0.02019 SOP= 1.70842E+04 SSSOP= 1.23757E+00 T2= 6.07558E-02 RC= 3.32478E-01;

....VC.....ALPD.....W.....T1.....T2.....FC.....FT.....PFID.....BED.....WTL.....WPD.....THS.....THMA  
 120.0 35.0 0.279 0.0201 0.0727 470.6 167.6 15.13 54.60 56482 42917 84 177...  
 LO LBE LBF LAB ET1 ET2 E WSD NOSO WPT WKF SPT2  
 0.0398 0.0613 0.0238 0.0602 2658 1563 3.33 0.00 1 42919 13565 36474  
 PSID GMD DELD RC LT1R LT2R SPT1 CHID SO SS NS SSSO  
 12.06 29.08 22.46 0.277 1.974 0.548 36471.4 12.1 16288.5 20872.5 10644.0 1.2814  
 ITERATIONS ON TEST NUMBER 43127 ARE COMPLETE WHERE THE CUTTING SPEED = 120.0 THE RAKE ANGLE = 35.00 THE UNDEFORMED CHIP  
 THICKNESS = 0.02019 SOP= 1.62765E+04 SSSOP= 1.28148E+00 T2= 7.27741E-02 RC= 2.77571E-01;

....VC.....ALPD.....W.....T1.....T2.....FC.....FT.....PFID.....BED.....WTL.....WPD.....THS.....THMA  
 120.0 30.0 0.279 0.0201 0.0865 542.8 226.2 12.88 52.62 65143 52053 97 194...  
 LO LBE LBF LAB ET1 ET2 E WSD NOSO WPT WKF SPT2  
 0.0403 0.0687 0.0328 0.0654 2615 863 4.86 0.00 1 52054 13090 41392  
 PSID GMD DELD RC LT1R LT2R SPT1 CHID SO SS NS SSSO  
 17.83 28.69 20.04 0.233 1.996 0.465 41391.3 11.8 15720.3 21011.9 10181.3 1.3366  
 ITERATIONS ON TEST NUMBER 43126 ARE COMPLETE WHERE THE CUTTING SPEED = 120.0 THE RAKE ANGLE = 30.00 THE UNDEFORMED CHIP  
 THICKNESS = 0.02019 SOP= 1.56962E+04 SSSOP= 1.33747E+00 T2= 8.65525E-02 RC= 2.33384E-01;

....VC.....ALPD.....W.....T1.....T2.....FC.....FT.....PFID.....BED.....WTL.....WPD.....THS.....THMA  
 120.0 25.0 0.279 0.0201 0.1031 610.0 303.5 10.94 51.45 73201 60684 107 212...  
 LO LBE LBF LAB ET1 ET2 E WSD NOSO WPT WKF SPT2  
 0.0377 0.0777 0.0462 0.0708 2710 537 4.92 0.00 1 60682 12516 50388  
 PSID GMD DELD RC LT1R LT2R SPT1 CHID SO SS NS SSSO  
 24.82 30.62 20.12 0.195 1.869 0.365 50392.2 14.5 14723.0 20555.2 9937.5 1.3961  
 ITERATIONS ON TEST NUMBER 43125 ARE COMPLETE WHERE THE CUTTING SPEED = 120.0 THE RAKE ANGLE = 25.00 THE UNDEFORMED CHIP  
 THICKNESS = 0.02019 SOP= 1.46302E+04 SSSOP= 1.39656E+00 T2= 1.03197E-01 RC= 1.95741E-01;

....VC.....ALPD.....W.....T1.....T2.....FC.....FT.....PFID.....BED.....WTL.....WPD.....THS.....THMA  
 120.0 20.0 0.279 0.0201 0.1122 698.8 390.5 10.21 49.19 83860 76771 122 246...  
 LO LBE LBF LAB ET1 ET2 E WSD NOSO WPT WKF SPT2  
 0.0314 0.0812 0.0573 0.0705 2920 426 5.29 0.00 1 70769 13088 68742  
 PSID GMD DELD RC LT1R LT2R SPT1 CHID SO SS NS SSSO  
 32.74 34.34 19.97 0.179 1.558 0.289 68742.0 13.3 15243.3 22200.0 11120.5 1.4563  
 ITERATIONS ON TEST NUMBER 43124 ARE COMPLETE WHERE THE CUTTING SPEED = 120.0 THE RAKE ANGLE = 20.00 THE UNDEFORMED CHIP  
 THICKNESS = 0.02019 SOP= 1.52352E+04 SSSOP= 1.45714E+00 T2= 1.12228E-01 RC= 1.79989E-01;

....VC.....ALFD.....W.....T1.....T2.....FC.....PT.....PFID.....BED.....WTL.....WPD.....THS.....THMA  
 80.0 45.0 0.279 0.0201 0.0534 378.5 112.3 20.04 61.53 30281 19785 56 150...  
 LO LBE LBP LAB ET1 ET2 E WSD NOSO WPT WKF SPT2  
 0.0302 0.0483 0.0185 0.0485 2301 3534 2.27 0.00 1 19784 10496 41019  
 PSID GND DELD RC LT1R LT2R SPT1 CHID SO SS NS SSSO  
 6.46 36.59 28.00 0.377 1.496 0.565 41020.1 15.8 17499.3 21308.1 12370.2 1.2176  
 ITERATIONS ON TEST NUMBER 43089 ARE COMPLETE WHERE THE CUTTING SPEED = 80.0 THE RAKE ANGLE = 45.00 THE UNDEFORMED CHIP  
 THICKNESS = 0.02019 SOP= 1.73766E+04 SSSOP= 1.21827E+00 T2= 5.34416E-02 RC= 3.77982E-01;

....VC.....ALFD.....W.....T1.....T2.....FC.....PT.....PFID.....BED.....WTL.....WPD.....THS.....THMA  
 80.0 40.0 0.279 0.0201 0.0635 424.7 139.0 17.02 58.13 33977 24321 65 150...  
 LO LBE LBP LAB ET1 ET2 E WSD NOSO WPT WKF SPT2  
 0.0350 0.0552 0.0214 0.0549 1798 1745 2.84 0.00 1 24323 9655 38692  
 PSID GND DELD RC LT1R LT2R SPT1 CHID SO SS NS SSSO  
 9.44 32.15 24.99 0.317 1.734 0.551 38690.1 14.1 16689.3 20985.1 11019.8 1.2573  
 ITERATIONS ON TEST NUMBER 43088 ARE COMPLETE WHERE THE CUTTING SPEED = 80.0 THE RAKE ANGLE = 40.00 THE UNDEFORMED CHIP  
 THICKNESS = 0.02019 SOP= 1.66230E+04 SSSOP= 1.25707E+00 T2= 6.35240E-02 RC= 3.17989E-01;

....VC.....ALFD.....W.....T1.....T2.....FC.....PT.....PFID.....BED.....WTL.....WPD.....THS.....THMA  
 80.0 35.0 0.279 0.0201 0.0769 495.6 180.2 14.21 54.98 39649 30574 78 158...  
 LO LBE LBP LAB ET1 ET2 E WSD NOSO WPT WKF SPT2  
 0.0388 0.0633 0.0274 0.0618 1617 863 3.56 0.00 1 30573 9075 39732  
 PSID GND DELD RC LT1R LT2R SPT1 CHID SO SS NS SSSO  
 14.07 28.93 20.77 0.262 1.922 0.504 39730.6 12.1 16040.8 21101.3 9778.4 1.3154  
 ITERATIONS ON TEST NUMBER 43087 ARE COMPLETE WHERE THE CUTTING SPEED = 80.0 THE RAKE ANGLE = 35.00 THE UNDEFORMED CHIP  
 THICKNESS = 0.02019 SOP= 1.60369E+04 SSSOP= 1.31646E+00 T2= 7.69056E-02 RC= 2.62659E-01;

....VC.....ALFD.....W.....T1.....T2.....FC.....PT.....PFID.....BED.....WTL.....WPD.....THS.....THMA  
 80.0 30.0 0.279 0.0201 0.0898 574.8 241.0 12.36 52.74 45986 37067 90 174...  
 LO LBE LBP LAB ET1 ET2 E WSD NOSO WPT WKF SPT2  
 0.0393 0.0703 0.0358 0.0663 1617 514 4.24 0.00 1 37074 8918 45070  
 PSID GND DELD RC LT1R LT2R SPT1 CHID SO SS NS SSSO  
 19.56 28.63 18.87 0.224 1.946 0.437 45061.6 10.8 15815.9 21667.8 9679.0 1.3699  
 ITERATIONS ON TEST NUMBER 43086 ARE COMPLETE WHERE THE CUTTING SPEED = 80.0 THE RAKE ANGLE = 30.00 THE UNDEFORMED CHIP  
 THICKNESS = 0.02019 SOP= 1.59060E+04 SSSOP= 1.36999E+00 T2= 8.94951E-02 RC= 2.24706E-01;

....VC.....ALFD.....W.....T1.....T2.....FC.....PT.....PFID.....BED.....WTL.....WPD.....THS.....THMA  
 80.0 25.0 0.279 0.0201 0.1099 688.4 343.4 10.23 51.51 55072 46224 104 200...  
 LO LBE LBP LAB ET1 ET2 E WSD NOSO WPT WKF SPT2  
 0.0362 0.0813 0.0521 0.0723 1567 307 5.27 0.00 1 46222 8848 59328  
 PSID GND DELD RC LT1R LT2R SPT1 CHID SO SS NS SSSO  
 27.80 30.36 18.27 0.183 1.794 0.329 59335.8 11.5 15102.0 22200.0 9223.0 1.4699  
 ITERATIONS ON TEST NUMBER 43085 ARE COMPLETE WHERE THE CUTTING SPEED = 80.0 THE RAKE ANGLE = 25.00 THE UNDEFORMED CHIP  
 THICKNESS = 0.02019 SOP= 1.51020E+04 SSSOP= 1.46999E+00 T2= 1.09968E-01 RC= 1.83688E-01;

....VC.....ALFD.....W.....T1.....T2.....FC.....PT.....PFID.....BED.....WTL.....WPD.....THS.....THMA  
 80.0 20.0 0.279 0.0201 0.1206 742.1 407.4 9.47 48.76 59374 50844 112 208...  
 LO LBE LBP LAB ET1 ET2 E WSD NOSO WPT WKF SPT2  
 0.0358 0.0873 0.0603 0.0751 1704 300 5.29 0.00 1 50853 8530 63420  
 PSID GND DELD RC LT1R LT2R SPT1 CHID SO SS NS SSSO  
 32.60 31.74 18.69 0.167 1.775 0.297 63416.9 12.1 14800.0 22200.0 9947.6 1.5000  
 ITERATIONS ON TEST NUMBER 43084 ARE COMPLETE WHERE THE CUTTING SPEED = 80.0 THE RAKE ANGLE = 20.00 THE UNDEFORMED CHIP  
 THICKNESS = 0.02019 SOP= 1.48000E+04 SSSOP= 1.50000E+00 T2= 1.20627E-01 RC= 1.67457E-01;

## PR2: PROCEDURE OPTIONS (MAIN)

```

1      PR2: PROCEDURE OPTIONS (MAIN)
2      DCL E(99) , ET(99) , T(99) , S(99) , SO(99) , A(49) , B(7) ,
          R(10,99) , NT(99) FIXED BINARY (31,0) , SS(99) , SS(99) ,
          (LE(99) , LT(99) , LSO(99) , LSS(99) , LSP(99) , LS(99) ) DECIMAL ;
3      NTROL = 1 ;
4      STT:
5      LE(*) = 0 ; LT(*) = 0 ; T(*) = 0 ;
6      LS(*) = 10**37 ;
7      S(*) = 10**37 ;
8      NTS = 29 ;
9      DO M = 1 TO NTS
10     IF NTROL = 1 THEN DO ;
11         GET EDIT ( NT(M) , E(M) , ET(M) , T(M) , SO(M) , SS(M) , CM)
12         ( 6 P(12,3) , P(8,3) )
13     END ;
14     IF NTROL = 2 THEN DO ;
15         GET EDIT ( NT(M) , E(M) , ET(M) , T(M) , SO(M) )
16         ( P(12,1) , 3 P(15,3) , P(23,9) )
17     END ;
18     S(M) = SO(M) ;
19     T(M) = T(M)/1000
20     LE(M) = LOG( P(M) )
21     LT(M) = LOG( ET(M) )
22     LS(M) = LOG( SO(M) )
23     END /* DO M = 1 TO NTS */
24     DO Q = -1 , 0 , 1 ; IF Q = 1 THEN P = 0 ; ELSE P = 1 ;
25     DO M = 1 TO NTS ;
26     LS(M) = P*LOG(SS(M)) + Q*LOG(SO(M)) ;
27     S(M) = ((SS(M)**P)*(SO(M)**Q)) ;
28     END ;
29     R(*,*) = 0.0 ;
30     R(1,*) = 1/LS(*) ;
31     R(2,*) = T(*)/LS(*) ;
32     R(3,*) = LE(*)/LS(*) ;
33     R(4,*) = LE(*)*T(*)/LS(*) ;
34     R(5,*) = LT(*)*T(*)/LS(*) ;
35     R(6,*) = LT(*)*LE(*)*T(*)/LS(*) ;
36     R(7,*) = LT(*)/LS(*) ;
37     DO M = 2 TO 7 ;
38     B(M) = 0.0 ;
39     M = 0 ;
40     DO I = 1 TO N ;
41     DO J = 1 TO M ;
42     M = M + 1 ; A(M) = SUM(R(I,*)*R(J,*) ) ; END ; B(I) = SUM(R(I,*) ) ;
43     END /* DO I = 1 TO N */ ;
44     PUT EDIT (':') ( PAGE , X(119) , A(1) ) ;
45     CALL PR5 ( A , B , N ) ;
46     PUT DATA (B)
47     SPO = EXP(B(1)) ; GK = EXP(B(2)) ; PUT DATA ( SPO , GK ) ;
48     LSP(*) = B(1) + T(*)*B(2) + LE(*)*B(3) + LE(*)*T(*)*B(4) +
49             LT(*)**(*)*B(5) + LT(*)*LE(*)*T(*)*B(6) + LT(*)*R(7)
50     SPSO = 0.0 ;
51     NPT = 29 ;

```

## PR2: PROCEDURE OPTIONS (MAIN)

```

60      DO M = 1 TO NPT ;
61      PSF = EXP(LSP(M))
62      EPSF = 100*(PSF-S(M))/S(M)
63      PUT EDIT ( MT(M) , S(M) , PSF , EPSF ) ( SKIP , P(5) , 3 F(12,3) )
64      SFSQ = SFSQ + ( S(M) - PSF )**2 ;
65      END ;
66      LST:
67      RMSQ = 100*(SQRT(SFSQ/30)) ;
68      PUT DATA ( RMSQ ) ;
69      END ;
70      IF NTROL = 1 THEN DO ; NTROL = 2 ; GO TO STT ; END ;
71      PR5: PROCEDURE (AH , BH , MM )
72      ON ZERODIVIDE GO TO LL4 ; ON UNDERFLOW GO TO LL4
73      ON OVERFLOW GO TO LL4 ; ON FIXEDOVERFLOW GO TO LL4
74      DECLARE A(49) , B(7) , AH(60) , BH(10)
75      DO KKK = 1 TO (MM*MM) ; A(KKK) = AH(KKK) ; END ; N = MM
76      DO KKK = 1 TO N ; B(KKK) = BH(KKK) ; END
77      DO M = 1 TO N
78      PUT EDIT ((A(N*L+M) DO L = 0 TO (N-1)) , B(M)) (SKIP , (N+1) F(12,6))
79      END
80      TOL = 0.0001
81      KS = 0
82      JJ = -N
83      DO J = 1 TO N
84      JY = J+1
85      JJ = JJ+N+1
86      BIGA = 0.0
87      IT = JJ-J
88      /* SEARCH FOR MAX COEFFICIENT IN COLUMN */
89      DO I = J TO N
90      IJ = IT+I
91      IF ( ABS(BIGA) - ABS(A(IJ))) < 0.0 THEN DO
92      BIGA = A(IJ)
93      IMAX = I
94      END /* (ABS(BIGA) - ABS(A(IJ))) < 0.0 */
95      END /* I = J TO N */
96      /* TEST FOR PIVOT LESS THAN TO L */
97      /* INTERCHANGE ROWS IF NECESSARY */
98      I1 = J+N*(J-2)
99      IT = IMAX-J
100      DO K = J TO N
101      I1 = I1+N
102      I2 = I1 + IT
103      SAVE = A(I1)
104      A(I1) = A(I2)
105      A(I2) = SAVE
106      /* DIVIDE EQUATION BY LEADING COEFFICIENT */
107      A(I1) = A(I1)/BIGA
108      END /* IF (ABS(A(I1)) < 0.0 */
109      SAVE = B(IMAX)
110      B(IMAX) = B(J)
111      B(J) = SAVE/BIGA
112      IF J = N THEN GO TO HXSOL

```

## PR2: PROCEDURE OPTIONS (MAIN)

```

126      /* ELIMINATE NEXT VARIABLE      */
127      IQS = N*(J-1)
128      DO IX = JY TO N
129          IXJ = IQS + IX
130          IT = J - IX
131          DO JX = JY TO N
132              IXJX = N*(JX-1) + IX
133              JJX = IXJX + IT
134              A(IXJX) = A(IXJX) - (A(IXJ))*A(JJX)
135          END /* DO JX = JY TO N */
136      B(IX) = B(IX) - (B(J))*A(IXJ)
137      END /* DO IX = JY TO N */
138  BK SOL: /* BACK SOLUTION */
139      NY = N-1
140      IT = N*N
141      DO J = 1 TO NY
142          IA = IT - J
143          IB = N - J
144          IC = N
145          DO K = 1 TO J
146              B(IB) = B(IB) - (A(IA))*B(IC)
147          IA = IA - N
148          IC = IC - 1
149      END /* DO K = 1 TO J */
150      END /* DO J = 1 TO NY */
151      DO KKK = 1 TO N ; BH(KKK) = B(KKK) ; END
152      DO M = 1 TO N
153          PUT EDIT ((A(N*L*N) DO L = 0 TO (N-1)), B(N)) (SKIP, (N+1) P(12,6))
154      END
155  LL4:
156      RETURN
157      END PR5
158  END /*PR2*/

```



624.126953	86.132904	130.810592
86.132904	12.746530	19.155075
1.000000	0.138005	0.032609
86.132904	1.000000	1.282411

B(4) = 0.00000E+00      B(5) = 0.02070E+00  
 GK = 3.60532E+00;

43089	1.229	1.196	-2.671
43129	1.209	1.188	-1.733
43169	1.196	1.184	-1.086
43249	1.183	1.180	-0.325
43329	1.167	1.172	0.483
43489	1.171	1.166	-0.365
43088	1.283	1.240	-3.341
43128	1.250	1.224	-2.075
43168	1.224	1.216	-0.723
43248	1.202	1.209	0.553
43328	1.190	1.202	0.998
43488	1.190	1.196	0.497
43087	1.360	1.314	-3.380
43127	1.310	1.288	-1.988
43167	1.262	1.260	-0.165
43247	1.228	1.247	1.600
43327	1.211	1.236	2.046
43487	1.201	1.226	2.036
43086	1.421	1.383	-2.715
43126	1.369	1.386	-1.669
43166	1.322	1.320	-0.188
43246	1.285	1.301	1.292
43326	1.249	1.277	2.222
43486	1.216	1.250	2.807
43085	1.462	1.424	-2.558
43125	1.411	1.391	-1.375
43165	1.362	1.359	-0.224
43245	1.322	1.343	1.538
43325	1.295	1.328	2.242

B(1) = 3.26099E-02  
 B(6) = 0.00000E+00

B(2) = 1.28241E+00  
 B(7) = 0.00000E+00;

B(3) = 0.00000E+00  
 SPO = 1.03310E+00

RMSQ = 2.18457E+00;

624.126953	86.132904	619.010498	130.810592		
86.132904	12.746530	91.648910	19.155075		
619.010498	91.648910	660.296386	137.670013		
1.000000	0.138005	0.991802	0.032360		
86.132904	1.000000	7.450911	1.541179		
619.010498	0.859726	1.000000	-0.0357548	B(1) = 3.23601E-02	B(2) = 1.54117E+00
B(4) = 0.00030E+00	B(5) = 0.00000E+00	B(6) = 0.00000E+00		B(7) = 0.00000E+00;	B(3) = -3.57547E-02
GR = 4.67009E+00;					SFO = 1.03288E+00

43089	1.229	1.197	-2.619
43129	1.209	1.188	-1.723
43169	1.196	1.184	-1.022
43249	1.183	1.180	-0.269
43329	1.167	1.174	0.586
43409	1.171	1.169	-0.115
43088	1.283	1.238	-3.565
43128	1.250	1.221	-2.358
43168	1.224	1.213	-0.914
43248	1.202	1.208	0.483
43328	1.190	1.202	1.066
43408	1.190	1.198	0.647
43087	1.360	1.313	-3.501
43127	1.310	1.281	-2.218
43167	1.262	1.257	-0.435
43247	1.228	1.245	1.443
43327	1.211	1.235	1.977
43407	1.201	1.225	1.929
43086	1.421	1.388	-2.377
43126	1.369	1.347	-1.565
43166	1.322	1.320	-0.148
43246	1.285	1.302	1.303
43326	1.249	1.276	2.177
43406	1.216	1.247	2.562
43085	1.462	1.432	-2.057
43125	1.411	1.396	-1.038
43165	1.362	1.361	-0.117
43245	1.322	1.344	1.612
43325	1.295	1.325	2.308

RMSQ = 2.14674E+00;

624.126953	86.132904	619.010498	91.648895	130.810592
86.132904	12.746530	91.648910	14.556415	19.155075
619.010498	91.648910	660.296386	104.636795	137.670013
91.648895	14.556415	104.636795	17.711868	21.684661
1.000000	0.138005	0.991802	0.146843	0.334815
86.132904	1.000000	7.450911	2.208122	-3.403320
619.010498	0.859726	1.000000	-0.083171	0.067197
91.648895	1.908375	-0.183641	1.000000	1.891840
B(3) = 6.71970E-02	B(4) = 1.89184E+00	B(5) = 0.00000E+00		
SFO = 1.39768E+00	GR = 3.32626E-02;			
43089	1.229	1.190	-3.198	
43129	1.209	1.193	-1.307	
43169	1.196	1.192	-0.370	
43249	1.183	1.189	0.471	
43329	1.167	1.183	1.359	
43409	1.171	1.176	0.428	
43088	1.283	1.242	-3.222	
43128	1.250	1.236	-1.134	
43168	1.224	1.221	-0.320	
43248	1.202	1.205	0.239	
43328	1.190	1.189	-0.032	
43408	1.190	1.181	-0.784	
43087	1.360	1.326	-2.545	
43127	1.310	1.292	-1.380	
43167	1.262	1.266	0.334	
43247	1.228	1.239	0.916	
43327	1.211	1.219	0.677	
43407	1.201	1.217	1.292	
43086	1.421	1.388	-2.332	
43126	1.369	1.349	-1.438	
43166	1.322	1.309	-0.972	
43246	1.285	1.283	-0.110	
43326	1.249	1.257	0.626	
43406	1.216	1.252	2.905	
43085	1.462	1.466	0.253	
43125	1.411	1.410	-0.013	
43165	1.362	1.377	1.116	
43245	1.322	1.344	1.931	
43325	1.295	1.314	1.414	

B(1) = 3.34815E-01  
B(6) = 0.00000E+00

B(2) = -3.40332E+00  
B(7) = 0.00000E+00;

RMSQ = 1.74347E+00;

624.126953	86.132904	619.010498	91.648895	736.513183	130.810592
86.132904	12.746530	91.648910	14.556415	107.961090	19.155075
619.010498	91.648910	667.296386	104.636795	776.242675	137.670013
91.648895	14.556415	104.636795	17.711868	122.042526	21.684661
736.513183	107.961090	776.242675	122.042526	920.776855	161.579864
1.000000	0.146584	1.053941	0.165703	1.250183	0.113628
86.132904	1.000000	7.243497	2.198455	8.173068	1.805624
619.010498	0.911865	1.000000	0.046628	-3.941774	-0.012397
91.648895	1.122151	-0.084095	1.000000	-32.723373	0.340303
624.126953	0.120822	-0.005322	0.018555	1.000000	-0.161770
B(3) = -1.23976E-02	B(4) = 3.40303E-01	B(5) = -1.61770E-01	B(6) = 0.00000E+00	B(1) = 1.13628E-01	B(2) = 1.80562E+00
SFO = 1.12033E+00	GR = 6.08377E+00;				B(7) = 0.00000E+00;
43089	1.229	1.224	-0.408		
43129	1.209	1.208	-0.080		
43169	1.196	1.198	0.185		
43249	1.183	1.187	0.291		
43329	1.167	1.174	0.588		
43409	1.171	1.162	-0.737		
43088	1.283	1.272	-0.916		
43128	1.250	1.242	-0.605		
43168	1.224	1.227	0.227		
43248	1.202	1.209	0.567		
43328	1.190	1.195	0.421		
43408	1.190	1.181	-0.764		
43087	1.360	1.356	-0.385		
43127	1.310	1.303	-0.545		
43167	1.262	1.266	0.292		
43247	1.228	1.238	0.854		
43327	1.211	1.219	0.669		
43407	1.201	1.200	-0.071		
43086	1.421	1.430	0.618		
43126	1.369	1.365	-0.264		
43166	1.322	1.320	-0.166		
43246	1.285	1.293	-0.133		
43326	1.249	1.248	-0.076		
43406	1.216	1.214	-0.187		
43085	1.462	1.477	1.049		
43125	1.411	1.410	-0.057		
43165	1.362	1.357	-0.381		
43245	1.322	1.321	-0.096		
43325	1.295	1.290	-0.407		
				RMSQ = 5.89783E-01;	

624.126953	86.132904	619.010498	91.648895	736.513183	776.242675	130.810592
86.132904	12.746530	91.648891	14.556415	107.961090	122.042556	19.155075
619.010498	91.648891	660.296386	104.636795	776.242675	877.791015	137.670013
91.648895	14.556415	104.636795	17.711868	122.042526	147.047607	21.684661
736.513183	107.961090	776.242675	122.042526	920.776855	1030.567382	161.579864
776.242675	122.042556	877.791015	147.047607	1030.567382	1229.704833	181.014465
1.000000	0.157222	1.130820	0.189435	1.327634	1.584175	0.117229
86.132904	1.000000	7.234224	2.216387	7.678994	17.716308	1.944751
619.010498	-5.673248	1.000000	-0.038096	-1.492310	-1.721129	-0.017408
91.648895	0.147179	-0.066362	1.000000	-28.913238	-24.428405	0.227688
736.513183	-7.835083	0.059402	0.021621	1.000000	1.403723	-0.179894
624.126953	-0.795469	0.002679	0.002996	-0.192892	1.000000	0.016155

B(2) = 1.94475E+00  
B(7) = 0.00000E+00;

43089	1.229
43129	1.209
43169	1.196
43249	1.183
43329	1.167
43489	1.171
43088	1.283
43128	1.250
43168	1.224
43248	1.202
43328	1.190
43488	1.190
43087	1.360
43127	1.310
43167	1.262
43247	1.228
43327	1.211
43487	1.201
43086	1.421
43126	1.369
43166	1.322
43246	1.285
43326	1.249
43486	1.216
43085	1.462
43125	1.411
43165	1.362
43245	1.322
43325	1.295

B(3) = -1.74084E-02  
SP0 = 1.12437E+00

1.225	-0.338
1.208	-0.032
1.199	0.220
1.187	0.306
1.174	0.581
1.162	-0.763
1.271	-0.923
1.242	-0.610
1.227	0.228
1.209	0.560
1.194	0.404
1.180	-0.803
1.355	-0.419
1.302	-0.575
1.266	0.274
1.238	0.842
1.219	0.650
1.200	-0.107
1.429	0.538
1.365	-0.282
1.320	-0.155
1.283	-0.105
1.248	-0.061
1.214	-0.196
1.476	0.973
1.410	-0.042
1.358	-0.331
1.322	-0.014
1.291	-0.325

B(4) = 2.27688E-01  
GK = 6.94189E+00;

RESQ = 5.76557E-01;

B(5) = -1.79894E-01

B(1) = 1.17229E-01  
B(6) = 1.61554E-02

624.126953	96.132904	619.010498	91.648895	736.513183	776.242675	5379.683593	130.810592
86.132904	12.746530	91.648910	14.556415	107.961090	122.042556	736.513183	19.155075
619.010498	91.648910	660.296386	104.636795	776.242675	877.791015	5289.812500	137.670013
91.648895	14.556415	104.636795	17.711868	122.042526	147.047607	776.242675	21.684661
736.513183	107.961090	776.242675	122.042526	920.776855	1030.567382	6339.351562	161.579864
776.242675	122.042556	877.791015	147.047607	1030.567382	1229.704833	6620.015625	181.014465
5379.683593	736.513183	5289.812500	776.242675	6339.351562	6620.015625	46658.593750	1114.195800
1.000000	0.136906	0.983294	0.144291	1.178186	1.230558	8.673110	-0.004875
86.132904	1.000000	7.261648	2.222094	7.346454	17.406021	-7.128849	3.592204
619.010498	6.902435	1.000000	-0.012623	-2.592805	-2.713879	-19.766647	-0.016740
91.648895	2.009097	-0.070388	1.000000	-43.174942	-38.944717	-303.502841	-0.498263
736.513183	7.127746	0.274505	-0.065087	1.000000	1.017687	7.598006	-0.369175
776.242675	0.954386	0.024505	0.007746	-0.150156	1.000000	-6.134042	0.098999
624.126953	0.685943	0.328977	0.022424	0.070603	-0.040078	1.000000	0.0139718

B(2) = 3.59220E+00	B(3) = -1.67404E-02	B(4) = -4.94263E-01	B(5) = -3.69175E-01	B(6) = 9.89996E-02
B(7) = 1.39716E-02;	SPO = 9.95135E-01	GE = 3.63140E+01;		

43089	1.229	1.225	-0.337
43129	1.209	1.208	-0.065
43169	1.196	1.198	0.192
43209	1.193	1.187	0.296
43329	1.167	1.174	0.599
43489	1.171	1.162	-0.711
43088	1.283	1.272	-0.894
43128	1.250	1.242	-0.622
43168	1.224	1.227	0.226
43248	1.202	1.209	0.560
43328	1.190	1.194	0.393
43488	1.190	1.180	-0.829
43087	1.360	1.355	-0.402
43127	1.310	1.303	-0.554
43167	1.262	1.266	0.292
43247	1.228	1.238	0.852
43327	1.211	1.219	0.636
43487	1.201	1.200	-0.131
43086	1.421	1.429	0.562
43126	1.369	1.365	-0.246
43166	1.322	1.321	-0.106
43246	1.285	1.284	-0.087
43326	1.249	1.248	-0.082
43486	1.216	1.213	-0.202
43085	1.462	1.474	0.848
43125	1.411	1.410	-0.053
43165	1.362	1.358	-0.322
43245	1.322	1.322	0.006
43325	1.295	1.291	-0.325

RMSQ = 5.59506E-01;

0.292032	0.045670	2.910132
0.045670	0.007701	0.455084
1.000000	0.156390	9.973781
0.045670	1.000000	-0.055555

B(4) = 0.00000E+00  
 GK = 9.45959E-01;  
 B(5) = 0.00000E+00

43089	22495.300	21320.437	-5.222
43129	21779.003	21326.843	-2.076
43169	21616.609	21330.058	-1.325
43249	21446.996	21333.230	-0.530
43329	21541.496	21339.050	-0.939
43489	21951.199	21343.629	-2.767
43088	21316.796	21286.812	-0.140
43128	20774.300	21299.015	2.525
43168	20727.597	21305.457	2.787
43248	21105.410	21310.761	0.972
43328	21616.691	21316.187	-1.390
43488	21923.500	21320.519	-2.750
43087	20934.898	21233.550	1.426
43127	20669.996	21255.167	2.831
43167	20459.695	21272.406	3.972
43247	20808.304	21281.656	2.274
43327	21055.695	21290.039	1.112
43487	20763.703	21297.738	2.571
43086	21937.703	21186.843	-3.422
43126	21397.496	21211.652	-0.868
43166	21461.402	21229.683	-1.079
43246	21416.605	21242.644	-0.812
43326	21294.507	21260.113	-0.161
43486	20253.003	21279.628	5.069
43085	21642.496	21159.664	-2.230
43125	21564.906	21181.328	-1.778
43165	21096.699	21202.691	0.502
43245	20937.593	21213.875	1.319
43325	21102.109	21226.464	0.589

B(1) = 9.97378E+00  
 B(6) = 0.00000E+00

B(2) = -5.55551E-02  
 B(7) = 0.00000E+00;

B(3) = 0.00000E+00  
 SPO = 2.14564E+04

RMSQ = 4.56106E+04;

0.292032	0.045670	0.327606	2.910132		
0.045670	0.007701	0.055009	0.455084		
0.327606	0.055009	0.393718	3.264145		
1.000000	0.167913	1.201803	9.999094		
0.045670	1.000000	5.941495	2.547584		
0.292032	0.000032	1.000000	-0.385461	B(1) = 9.99909E+00	B(2) = 2.54758E+00
B(4) = 0.00000E+00	B(5) = 0.00000E+00	B(6) = 0.00000E+00			B(3) = -3.85461E-01
GR = 1.27762E+01;					SFO = 2.20065E+04

43089	22495.300	21587.003	-4.037
43129	21779.003	21515.750	-1.208
43169	21616.609	21559.785	-0.262
43249	21446.996	21650.734	0.949
43329	21541.496	21878.992	1.566
43489	21951.199	22155.648	0.931
43088	21316.796	20789.401	-2.473
43128	20774.300	20714.218	-0.289
43168	20727.597	20957.292	1.108
43248	21105.410	21259.585	0.730
43328	21616.691	21600.925	-0.072
43488	21923.500	21810.910	-0.513
43087	20934.898	20799.034	-0.648
43127	20669.996	20649.050	-0.101
43167	20459.695	20642.257	0.892
43247	20808.304	20941.207	0.638
43327	21055.695	21176.179	0.572
43487	20763.703	21123.191	1.731
43086	21937.703	21678.605	-1.181
43126	21397.496	21227.902	-0.792
43166	21461.402	21157.789	-1.414
43246	21416.605	21148.056	-1.253
43326	21294.507	21098.449	-0.920
43486	20253.003	20743.277	2.420
43085	21642.496	21948.101	1.412
43125	21564.906	21639.750	0.347
43165	21096.699	21194.746	0.464
43245	20937.593	21163.863	1.080
43325	21102.104	21201.820	0.472

RMSQ = 2.65034E+04;



0.292032	0.045670	0.327606	0.055009	2.910132
0.045670	0.007701	0.055009	0.009873	0.455084
0.327606	0.055009	0.393718	0.070246	3.264145
0.055009	0.009873	0.070246	0.013257	0.548114
1.000000	0.167913	1.201803	0.214424	9.855410
0.045670	1.000000	6.941495	2.261244	4.903636
0.292032	0.000032	1.000000	-0.094067	-0.437919
0.055009	0.000636	-0.000105	1.000000	-0.880994

$B(3) = -4.37919E-01$        $B(4) = -8.80894E-01$        $B(5) = 0.00000E+00$   
 $SP0 = 1.90612E+04$        $GR = 1.34779E+02$

43089	22495.300	21638.511	-3.808
43129	21779.003	21462.464	-1.453
43169	21616.609	21482.101	-0.622
43249	21446.996	21563.960	0.545
43329	21541.496	21788.976	1.148
43489	21951.199	22088.539	0.625
43088	21316.796	20752.855	-2.645
43128	20774.300	20586.308	-0.904
43168	20727.597	20891.000	0.788
43248	21105.410	21276.683	0.811
43328	21616.691	21705.765	0.412
43488	21923.500	21952.015	0.130
43087	20934.898	20723.960	-1.007
43127	20669.996	20572.589	-0.471
43167	20459.695	20570.468	0.541
43247	20808.304	20993.796	0.891
43327	21055.695	21303.996	1.179
43487	20763.703	21182.035	2.014
43086	21937.703	21726.207	-0.964
43126	21397.496	21250.341	-0.687
43166	21461.402	21266.218	-0.909
43246	21416.605	21308.015	-0.507
43326	21294.507	21262.101	-0.152
43486	20253.003	20707.503	2.284
43085	21642.496	21778.566	0.628
43125	21564.906	21589.968	0.116
43165	21096.699	21112.378	0.074
43245	20937.593	21166.324	1.092
43325	21102.109	21317.304	1.019

RMSQ= 2.51087E+04;

$B(1) = 9.85541E+00$   
 $B(6) = 0.00000E+00$

$B(2) = 4.90363E+00$   
 $B(7) = 0.00000E+00$

0.292032	0.045670	0.327606	0.055009	0.379511	2.910132	
0.045670	0.007701	0.055009	0.009873	0.063261	0.455084	
0.327606	0.055009	0.393718	0.070246	0.452270	3.264195	
0.055009	0.009873	0.070246	0.013257	0.080291	0.548114	
0.379511	0.063261	0.452270	0.080291	0.523504	3.781418	
1.000000	0.166692	1.191716	0.211564	1.373414	9.669666	
0.045670	1.000000	6.788734	2.251497	7.751526	9.024670	
0.327606	0.000399	1.000000	0.062283	-4.618093	-0.492552	
0.055009	0.000703	-0.000081	1.000000	-34.566223	-2.162377	
0.292032	0.000088	-0.000017	0.000012	1.000000	-0.120091	B(1) = 9.66966E+00
B(3) = -4.92552E-01	B(4) = -2.16237E+00	B(5) = -1.20091E-01	B(6) = 0.00000E+00	B(2) = 9.02467E+00	B(7) = 0.00000E+00;	
SPO = 1.58300E+04	GR = 8.30547E+03;					
43089	22495.300	22079.777	-1.847			
43129	21779.003	21630.218	-0.683			
43169	21616.609	21537.058	-0.369			
43249	21446.996	21447.820	0.236			
43329	21541.496	21621.371	0.370			
43489	21951.199	21849.425	-0.463			
43088	21316.796	21106.195	-0.987			
43128	20774.300	20647.101	-0.612			
43168	20727.597	20957.992	1.111			
43248	21105.410	21313.769	0.987			
43328	21616.691	21767.210	0.696			
43488	21923.500	21942.933	0.088			
43087	20934.898	21039.859	0.501			
43127	20669.996	20674.765	0.023			
43167	20459.695	20548.039	0.431			
43247	20808.304	20978.906	0.819			
43327	21055.695	21302.511	1.172			
43487	20763.703	20963.167	0.960			
43086	21937.703	22158.859	1.008			
43126	21397.496	21403.148	0.026			
43166	21461.402	21378.812	-0.384			
43246	21416.605	21299.464	-0.546			
43326	21294.507	21152.804	-0.665			
43486	20253.003	20225.671	-0.138			
43085	21642.496	21807.996	0.764			
43125	21564.906	21517.308	-0.220			
43165	21096.699	20829.667	-1.265			
43245	20437.593	20818.585	-0.568			
43325	21102.109	21015.832	-0.408			
			RMSQ = 1.49709E+04;			

0.292032	0.045670	0.327606	0.055009	0.379511	0.452270	2.910132
0.045670	0.007701	0.055009	0.009873	0.063261	0.080291	0.455084
0.327606	0.055009	0.393718	0.070246	0.452270	0.572010	3.264145
0.055009	0.009873	0.070246	0.013257	0.080291	0.106872	0.548114
0.379511	0.063261	0.452270	0.080291	0.523504	0.657674	3.781414
0.452270	0.080291	0.572010	0.106872	0.657674	0.867514	4.506116
1.000000	0.177529	1.264753	0.236302	1.454162	1.918133	9.718111
0.045670	1.000000	6.761841	2.267619	7.313968	17.476501	11.524127
0.327606	-0.003150	1.000000	-0.035426	-1.595391	-1.958060	-0.575324
0.055009	0.000107	-0.000052	1.000000	-30.882980	-29.432968	-3.957736
0.379511	-0.004112	0.000089	0.000013	1.000000	1.478090	-0.423331
0.292032	-0.000406	-0.000004	0.000002	-0.000107	1.000000	0.249101
B(2) = 1.15241E+01	B(3) = -5.75324E-01	B(4) = -3.95773E+00	B(5) = -4.23331E-01	B(1) = 0.71811E+00		
B(7) = 0.00000E+00;	SFO = 1.66159E+04	GK = 1.01126E+05;		B(6) = 2.49101E-01		
43089	22495.300	22388.929	-0.472			
43129	21779.003	21827.179	0.221			
43169	21616.609	21672.238	0.257			
43249	21446.996	21541.390	0.440			
43329	21541.496	21589.597	0.223			
43409	21951.199	21722.726	-1.040			
43088	21316.796	21151.636	-0.774			
43128	20774.300	20654.742	-0.575			
43168	20727.597	20973.746	1.187			
43248	21105.410	21282.570	0.839			
43328	21616.691	21694.136	0.358			
43408	21923.500	21775.246	-0.676			
43087	20934.898	20887.656	-0.225			
43127	20669.996	20610.488	-0.287			
43167	20459.695	20497.464	0.184			
43247	20808.304	20919.949	0.536			
43327	21055.695	21207.058	0.718			
43407	20763.703	20783.535	0.095			
43086	21937.703	22001.519	0.290			
43126	21397.496	21391.046	-0.030			
43166	21461.402	21426.859	-0.160			
43246	21416.605	21362.609	-0.252			
43326	21294.507	21146.531	-0.694			
43406	20253.003	20102.027	-0.745			
43085	21642.496	21650.652	0.037			
43125	21564.906	21600.578	0.165			
43165	21096.699	20976.785	-0.568			
43245	20937.593	21031.593	0.448			
43325	21102.109	21211.468	0.518			
			PMSQ = 1.04891E+04;			

0.292032	0.045670	0.327606	0.055009	0.379511	0.452270	2.453555	2.910132
0.045670	0.007701	0.055009	0.009873	0.063261	0.080291	0.379511	0.455084
0.327606	0.055009	0.393718	0.070246	0.452270	0.572010	2.723141	3.264145
0.055009	0.009873	0.070246	0.013257	0.080291	0.106872	0.452270	0.548114
0.379511	0.063261	0.452270	0.080291	0.523504	0.657674	3.176957	3.791414
0.452270	0.080291	0.572010	0.106872	0.657674	0.867514	3.745814	4.506116
2.453555	0.379511	2.723141	0.452270	3.176957	3.745814	20.762664	24.449050
1.000000	0.154678	1.109875	0.184332	1.294837	1.526687	8.462277	13.028878
0.045670	1.000000	6.717787	2.274337	6.972425	17.130538	-7.878376	-33.861724
0.327606	0.004335	1.000000	-0.003884	-2.461212	-3.317168	-20.572586	-0.534207
0.055009	0.001364	-0.000054	1.000000	-43.399826	-43.204467	-280.449462	15.834304
0.379511	0.004559	0.000155	-0.000034	1.000000	1.100068	7.013899	4.769542
0.452270	0.000637	0.000001	0.000005	-0.000075	1.000000	-5.931029	-2.034223
0.292032	0.000499	0.000098	0.000014	0.000021	-0.000024	1.000000	-0.3808088 (1) = 1.302888E+01
B(2) = -3.38617E+01		B(3) = -5.34207E-01		B(4) = 1.58343E+01		B(5) = 4.76954E+00	
B(7) = -3.80808E-01;		SFO = 4.55375E+05		GR = 1.96806E-15;		B(6) = -2.03422E+00	
43089	22495.300	22323.031	-0.765				
43129	21779.003	21989.085	0.937				
43169	21616.609	21804.234	0.867				
43249	21446.996	21557.687	0.516				
43329	21541.496	21425.449	-0.538				
43489	21951.199	21332.679	-2.817				
43088	21316.796	21047.281	-1.264				
43128	20774.300	20796.003	0.104				
43168	20727.597	21032.875	1.472				
43248	21105.410	21303.261	0.937				
43328	21616.691	21751.500	0.623				
43488	21923.500	21915.515	-0.036				
43087	20934.898	20842.085	-0.443				
43127	20669.996	20564.078	-0.512				
43167	20459.695	20489.589	0.146				
43247	20808.304	20929.449	0.582				
43327	21055.695	21334.003	1.321				
43487	20763.703	20982.750	1.054				
43086	21437.703	21773.855	-0.746				
43126	21397.496	21160.593	-1.107				
43166	21461.402	21145.058	-1.474				
43246	21416.605	21274.109	-0.665				
43326	21294.507	21305.640	0.052				
43486	20253.003	20233.312	-0.097				
43085	21642.496	22237.656	2.749				
43125	21564.906	21557.011	-0.036				
43165	21046.699	20883.671	-1.009				
43245	20937.593	20889.924	-0.228				
43325	21102.109	21200.367	0.465				

RMSQ= 2.11074E+04;

0.306418	0.048084	2.980889
0.048084	0.008136	0.466946
1.000000	0.156925	9.948768
0.048084	1.000000	-1.405884

B(4) = 0.00000E+00      B(5) = 0.00000E+00  
 GK = 2.45150E-01;

43089	18298.511	17815.742	-2.638
43129	18011.007	17951.656	-0.329
43169	18064.402	18020.148	-0.244
43249	18115.105	18087.933	-0.149
43329	18451.300	18213.464	-1.288
43409	18743.207	18312.390	-2.298
43088	16604.292	17118.140	3.094
43128	16611.898	17368.058	4.551
43168	16921.097	17501.339	3.429
43248	17551.800	17612.132	0.343
43328	18163.003	17725.972	-2.406
43408	18415.507	17817.207	-3.248
43087	15384.398	16066.472	4.433
43127	15774.800	16485.703	4.506
43167	16205.199	16827.390	3.839
43247	16941.703	17013.265	0.422
43327	17376.011	17184.042	-1.104
43407	17277.000	17341.941	0.375
43086	15427.800	15195.671	-1.504
43126	15626.101	15652.324	0.167
43166	16224.003	15992.593	-1.426
43246	16663.304	16241.339	-2.532
43326	17080.804	16582.929	-2.686
43406	16649.199	16972.589	1.942
43085	14799.703	14710.085	-0.605
43125	15282.199	15095.734	-1.220
43165	15481.097	15485.878	0.030
43245	15827.406	15693.980	-0.843
43325	16283.605	15931.246	-2.163

B(1) = 9.94876E+00  
 B(6) = 0.00000E+00

B(2) = -1.40588E+00  
 B(7) = 0.00000E+00;

B(3) = 0.00000E+00  
 SFD = 2.09264E+04

RMSQ = 3.59560E+04;

0.306419	0.048084	0.344847	2.980889		
0.048084	0.008136	0.058095	0.466946		
0.344847	0.058095	0.415674	3.348868		
1.000000	0.168467	1.205387	9.972346		
0.048084	1.000000	6.929051	0.946582		
0.306419	0.000035	1.000000	-0.348972	B(1) = 9.97234E+00	B(2) = 9.46582E-01
B(4) = 0.00000E+00	B(5) = 0.00000E+00	B(6) = 0.00000E+00		B(7) = 0.00000E+00;	B(3) = -3.48972E-01
GK = 2.57688E+00;					SFO = 2.14256E+04

43089	18298.511	18020.421	-1.519
43129	18011.007	18099.132	0.489
43169	18064.402	18199.574	0.748
43249	18115.105	18335.527	1.216
43329	18451.300	18634.699	0.993
43489	18743.207	18946.917	1.086
43088	16604.292	16756.511	0.916
43128	16611.898	16937.437	1.959
43168	16921.097	17244.308	1.910
43248	17551.800	17576.308	0.139
43328	18163.003	17943.062	-1.210
43488	18415.507	18191.000	-1.219
43087	15384.398	15766.363	2.482
43127	15774.800	16058.554	1.798
43167	16205.199	16375.084	1.050
43247	16941.703	16767.273	-1.029
43327	17376.011	17101.921	-1.577
43487	17277.000	17214.812	-0.359
43086	15427.800	15509.898	0.532
43126	15626.101	15659.789	0.215
43166	16224.063	15941.140	-1.743
43246	16663.304	16174.179	-2.935
43326	17040.804	16468.039	-3.361
43486	16649.199	16585.295	-0.393
43085	14799.703	15199.296	2.790
43125	15282.199	15386.191	0.680
43165	15481.097	15476.769	-0.027
43245	15827.406	15657.234	-1.075
43325	16283.605	15911.917	-2.292

RMSQ = 2.37746E+04;

0.306418	0.048084	0.344847	0.058095	2.980889		
0.048084	0.008136	0.058095	0.010459	0.466946		
0.344847	0.058095	0.415674	0.074387	3.348868		
0.058095	0.010459	0.074387	0.014076	0.563269		
1.000000	0.168467	1.205387	0.215710	9.503749		
0.048084	1.000000	6.929051	2.262593	8.624809		
0.306418	0.000035	1.000000	-0.084018	-0.519515		
0.058095	0.000671	-0.000110	1.000000	-2.871274		
B(3) = -5.19515E-01	B(4) = -2.87127E+00	B(5) = 0.00000E+00	B(1) = 9.50374E+00	B(2) = 8.62480E+00		
SPO = 1.34099E+04	GR = 5.56810E+03;		B(6) = 0.00000E+00	B(7) = 0.00000E+00;		
43089	18298.511	18160.062	-0.756			
43129	18011.007	17952.410	-0.325			
43169	18064.402	17985.515	-0.836			
43249	18115.105	18095.785	-0.106			
43329	18451.300	18384.187	-0.363			
43489	18743.207	18758.300	0.090			
43088	16604.292	16661.175	0.342			
43128	16611.898	16599.257	-0.076			
43168	16921.097	17067.105	0.862			
43248	17551.800	17621.941	0.399			
43328	18163.003	18227.660	0.355			
43488	18415.507	18576.199	0.872			
43087	15384.398	15583.242	1.292			
43127	15774.800	15866.851	0.583			
43167	16205.199	16191.652	-0.083			
43247	16941.703	16905.468	-0.213			
43327	17376.011	17440.859	0.373			
43487	17277.000	17371.605	0.547			
43086	15427.800	15623.125	1.266			
43126	15626.101	15715.578	0.572			
43166	16224.003	16210.453	-0.083			
43246	16663.304	16577.554	-0.514			
43326	17040.804	16888.933	-0.891			
43486	16649.199	16493.031	-0.937			
43085	14799.703	14822.132	0.151			
43125	15282.199	15273.210	-0.058			
43165	15481.097	15283.527	-1.276			
43245	15827.406	15664.925	-1.026			
43325	16283.605	16197.691	-0.527			
			PM5Q = 9.86341E+03;			

0.306418	0.048084	0.344847	0.058095	0.399246	2.980889
0.048084	0.008136	0.058095	0.010459	0.066775	0.466946
0.344847	0.058095	0.415674	0.074387	0.477247	3.348868
0.058095	0.010459	0.074387	0.014076	0.084985	0.563269
0.399246	0.066775	0.477247	0.084985	0.552110	3.878406
1.000000	0.167254	1.195370	0.212864	1.382882	9.572257
0.048084	1.000000	6.773320	2.252860	7.739502	7.104135
0.344847	0.000418	1.000000	0.062543	-4.636077	-0.498711
0.058095	0.000742	-0.000086	1.000000	-34.649826	-2.399552
0.306418	0.000093	-0.000018	0.000013	1.000000	0.043356
B(3) = -4.98711E-01	B(4) = -2.39955E+00	B(5) = 4.33566E-02	B(6) = 0.00000E+00	B(1) = 9.57225E+00	B(2) = 7.10913E+00
SFO = 1.43607E+04	GR = 1.22308E+03;				B(7) = 0.00000E+00;
43089	18298.511	18027.589	-1.480		
43129	18011.007	17902.382	-0.603		
43169	18064.402	17969.503	-0.525		
43249	18115.105	18116.402	0.007		
43329	18451.300	18435.804	-0.083		
43409	18743.207	18831.914	0.473		
43088	16604.292	16560.945	-0.261		
43128	16611.898	16583.468	-0.171		
43168	16921.097	17048.476	0.752		
43248	17551.800	17610.957	0.337		
43328	18163.003	18207.976	0.247		
43408	18415.507	18577.332	0.878		
43087	15384.398	15499.589	0.748		
43127	15774.800	15839.910	0.412		
43167	16205.199	16199.480	-0.035		
43247	16941.703	16909.933	-0.187		
43327	17376.011	17440.527	0.371		
43407	17277.000	17436.734	0.924		
43086	15427.800	15511.656	0.543		
43126	15626.101	15675.015	0.313		
43166	16224.003	16178.996	-0.277		
43246	16663.304	16578.976	-0.506		
43326	17040.804	16919.421	-0.712		
43406	16649.199	16634.898	-0.085		
43085	14799.703	14815.546	0.107		
43125	15292.199	15291.910	0.063		
43165	15481.097	15358.921	-0.789		
43245	15827.406	15759.117	-0.431		
43325	16283.605	16280.542	-0.018		
			RMSQ = 8.65358E+03;		



0.306418	0.048084	0.344847	0.058095	0.399246	0.477247	2.980889
0.048084	0.008136	0.058095	0.010459	0.066775	0.084985	0.466946
0.344847	0.058095	0.415674	0.074387	0.477247	0.605229	3.348868
0.058095	0.010459	0.074387	0.014076	0.084985	0.113384	0.563269
0.399246	0.066775	0.477247	0.084985	0.552110	0.695539	3.078406
0.477247	0.084985	0.605229	0.113384	0.695539	0.919620	4.628789
1.000000	0.178073	1.268166	0.237579	1.457396	1.926925	9.609584
0.048084	1.000000	6.750127	2.268885	7.333263	17.468063	8.784224
0.344847	-0.003312	1.000000	-0.035221	-1.597477	-1.962958	-0.554608
0.058095	0.000113	-0.000055	1.000000	-31.042663	-29.684585	-3.629442
0.399246	-0.004319	0.000095	0.000014	1.000000	1.489620	-0.167581
0.306418	-0.000426	-0.000005	0.000002	-0.000113	1.000000	0.173826
B(2) = 8.78422E+00	B(3) = -5.54608E-01	B(4) = -3.62944E+00	B(5) = -1.67581E-01	B(1) = 9.60958E+00	B(6) = 1.73826E-01	
B(7) = 0.00000E+00;	SP0 = 1.49069E+04	GR = 6.53040E+03;				
43089	18298.511	18199.921	-0.538			
43129	18011.007	18015.457	0.024			
43169	18064.402	18048.386	-0.088			
43249	18115.105	18142.871	0.153			
43329	18451.300	18417.914	-0.180			
43489	18743.207	18756.261	0.069			
43088	16604.292	16585.304	-0.114			
43128	16611.898	16589.890	-0.132			
43168	16921.097	17058.316	0.810			
43248	17551.800	17592.339	0.230			
43328	18163.003	18162.796	-0.001			
43488	18415.507	18475.089	0.323			
43087	15384.398	15421.550	0.241			
43127	15774.800	15806.905	0.203			
43167	16205.199	16173.472	-0.195			
43247	16941.703	16876.394	-0.385			
43327	17376.011	17384.097	0.046			
43487	17277.000	17332.535	0.321			
43086	15427.800	15432.128	0.028			
43126	15626.101	15668.062	0.268			
43166	16224.003	16202.632	-0.131			
43246	16863.304	16611.183	-0.312			
43326	17040.804	16914.257	-0.742			
43486	16649.199	16567.171	-0.492			
43085	14799.703	14742.343	-0.387			
43125	15282.199	15333.867	0.338			
43165	15481.097	15437.000	-0.288			
43245	15827.406	15873.117	0.288			
43325	16283.605	16385.968	0.628			
			RMSQ = 5.31144E+03;			

0.263739	0.055824	2.765046
0.055824	0.012175	0.584620
1.000000	0.211666	10.865621
0.055824	1.000000	-1.802980

B(4) = 0.00000E+00      B(5) = 0.00000E+00  
 GK = 1.68806E-01;

43089	42632.031	40004.156	-6.164
43129	37698.023	38836.640	3.020
43169	34059.011	37957.148	11.445
43249	30693.992	36430.277	18.688
43329	31731.992	34832.300	9.770
43489	32672.992	32328.394	-1.054
43088	41127.035	39818.649	-3.181
43128	37776.007	38533.675	2.005
43168	29895.000	38196.050	27.767
43248	27983.015	36467.472	30.320
43328	27377.992	35150.015	28.387
43488	27209.011	32961.550	21.142
43087	41359.015	39097.144	-5.468
43127	37492.007	37852.351	0.961
43167	33372.011	37193.289	11.450
43247	29662.015	35682.035	20.295
43327	27184.011	34773.386	27.918
43487	25951.015	32994.007	27.139
43086	48631.015	37734.496	-22.406
43126	43278.039	36499.101	-15.663
43246	36792.031	33915.261	-7.819
43166	40472.007	35499.496	-12.286
43326	34994.019	32986.644	-5.736
43486	31831.011	31743.734	-0.274
43085	56805.015	36974.660	-34.909
43125	52583.019	35313.511	-32.842
43165	51245.011	34236.332	-33.190
43245	39992.027	33200.558	-16.982
43325	35642.007	32378.839	-9.155

B(1) = 1.38656E+01  
 B(6) = 0.00000E+00

B(2) = -1.80298E+00  
 B(7) = 0.00000E+00;

B(3) = 0.00000E+00  
 SPO = 5.23455E+04

BMSQ = 7.08201E+05;

0.263739	0.055824	0.293575	2.765046
0.055824	0.012175	0.062208	0.584620
0.293575	0.062208	0.350118	3.089327
1.000000	0.211898	1.192600	10.331525
0.055824	1.000000	-12.615931	-1.897634
0.263739	-0.000061	1.000000	0.497817

B(4) = 0.00000E+00

B(5) = 0.00000E+00

B(1) = 1.03315E+01

B(2) = -1.89763E+00

B(3) = 4.97817E-01

B(7) = 0.00000E+00;

SPO = 3.06849E+04

GR = 1.49922E-01;

43089	42632.031	34544.558	-18.970
43129	37698.023	33034.746	-12.370
43169	34059.011	31877.460	-6.405
43249	30693.992	30098.078	-1.941
43329	31731.992	27869.242	-12.173
43489	32672.992	25030.667	-23.390
43088	41127.035	39624.914	-3.652
43128	37776.007	37177.046	-1.585
43168	29895.000	35640.171	19.217
43248	27983.015	32834.046	17.335
43328	27377.992	30480.613	11.332
43488	27209.011	27796.964	2.160
43087	41359.015	45060.187	8.948
43127	37492.007	41388.726	10.393
43167	33372.011	38742.496	16.092
43247	29662.015	35481.050	19.617
43327	27184.011	33250.339	22.315
43487	25951.015	30895.515	19.053
43086	48631.015	46879.359	-3.601
43126	43278.039	43396.820	0.274
43246	36792.031	37022.398	0.626
43166	40472.007	40249.570	-0.549
43326	34994.019	34350.832	-1.837
43486	31831.011	31937.316	0.333
43085	56805.015	48726.324	-14.221
43125	52583.019	44502.699	-15.366
43165	51245.011	41681.730	-18.661
43245	39992.027	39188.039	-2.010
43325	35642.007	36765.691	3.152

RMSQ = 4.25332E+05;

0.263739	0.055824	0.293575	0.062208	2.765046	
0.055824	0.012175	0.062208	0.013563	0.584620	
0.293575	0.062208	0.350118	0.074297	3.089327	
0.062208	0.013563	0.074297	0.016198	0.653962	
1.000000	0.211898	1.192600	0.253077	10.426337	
0.055824	1.000000	0.282781	1.191730	-2.342193	
0.263739	-0.000061	1.000000	0.213231	0.488604	
0.062208	0.000346	-0.004466	1.000000	0.417998	
B(3) = 4.08604E-01	B(4) = 4.17998E-01	B(5) = 0.00000E+00	B(1) = 1.04263E+01	B(2) = -2.34219E+00	
SFO = 3.37365E+04	GR = 9.61165E-02		B(6) = 0.00000E+00	B(7) = 0.00000E+00	
43089	42632.031	34781.546	-19.414		
43129	37698.023	33220.765	-11.876		
43169	34059.011	32019.503	-5.988		
43249	30693.992	30148.378	-1.777		
43329	31731.992	27809.769	-12.360		
43489	32672.992	24774.464	-24.174		
43088	41127.035	39593.109	-3.729		
43128	37776.007	37194.921	-1.538		
43168	29895.000	35693.234	19.395		
43248	27993.015	32860.734	17.430		
43328	27377.992	30456.117	11.243		
43488	27209.011	27652.968	1.631		
43087	41359.015	44742.113	8.179		
43127	37492.007	41256.238	10.040		
43167	33372.011	38690.468	15.936		
43247	29662.015	35477.972	19.607		
43327	27194.011	33240.953	22.281		
43487	25951.015	30852.675	18.888		
43086	48631.015	46577.042	-4.223		
43126	43278.039	43297.480	0.044		
43246	36792.031	37117.425	0.894		
43166	40472.007	40256.671	-0.532		
43326	34994.019	34433.914	-1.600		
43486	31831.011	31998.562	0.526		
43085	56805.015	48471.367	-14.670		
43125	52583.019	44546.261	-15.283		
43165	51245.011	41851.812	-18.329		
43245	39992.027	39436.093	-1.390		
43325	35642.007	37020.632	3.867		
			RMSQ = 4.24024E+05;		

0.263739	0.055824	0.293575	0.062208	0.463028	2.765046	
0.055824	0.012175	0.062208	0.013563	0.101920	0.584620	
0.293575	0.062208	0.350118	0.074297	0.493960	3.089327	
0.062208	0.013563	0.074297	0.016198	0.108670	0.653962	
0.463028	0.101920	0.493960	0.108670	0.877681	4.835453	
1.000000	0.220118	1.066804	0.234695	1.895525	9.184440	
0.055824	1.000000	-15.303975	-2.236349	25.907684	28.875244	
0.293575	-0.000112	1.000000	0.213524	-0.952242	0.604701	
0.062208	-0.000129	0.005956	1.000000	-5.952471	-9.024642	
0.263739	-0.002228	0.000930	0.000011	1.000000	-1.912057	B(1) = 9.18444E+00
B(3) = 6.04701E-01	B(4) = -9.02464E+00	B(5) = -1.91205E+00	B(6) = 0.00000E+00	B(2) = 2.88752E+01	B(7) = 0.00000E+00;	
SFO = 9.74432E+03	GM = 3.47023E+12;					
43089	42632.031	39803.226	-6.635			
43129	37698.023	36618.093	-2.864			
43169	34059.011	32728.191	-3.907			
43249	30693.992	25935.773	-15.502			
43329	31731.992	25772.351	-18.781			
43489	32672.992	30583.894	-6.393			
43088	41127.035	40963.765	-0.396			
43128	37776.007	38772.210	2.637			
43168	29895.000	33746.781	12.884			
43248	27983.015	29442.046	5.213			
43328	27377.992	27521.265	0.523			
43488	27209.011	27003.062	-0.756			
43087	41359.015	43301.074	4.695			
43127	37492.007	41077.566	9.563			
43167	33372.011	38413.000	15.105			
43247	29662.015	34809.953	17.355			
43327	27184.011	32183.105	18.389			
43487	25951.015	28132.859	8.497			
43086	48631.015	46618.550	-4.138			
43126	43278.039	43921.683	1.487			
43246	36792.031	39271.394	6.738			
43166	40472.007	42576.203	5.199			
43326	34994.019	37683.390	7.685			
43486	31831.011	32683.339	2.677			
43095	56805.015	46982.390	-17.291			
43125	52583.019	44967.718	-14.482			
43165	51245.011	42597.605	-16.874			
43245	39992.027	38472.210	-3.800			
43325	35642.007	36475.472	2.338			
				RMSQ = 3.61799E+05;		

0.263739	0.055824	0.293575	0.062208	0.463028	0.493960	2.765046
0.055824	0.012175	0.062208	0.013563	0.101920	0.108670	0.584620
0.293575	0.062208	0.350118	0.074297	0.493960	0.567074	3.089327
0.062208	0.013563	0.074297	0.016198	0.108670	0.124767	0.653962
0.463028	0.101920	0.493960	0.108670	0.877681	0.895849	4.835453
0.493960	0.108670	0.567074	0.124767	0.895849	0.987362	5.176922
1.000000	0.219998	1.148013	0.252586	1.813603	1.998867	10.722923
0.055824	1.000000	-5.504475	-0.060656	16.176544	8.302606	8.994637
0.293575	-0.000105	1.000000	0.222020	-0.993042	0.808153	-0.779686
0.062208	-0.000121	0.002211	1.000000	-4.798798	12.016633	8.233015
0.463028	0.000055	-0.002462	0.000003	1.000000	4.676522	-0.456341
0.263739	-0.002197	-0.021297	-0.000012	-0.000038	1.000000	-1.286008
B(2) = 8.99463E+00	B(3) = -7.79686E-01	B(4) = 8.20331E+00	B(5) = -4.56341E-01	B(1) = 1.07229E+01	B(6) = -1.28600E+00	
B(7) = 0.00000E+00;	SFO = 4.53843E+04	GR = 8.05974E+03;				
43089	42632.031	41136.214	-3.508			
43129	37698.023	38357.871	1.750			
43169	34059.011	35200.769	3.352			
43249	30693.992	29466.992	-3.997			
43329	31731.992	30111.113	-5.108			
43489	32672.992	34147.117	4.511			
43088	41127.035	37868.382	-7.923			
43128	37776.007	35970.230	-4.780			
43168	29895.000	32245.871	7.863			
43248	27983.015	28764.464	2.792			
43328	27377.992	27740.292	1.323			
43488	27209.011	27077.437	-0.483			
43087	41359.015	40221.980	-2.749			
43127	37492.007	37690.222	0.528			
43167	33372.011	34755.882	4.146			
43247	29662.015	31226.421	5.274			
43327	27184.011	28948.875	6.492			
43487	25951.015	25156.113	-3.063			
43086	48631.015	48697.199	0.136			
43126	43278.039	44603.820	3.063			
43246	36792.031	37117.496	0.884			
43166	40472.007	41533.839	2.623			
43326	34994.019	34052.093	-2.691			
43486	31831.011	28634.378	-10.042			
43085	56805.015	55999.160	-1.418			
43125	52583.019	52963.902	0.724			
43165	51245.011	48282.257	-5.781			
43245	39992.027	41513.089	3.803			
43325	35642.007	37041.574	3.926			
			RMSQ = 1.41249E+05;			

0.263739	0.055824	0.293575	0.062208	0.463028	0.493960	2.166766	2.765046
0.055824	0.012175	0.062208	0.013563	0.101920	0.108670	0.463028	0.584620
0.293575	0.062208	0.350118	0.074297	0.493960	0.567074	2.310463	3.089327
0.062208	0.013563	0.074297	0.016198	0.108670	0.124767	0.493961	0.653962
0.463028	0.101920	0.493960	0.108670	0.877681	0.895849	3.952233	4.835453
0.493960	0.108670	0.567074	0.124767	0.895849	0.987362	4.037564	5.176922
2.166766	0.463028	2.310463	0.493961	3.952233	4.037564	18.319320	22.652999
1.000000	0.213695	1.066318	0.227971	1.824023	1.863405	8.454682	14.065599
0.055824	1.000000	12.961079	3.905218	-1.652958	21.491287	-44.553787	-11.090393
0.293575	-0.000527	1.000000	0.214773	-0.965562	0.714235	-4.443655	-1.813988
0.062208	0.000270	0.004454	1.000000	-3.792126	12.962867	1.109244	14.867738
0.463028	0.002973	-0.038318	0.000003	1.000000	0.934003	6.784339	1.081575
0.493960	0.000245	-0.000506	-0.000014	-0.000041	1.000000	-0.504532	-1.347826
0.263739	-0.000535	0.019280	0.000031	-0.000031	-0.000054	1.000000	-0.255159
B(2) = -1.10903E+01      B(3) = -1.81398E+00      B(4) = 1.48677E+01      B(5) = 1.08157E+00      B(6) = -1.34782E+00							
B(7) = -2.55159E-01;      SFO = 1.28413E+06      GK = 1.52582E-05;							
43089	42632.031	43095.378	1.086				
43129	37698.023	38239.128	1.435				
43169	34059.011	34431.320	1.093				
43249	30693.992	29140.832	-5.060				
43329	31731.992	30170.816	-4.919				
43489	32672.992	33847.503	3.594				
43088	41127.035	39291.476	-4.463				
43128	37776.007	35764.039	-5.326				
43168	29895.000	31791.300	6.343				
43248	27983.015	28254.582	0.970				
43328	27377.992	27611.015	0.851				
43488	27209.011	27777.937	2.090				
43087	41359.015	41191.410	-0.405				
43127	37492.007	37411.144	-0.215				
43167	33372.011	34080.261	2.122				
43247	29662.015	30490.613	2.793				
43327	27184.011	28523.804	4.928				
43487	25951.015	25964.929	0.053				
43086	48631.015	49075.625	0.914				
43126	43278.039	44062.398	1.812				
43246	36792.031	36377.437	-1.126				
43166	40472.007	40490.769	0.046				
43326	34994.019	33472.000	-4.349				
43486	31831.011	29415.246	-7.589				
43085	56805.015	56575.460	-0.408				
43125	52583.019	52645.839	0.119				
43165	51245.011	47960.507	-6.409				
43245	39992.027	41985.093	4.983				
43325	35642.007	37832.214	6.145				

RMSQ= 1.21400E+05;

## BIBLIOGRAPHY\*

1. Ernst, H. and Merchant, M. E., "Chip Formation, Friction and High Quality Machined Surfaces," Surface Treatment of Metals (American Society Metals), 1941, p. 259.
2. Merchant, M. E., "Mechanics of the Metal Cutting Process," J. Appl. Phys., Vol. 16, 1945, No. 5, p. 267 and No. 6, p. 318.
3. Bridgeman Phys. Rev., 1935, Vol. 48, p. 825, Proc. Amer. Acad. 1937, Vol. 71, p. 386, J. Appl. Phys., Vol. 8, 1937, No. 5, p. 328; J. Appl. Phys., Vol. 14, 1943, p. 273, "The Physics of High Pressure," 1949 (Bell & Sons, Limited, London).
4. Crossland, B., "The Effect of Fluid Pressure on the Shear Properties of Metals," Proc. Inst. Mech. Eng. (1954), Vol. 168, p. 935.
5. Lee, E. H. and Shaffer, B. W., "The Theory of Plasticity Applied to a Problem of Machining," J. Appl. Mech., Trans. Amer. Soc. Mech. Engrs., Vol. 73, p. 405.
6. Sata, Toshio, "Recent Developments Concerning Cutting Mechanics," Proceedings of the International Research in Production Engineering Conference, 1963, pp. 18-25.
7. Stabler, G. V., "The Fundamental Geometry of Cutting Tools," Proc. Inst. Mech. Engrs., London, Vol. 165, 1951, p. 14.
8. Huchs, H., "Plastizitätmechanische Grundlagen und Kenngrößen der Serspannung," Dissertation, Tech. Hock. Aachen, 1951.
9. Shaw, M. C., Cook, N. H., and Finnie, I., "The Shear-Angle Relationship in Metal Cutting," Trans. ASME, 1953, pp. 273-288.
10. Weisz, M., "Étude Metallographique de la Formation du Copeau d'Usinage, l'Institut de Recherches de la Siderurgie," Ser. A., No. 142, 1957.
11. Colding, B. N., "A Yield Criterion Applied to the Shear Angle Relationship," Les Annales du College International pour L'Etude Scientifique des Technique de Production Mechanique, Vol. 7, 1958.

---

\* Abbreviations used conform to the practice of the Transaction of the American Society of Mechanical Engineers.



12. Sata, T. and Mizuno, M., "Friction Process on Cutting Tool and Cutting Mechanism," J. Sci. Res. Inst., Tokyo, Vol. 49, 1955, pp. 163-174.
13. Oxley, P. L. B., "A Strain-Hardening Solution for the 'Shear Angle' on the Orthogonal Metal Cutting," International J. Mech. Sci. Vol. 3, 1961, pp. 68-79.
14. Zorev, N. N., "Problems of Metal Cutting Mechanics," Moscoe, 1956.
15. Boothroyd, G. and Bailey, J. A., "Effects of Strain Rate and Temperature in Orthogonal Metal Cutting," J. Mech. Engr. Sci., Vol. 8, No. 3, 1961, pp. 264-275.
16. Bailey, J. A. and Singer, A. R. E., "Effect of Strain Rate and Temperature on the Resistance to Deformation of Aluminum, Two Aluminum Alloys and Lead," J. Inst. Metals, Vol. 92, 1964, p. 404.
17. Pugh, H. L. D., "Mechanics of the Cutting Process," Proceedings of the Conference on Technology of Engineering Manufacture.
18. Palmer, W. B. and Oxley, P. L. B., "Mechanics of Orthogonal Machining," Proc. Inst. Mech. Engrs., Vol. 173, 1959, p. 623.
19. Nakayama, K., "Studies on the Mechanism of Metal Cutting," Bull. Fac. Engrg. Natl. Univ. Yokohama, Vol. 7, 1958, p. 1.
20. Wallace, P. W. and Boothroyd, G., "Tool Forces and Tool Chip Friction in Orthogonal Machining," J. Mech. Eng. Sci., Vol. 6, 1964, No. 1, p. 74.
21. Lubahn, J. D., "Derivation of Stress, Strain, Temperature, Strain-Rate Relation for Plastic Deformation," J. Appl. Mech., Sept. 1947, pp. A-229, A-230.
22. Albrecht, P., "Mechanics of the Cutting Process," Proceedings of the International Production Engineering Research Conference, 1963, pp. 32-41.
23. Shaw, M. C., "Resume and Critique of Papers in Part One," Proceedings of the International Production Engineering Research Conference, 1963, pp. 3-17.
24. Boothroyd, G., "Mechanics of Unlubricated Metal Cutting," The Engineer, Nov. 26, 1965.
25. Cumming, J. D., Kobayashi, S., and Thomsen, E. G., "A New Analysis of the Forces in Orthogonal Metal Cutting," J. Engr. for Ind., Nov. 1965, pp. 480-486.

26. Enahoro, H. E., "Effects of Cold Working on Chip Formation in Metal Cutting," Annals of the C.I.R.P., Vol. XIII, pp. 251-261.
27. Kobayashi, S., Herzog, R. P., Eggleston, D. M., and Thomsen, E. G., "A Critical Comparison of Metal Cutting Theories with New Experimental Data," J. Engr. for Ind., Nov. 1960, pp. 333-347.
28. Kobayashi, S. and Thomsen, E. G., "Metal Cutting Analysis - I," J. Engr. for Ind., Feb. 1962, pp. 63-70.
29. Kobayashi, S. and Thomsen, E. G., "Metal Cutting Analysis - II," J. Engr. for Ind., Feb. 1962, pp. 71-80.
30. Kullberg, G., "Mechanics of Orthogonal Cutting," Annals of the C.I.R.P., Vol. XII, No. 2, pp. 106-115.
31. Nakayama, N., "Mechanical Properties of Chips Produced on Metal Cutting," Proceedings of the International Research on Production Engineering Conference, 1963, pp. 83-88.
32. Ostafiev, V. A. and Kobayashi, Shiro, "Stress, Strain, and Strain-Rate in Metal Cutting," Proceedings of the 7th International M.T.D.R. Conference, U. of Birmingham, Sept. 1966, Pergamon Press, Oxford and N.Y.C., 1957.
33. Oxley, P. L. B., "Flow Stress Characteristics and the Machining Process," The Engineer, Jan. 27, 1967, pp. 140-144.
34. Oxley, P. L. B., "Mechanics of Metal Cutting," Proceedings of the International Research in Production Engineering Conference, 1963, pp. 50-60.
35. Oxley, P. L. B., "Rate of Strain Effect in Metal Cutting," J. Engr. for Ind., Nov. 1963, p. 335.
36. Oxley, P. L. B., "Mechanics of Metal Cutting for a Material of Variable Flow Stress," J. Engr. for Ind., Nov. 1963, p. 339.
37. Oxley, P. L. B., "Introducing Strain Rate Dependent Work Material Properties into the Analysis of Orthogonal Cutting," Annals of the C.I.R.P., Vol. XIII, 1966, pp. 127-138.
38. Rowe, G. W. and Spick, P. T., "A New Approach to Determinations of the Shear Plane Angle in Machining," J. Engr. for Ind., Aug. 1967, pp. 530-537.
39. Russell, J. K. and Brown, R. H., "Deformation During Chip Formation," J. Engr. for Ind., Feb. 1965, pp. 53-56.
40. Sata, Toshio, "Flow Stress in Metal Cutting," Sci. Pap. IPCR, Vol. 53, Sept. 1959, (Tokyo, Japan), pp. 188-200.

41. Thomsen, E. G., "Application of the Mechanics of Plastic Deformation to Metal Cutting," Annals of the C.I.R.P., Vol. XII, pp. 113-123.
42. Trigger, K. J., "Temperatures in Machining and Their Importance," Proceedings of the International Research in Production Engineering Conference, 1963, pp. 95-101.
43. Trigger, K. J. and von Turkovich, B. F., "Chip Formation in High Speed Cutting of Copper and Aluminum," J. Engr. for Ind., Nov. 1963, pp. 365-373.
44. von Turkovich, B. F., "Mechanics of Cutting," Proceedings of the International Research in Production Engineering Conference, 1963, pp. 26-31.
45. Weiner, J. H., "Shear Plane Temperature Distribution in Orthogonal Cutting and Discussion," Trans. of the ASME, Nov. 1965, pp. 1331-1341.
46. Zorev, N. N., "Interrelationship Between Shear Processes Occurring Along Tool Face and on Shear Plane in Metal Cutting," Proceedings of International Production Engineering Research Conference, 1963, pp. 42-49.
47. Boothroyd, G., "A Metal Cutting Dynamometer," The Engineer, Feb. 23, 1962.
48. Boothroyd, G., "Temperatures in Orthogonal Metal Cutting," Proc. Inst. Mech. Engr., Vol. 177, No. 29, 1963, pp. 789-810.
49. Rapier, A. C., "A Theoretical Investigation of the Temperature Distribution in Orthogonal Cutting," Brit. J. Appl. Phys., Vol. 5, 1954, p. 400.
50. Boothroyd, G., Personal communications, 1964.

## VITA

Cecil Reid Attaway was born in Fredericksberg, Virginia on May 19, 1940. He attended grammar school in Clinton, New Jersey and high school at Annandale, New Jersey. He entered Clemson University (then Clemson College) in 1958 and graduated with honors in June, 1962 in Mechanical Engineering. He received a commission as a Second Lieutenant in the United States Army Reserve in August, 1962.

In September, 1962 he enrolled in the Graduate Division of the Georgia Institute of Technology. In June, 1967 he was called to active duty by the United States Army and in June, 1968 was promoted to the rank of Captain. During his tour of duty he served as a Research and Development Coordinator for the Army Research Office, Durham, North Carolina. In 1968 he was awarded the degree of Master of Science by the Georgia Institute of Technology.